

Natural killer cell mediated killing of patient-derived lung cancer models in co-culture: An approach to unravel killing mechanisms.

Inaugural Dissertation

zur

Erlangung des Doktorgrades  
Dr. nat. med.

der Medizinischen Fakultät  
und  
der Mathematisch-Naturwissenschaftlichen Fakultät  
der Universität zu Köln

vorgelegt von

Alena Heimsoeth

aus Kirchheimbolanden

Goltstein 68, Köln

2024

Natural killer cell mediated killing of patient-derived lung cancer models in co-culture: An approach to unravel killing mechanisms.

Inaugural Dissertation

zur

Erlangung des Doktorgrades  
Dr. nat. med.

der Medizinischen Fakultät  
und  
der Mathematisch-Naturwissenschaftlichen Fakultät  
der Universität zu Köln

vorgelegt von

Alena Heimsoeth

aus Kirchheimbolanden

Goltstein 68, Köln

2024

Betreuer/in: Prof. Dr. Martin L. Sos  
Referent/in: Prof. Dr. Hamid Kashkar  
Referent/in: Prof. Dr. Kay Hofmann

Datum der mündlichen Prüfung: 24.05.2024

# Table of Contents

Abstract .....	5
Zusammenfassung .....	6
Introduction .....	7
<i>Lung cancer</i> .....	7
<i>NK cells</i> .....	7
NK cell receptor repertoire .....	8
Stages of tumor cell lysis .....	13
Lytic granules and death receptor pathway .....	14
<i>Cell death pathways</i> .....	17
Apoptosis.....	18
Necroptosis.....	19
Pyroptosis.....	19
Crosstalk.....	20
<i>NK cells in lung cancer</i> .....	20
<i>Immune escape of cancer cells</i> .....	21
Aim .....	23
Results .....	24
<i>Evaluation of the co-culturing method</i> .....	24
<i>How do tumor cells die?</i> .....	29
<i>What are the drivers for NK cell killing?</i> .....	34
<i>Tumor escape mechanisms</i> .....	38
<i>Summary</i> .....	42
Discussion.....	43
<i>EMT</i> .....	43
<i>Increased IFN<math>\gamma</math> signature</i> .....	44
<i>Cell death</i> .....	45
Efficiency of pan-caspase inhibition.....	46
Effect of granzymes.....	46
Cell death signatures as prognostic factor .....	46
Concluding remarks .....	48
Methods .....	49
List of figures .....	65
List of tables.....	66
List of abbreviations .....	67
Literature .....	72
Danksagung.....	88
Erklärung.....	89
Curriculum Vitae .....	89

## Abstract

Lung cancer is the most common malignancy and the leading cause of cancer mortality worldwide and the limited understanding of the complex interplay between the immune system and tumor cells hampers the development of novel therapies (Sung, 2021). Natural killer (NK) cells are lymphocytes and are highly cytotoxic against transformed cells without prior sensitization and thus play an important role in the development of lung cancer and other tumor types. It was shown that a NK cell gene signature within the tumor leads to a better overall survival (Habif, Crinier, Andre, Vivier, & Narni-Mancinelli, 2019; Larsen, Gao, & Basse, 2014; Takanami, Takeuchi, & Giga, 2001). The importance of NK cells in anti-tumor immunity is indisputable, but during tumor progression cancer cells escape their cytolytic function with various mechanisms (Sordo-Bahamonde, Lorenzo-Herrero, Payer, Gonzalez, & Lopez-Soto, 2020).

This work aims to unravel dynamics between NK cells and lung cancer cells, investigating the prospects of cancer cell vulnerability, mechanisms of cell death and dynamics within short- and long-term co-culture.

In this work I established a co-culture system of the human NK cell line NK-92 and patient-derived lung cancer cell lines in 2D and 3D to measure and mechanistically dissect NK cell killing efficacy.

NK-92 were able to induced cell death in the majority of cell lines with a heterogenous pattern of killing efficacy between the individual lung cancer cell lines. Key findings of this work were; firstly, the identification of an epithelial-to-mesenchymal phenotype (EMT) gene signature in NK resistant cancer cell lines also reflected in a reduced killing of TGF $\beta$  treated cell lines; secondly, increased IFN $\gamma$  signaling for highly sensitive cell lines; and thirdly, elevated cell death levels and less effect of caspase inhibition in highly vulnerable cancer cells.

## Zusammenfassung

Lungenkrebs ist die häufigste bösartige Erkrankung und die häufigste krebsbedingte Todesursache weltweit, und das begrenzte Verständnis des komplexen Zusammenspiels zwischen Immunsystem und Tumorzellen beeinflusst die Entwicklung neuartiger Therapien (Sung, 2021). Natürliche Killerzellen (NK) sind Lymphozyten, wirken ohne vorherige Sensibilisierung stark zytotoxisch gegenüber transformierten Zellen und spielen daher eine wichtige Rolle bei der Entstehung von Lungenkrebs und anderen Tumorarten. Es wurde gezeigt, dass eine NK-Zell-assoziierte Gensignatur innerhalb des Tumors zu einem besseren Gesamtüberleben führt (Habif, Crinier, Andre, Vivier, & Narni-Mancinelli, 2019; Larsen, Gao, & Basse, 2014; Takanami, Takeuchi, & Giga, 2001). Die Bedeutung von NK-Zellen für die Antitumorimmunität ist unbestritten, aber im Laufe der Tumorprogression entziehen sich Krebszellen ihrer zytolytischen Funktion durch die Entwicklung verschiedener Resistenzmechanismen (Sordo-Bahamonde et al., 2020).

Diese Arbeit zielt darauf ab, die Dynamik zwischen NK-Zellen und Lungenkrebszellen zu entschlüsseln und die Anfälligkeit von Krebszellen, die Mechanismen des Zelltods und die Dynamik innerhalb kurz- und langfristiger Co-Kultur zu untersuchen.

In dieser Arbeit habe ich ein Co-Kultursystem der menschlichen NK-Zelllinie NK-92 und von Patienten stammender Lungenkrebszelllinien in 2D und 3D etabliert, um die Wirksamkeit der Abtötung durch NK-Zellen zu messen und mechanistisch zu analysieren.

Die NK-92 Zellen konnten in den meisten Tumorzelllinien den Zelltod auslösen, wobei die Abtötungswirksamkeit zwischen den einzelnen Lungenkrebszelllinien sehr heterogen war. Die wichtigsten Ergebnisse dieser Arbeit waren: Erstens spiegelte sich die Identifizierung einer Gensignatur des epithelialen-mesenchymalen Transitions (EMT) Phänotyps in NK-resistenten Krebszelllinien auch in einer verringerten Abtötung von TGF $\beta$ -behandelten Zelllinien wider; zweitens eine verstärkte IFN $\gamma$ -Signalgebung für hochsensible Zelllinien; und drittens erhöhte Zelltodraten und eine geringere Wirkung der Caspase-Hemmung in Krebszellen die erhöhte Anfälligkeit für NK-Zell bedingten Zelltod aufwiesen.

## Introduction

### Lung cancer

Lung cancer is the most common malignancy and the leading cause of cancer mortality, accounting for 11.4% of newly diagnosed cancers and 18% of cancer-associated deaths worldwide in 2020 (Sung et al., 2021). The five-year survival rate is approximately 25.4% relative to 68.7% for cancer diagnosed patients in general ("Cancer Stat Facts: Lung and Bronchus Cancer,"). Some of the causes of lung cancer include tobacco smoking, as well as indirect exposure to tobacco, air pollution, poor safety measures of the industry in low- and middle-income countries such as coal and aluminum production companies, and exposure to building materials like asbestos (Islami, Torre, & Jemal, 2015). However, the most prevalent risk factor is smoking. Bruder (2018) estimated the risk for lung cancer association to smoking and found a 14% risk for current smokers versus 2% for never-smokers (Bruder et al., 2018).

### NK cells

Natural killer (NK) cells are lymphocytes and part of the innate immune system, phenotypically defined as CD56<sup>+</sup> and CD3<sup>-</sup> immune cells. They express a variety of germ-line encoded activating and inhibitory receptors and are highly cytotoxic against transformed cells without prior sensitization, a characteristic, that deems them for early stages of host defense. With the secretion of cytokines and chemokines (mainly interferon gamma (INF $\gamma$ ) and tumor necrosis factor alpha (TNF $\alpha$ )) NK cells can attract, as well as communicate with other immune cells of the innate or adaptive system (Vivier et al., 2018). Long-term studies did reveal a correlation between low NK cell cytotoxicity and increased risk of cancer, whereas NK cell tumor infiltration is associated with improved patient outcome in several malignancies (Imai, Matsuyama, Miyake, Suga, & Nakachi, 2000).

In this work, I used the 1992 isolated IL-2 dependent human NK cell line NK-92 for the establishment of a co-culture system (Gong, Maki, & Klingemann, 1994). NK-92 show a consistent and high cytotoxicity against transformed cells, are commonly used for tumor cell co-cultures and are involved in the development of NK cell-based cancer therapies (Snyder et al., 2018; X. Song et al., 2020; Tam et al., 1999).

## NK cell receptor repertoire

For the recognition of a target cell, the complex interplay of inhibitory and activating receptor signaling has to be strongly predominated by the activation signal (Figure 1). Interaction of major histocompatibility complex (MHC) I with NK cells, killer-immunoglobulin-like receptors (KIRs) and the CD94/natural-killer group 2, member A (NKG2A) heterodimer has been proposed as a crucial inhibitory mechanism for the self-tolerance of healthy cells (Raulet & Vance, 2006). However, in contrast to T-cell recognition of MHC I, NK cell binding is less allele-specific and peptide-dependent. Boyington et al. demonstrated in a crystal structure of KIR2DL2 and human leukocyte antigen-C (HLA-C) that only 36% of HLA surface peptides are covered by KIR, in comparison to 80% for T-cell receptor (TCR) binding. In the shared interface, 11 out of 12 residues are invariant in HLA-C for KIR binding, but only 8 out of 16 for TCR binding, meaning that the KIR receptors interact with a majority of conserved residues (Boyington, Motyka, Schuck, Brooks, & Sun, 2000). The KIR family as well as inhibitory receptors Ig-like transcript 2 (ILT2) detect allelic variants of HLA-A, B and mainly C, whereas CD94/NKG2A recognizes HLA-E (Joyce & Sun, 2011; Moretta & Moretta,

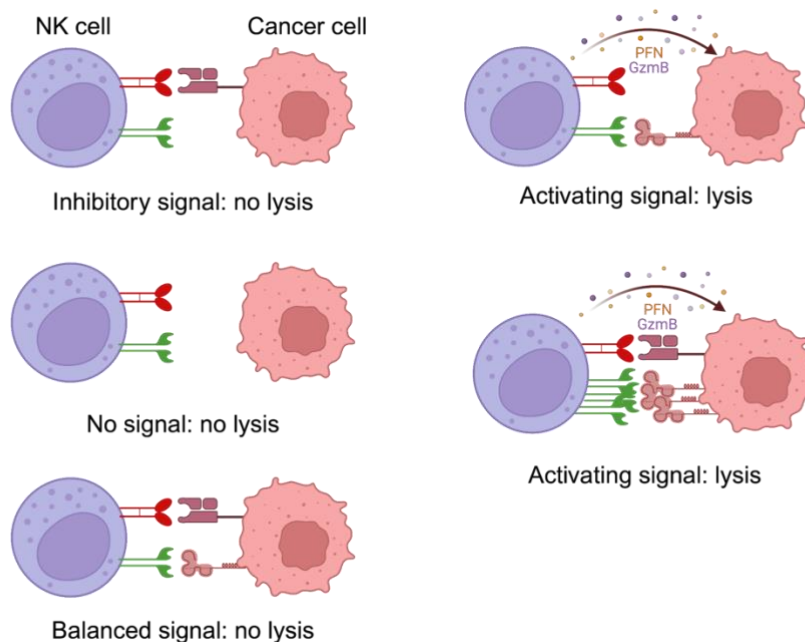


*Figure 1* Balancing inhibitory and activation signal in NK cell - tumor cell interaction

2004). Tumor cells commonly downregulate expression of MHC I, resulting in the loss of inhibitory signals towards NK cells. However, activating signaling via stress induced ligands is required in addition for NK cell activation (Shaver, Croom-Perez, & Copik, 2021) (Figure 1). NK cells express a variety of activating receptors, such as NKG2D,



activating KIRs, Natural cytotoxicity triggering receptor 80 (NKp80), CD94/NKG2C, DNAX-accessory molecule-1 (DNAM-1) and 2B4 (Moretta et al., 2006).

A list of all NK cell receptors involved in activation or inhibition of NK cell effector function and their ligands is shown in Table 1.

**Table 1** Natural Killer cell receptors and their ligands data consolidated from: (Aldemir et al., 2005; Beldi-Ferchiou & Caillat-Zucman, 2017; Bhatt et al., 2021; Campbell & Purdy, 2011; Claus, Urlaub, Fasbender, & Watzl, 2019; Deuss, Watson, Fu, Rossjohn, & Berry, 2019; Hosomi et al., 2013; Jandus et al., 2014; W. Jiang et al., 2022; Khan, Arooj, & Wang, 2020; Koch, Steinle, Watzl, & Mandelboim, 2013; Y. Li et al., 2009; Mizrahi, Markel, Porgador, Bushkin, & Mandelboim, 2007; Stanietzky et al., 2009; Van Laethem et al., 2022; Z. Zhang et al., 2015)

Receptor class	Receptor (NK cell)	Ligand (tumor cell)	Function
Natural cytotoxicity receptors (NCRs)	NKp46	heparin/heparan sulfate unknown	Activating Activating/Inhibitory
	NKp44	Sialylated/sulfated proteoglycans PCNA unknown	Activating Inhibitory Activating/Inhibitory
	NKp30	B7-H6 BAG6 heparin/heparan sulfate unknown	Activating Activating/Inhibitory
C-type lectin family	NKG2A/B/CD94	HLA-E	Inhibitory
	NKG2C/CD94	HLA-E	Activating
	NKG2D	MICA MICB ULBP family	Activating
Killer-immunoglobulin-like family	KIR2DL1	HLA-C	Activating
	KIR2DL2	HLA-C, HLA-B	
	KIR2DL3	HLA-C, HLA-B	
	KIR3DL1	HLA-B, HLA-A	
	KIR3DL2	HLA-A	
	KIR2DL5A	unknown	
	KIR2DL5B	unknown	
	KIR3DL3	HLA2	Inhibitory
	KIR2DL4	HLA-G	
	KIR2DS1	HLA-C	
	KIR2DS2	HLA-C	
	KIR2DS3	HLA-C	
	KIR2DS4	HLA-C	
	KIR2DS5	HLA-C (Blokhuis et al., 2017)	

	KIR3DS1	HLA-F, HLA-Bw4 (Garcia-Beltran et al., 2016)	
	ILT2	HLA-G	Inhibitory
Immunoglobulin superfamily receptors	DNAM-1	CD112 CD155	Activating
	TIGIT	PVR PVRL2	Inhibitory
	CD96	CD155	Activating/Inhibitory
signaling lymphocytic activation molecule (SLAM)-family	SLAMF4	CD48	Activating
	SLAMF6	SLAMF6	Activating
	SLAMF7	SLAMF7	Activating/Inhibitory
Immunoglobulin superfamily receptors	DNAM-1	CD112 CD155	Activating
	TIGIT	PVR PVRL2	Inhibitory
	CD96	CD155	Activating/Inhibitory
	CD100	CD72	Activating
	CD160	HLA-C	Enhancing cytokine release
	CEACAM1	CEACAM1 CEACAM5	Inhibitory
	KLRG1	E-,N-,R-cadherins	Inhibitory
	LAIR	Collagen	Inhibitory
	CD161	LLR1	Inhibitory
	Silec-7/9	Lectins	Inhibitory
	LAG-3	HLA-type II C-type lectin Gal-3 FGL-1 (?) (Burnell et al., 2022)	Inhibitory Unknown
	TIM3	HMGB1 CEACAM1 Galectin-9	Inhibitory

There are various intracellular adaptor proteins which transmit signals downstream of NK receptor activation. For receptors involved in activating functions, common motifs are the immunoreceptor tyrosine activation motif (ITAM), Death-associated protein 10 (DAP10) (containing a tyrosine based signaling motif (YINM)), and the immunoreceptor tyrosine based switch motif (ITSM) (Watzl & Urlaub, 2012). Upon receptor activation the ITAM motif gets phosphorylated by Src-family kinases, resulting in the recruitment

of Zeta Chain of T Cell Receptor Associated Protein Kinase 70 (ZAP70) or spleen tyrosine kinase (SYK). This leads to the phosphorylation of trans-membrane adaptor molecules Linker for activation of T cells (LAT) and non-T cell activation linker (NTAL) and the cytosolic adaptors lymphocyte cytosolic protein 2 (SLP76) and c-Abl Src homology 3 domain-binding protein-2 (3BP2) (Watzl & Urlaub, 2012). DAP10 is coupled to NKG2D and upon Src-family kinase phosphorylation, phosphoinositide 3-kinase (PI3K) or growth factor receptor-bound protein 2 (GRB2) is recruited, binding and activating vav guanine nucleotide exchange factor 1 (VAV1). VAV1 in turn phosphorylates SLP76 and phospholipase C, gamma 2 (PLC $\gamma$ 2). This signaling cascade finally leads to the activation of small coupled G proteins of the Ras homologous (Rho) -family and the initiation of actin reorganization and polarization of the microtubule organization center (MTOC) towards the target cell (Garrity, Call, Feng, & Wucherpfennig, 2005; Upshaw et al., 2006). SLAM-family members contain the ITSM in their cytoplasmic tail and following the Src-family kinase phosphorylation, adaptor molecules serum amyloid P component (SAP), EAT-2 and ethylene-responsive transcriptional coactivator-like protein (ERT), all of which contain the SH2 domain, are recruited. Whereas SLAM-4 and -6 seem to depend on the adaptor molecule SAP, SH2 domain-containing protein 1B (EATS-2) does play a crucial role in SLAM-7 signaling. SAP next recruits FYN, leading to the activation of LAT, PLC $\gamma$ 1 and VAV1 (Bloch-Queyrat et al., 2005; R. Chen et al., 2004). The downstream signaling of SLAM-7 is not fully understood, however there is evidence for signaling via PLC $\gamma$ 1/2 leading to extracellular-signal regulated kinase (ERK) pathway activation (Gutierrez-Guerrero et al., 2022; Perez-Quintero et al., 2014). Different signaling pathways ensure a robust NK cell signaling, which is even independent from single proteins which are crucial for one of those pathways (Colucci et al., 2002). The output of activation receptor pathways is either ERK activation for granule polarization and release, or Ca<sup>2+</sup> flux via calcium release-activated calcium modulator 1 (ORAI1) which is necessary for exocytosis of cytolytic granules and is mediated by PLC $\gamma$  (Maul-Pavicic et al., 2011; Regunathan et al., 2006). Another essential outcome is actin reorganization for receptor clustering and formation on the immunological synapse, driven by Vav-family and Rho-family activation (C. Li et al., 2008) (Figure 2).

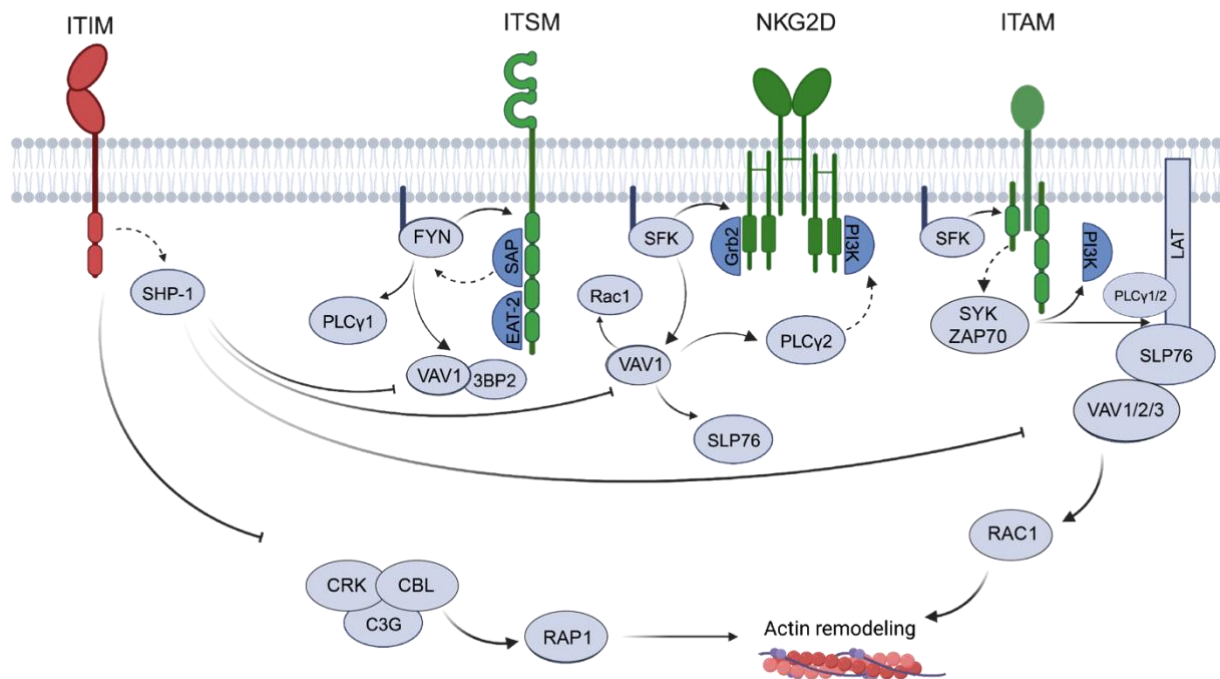


**Figure 2** Schematic overview of NK cell receptor downstream signaling and crosstalk. Adapted from (Watzl & Urlaub, 2012)

The main inhibitory receptors belong to the KIR or C-type lectin-like family. The structure of KIR receptors is reflected in the nomenclature, they can either contain 2 or 3 Ig-like domains (KIR2/3) and a long or short intracellular domain (KIR2DL/S). Receptors with a long domain contain an immunoreceptor tyrosin-based inhibitory motif (ITIM), whereas those with a short cytoplasmic tail are complexed with DAP12 and can deliver an activating signal. In the C-type lectin-like family, receptors build heterodimers with CD94 and, whereas NKG2A/B have an intracellular ITIM motif, NKG2C/E bind to DAP12 (Watzl & Urlaub, 2012). Following ligand binding, the ITIM motif is phosphorylated and recruits phosphatases small heterodimer partner 1/2 (SHP1/2) (Lu, Gong, Bar-Sagi, & Cole, 2001). A direct target of SHP1 is VAV1, which enables interference with actin reorganization (Stebbins et al., 2003). Additionally, KIR or NKG2A activation leads to phosphorylation of CT10-regulated kinase (CRK), followed by dissociation of the CRK complex which is involved in actin reorganization and lymphocyte function associated antigen 1 (LFA1)-mediated adhesion (Peterson & Long, 2008). To sum up, the engagement of inhibitor receptors interferes with attachment to the target cell and the building of the immunological synapse (Figure 2).

## Stages of tumor cell lysis

The whole process of target cell lysis can be subdivided into the initiation stage, the effector stage and the termination stage (Figure 3).

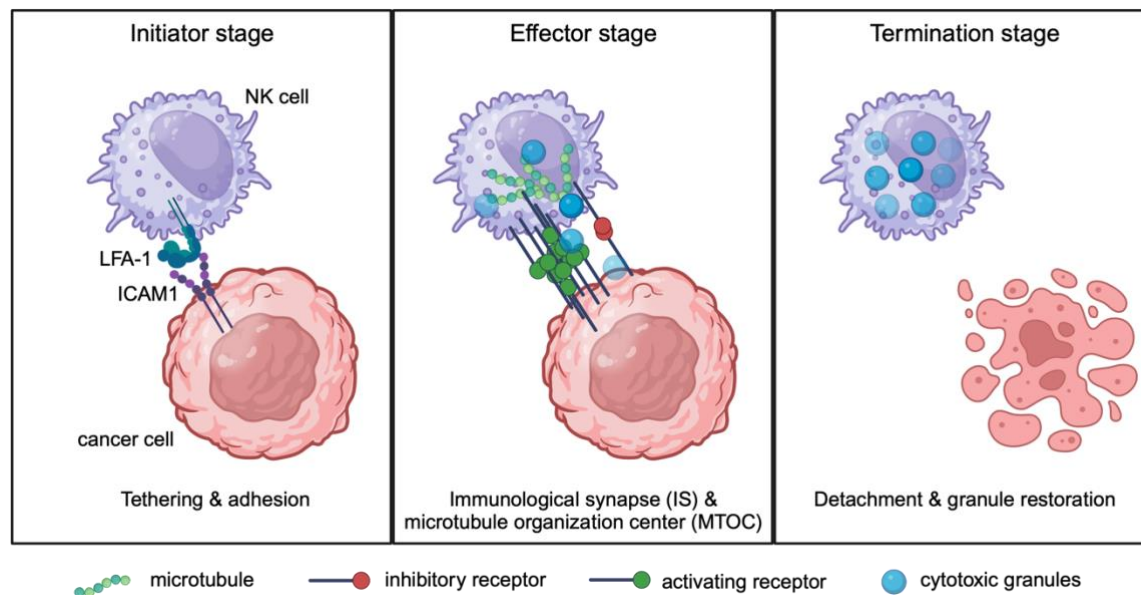


**Figure 3** Overview of NK cell mediated target cell lysis. *Initiator stage: Establishment of stable adhesion between NK and target cell by LFA-1 binding to ICAM1. Effector stage: The clustering of activation receptors, aggregation of lipid rafts and supramolecular clusters lead to for a robust activation signaling and the formation of the immunological synapse. Lytic granules are recruited via movement along the microtubules in a negative direction towards the MTOC, which polarizes towards the immunological synapse. Last step is granule docking at the IS and release. Termination stage: Detachment of the target cell and restoration of lytic capability.*

As a first contact between NK cell and target cell, tethering and adhesion via receptors such as CD2 and selectin CD62L is necessary (Santoni et al., 2021). Next, in the case of predominantly activating signaling, meaning engagement of a SLAM-family member and at least two coactivating receptors, stable adhesion is established by the integrin LFA-1. This is an essential step for further progress. LFA-1 is a heterodimer of CD11a and CD18 which, depending on its conformation, binds to Intercellular Adhesion Molecule 1 (ICAM1). Cation binding on the adhesion side of LFA-1 changes its conformation, whereas Mg<sup>+</sup> or Mn<sup>+</sup> binding increases its binding affinity and Ca<sup>2+</sup> stabilizes the inactive conformation (Urlaub, Hofer, Muller, & Watzl, 2017). Activation and association of LFA-1 with actin reorganization leads to a rapid and strong adhesion. Hoffmann et al. demonstrated an increase of force needed for separation of NK and target cell from 1nN to 3nN only 120s after tethering (Hoffmann, Cohnen, Ludwig, & Watzl, 2011). During initiation, inhibitory signaling can interfere and disrupt further adhesion and actin remodeling as described earlier.

The next steps are part of the effector stage, which establishes a stable NK cell – target cell interface, due to the recruitment, direction and fusion of cytolytic granules with the plasma membrane in the cleft between NK and target cell. For a stable interface, the

formation of fibrous actin (F-actin) from the cellular globular actin (G-actin) pool carried out by VAV1 and Wiskott–Aldrich syndrome protein (WASP) is essential (Graham et al., 2006; Orange et al., 2002). The clustering of activation receptors, aggregation of lipid rafts and supramolecular clusters are required for a robust activation signaling and the formation of the immunological synapse (Giurisato et al., 2007; Lou, Jevremovic, Billadeau, & Leibson, 2000; Treanor et al., 2006). Lytic granules are recruited via movement along the microtubules in a negative direction towards the MTOC, which polarizes towards the immunological synapse in an ERK, VAV1 and protein tyrosine kinase 2 (Pyk2)-dependent manner (X. Chen et al., 2006; Sancho et al., 2000). Once the granules arrive, the docking to the synapse is performed by the Ras-associated binding protein (Rab)-family member Ras-related protein Rab-27A (RAP27a) , which also primes the granules for the fusion with the inner leaflet of the membrane at the synapse together with MUNCH13-4 (Ménager et al., 2007; Stinchcombe et al., 2001). The final fusion and granule release are coordinated by the target synaptosome-associated protein receptor (t-SNAREs) vesicle associated membrane protein 7 (VAMP7) and syntaxin11 and vesicle synaptosome-associated protein receptor (v-SNARE) member syntaxin7 (Arneson et al., 2007; Casey, Meade, & Hewitt, 2007; Marcet-Palacios et al., 2008).

Finally, the termination stage includes detachment of the target cell and restoration of lytic capability. McCann et al. demonstrated that the lytic cleft between NK and target cell remains stable up to 45min after conjugation. This might be necessary to increase the concentration of lytic molecules in the synaptic cleft and for protection of neighboring cells (McCann, Eissmann, Onfelt, Leung, & Davis, 2007). After fulfilling the lytic activity the NK cell detaches and refills its lytic granules, although the mechanism of the process is still elusive (Orange, 2008).

#### Lytic granules and death receptor pathway

NK cell cytotoxicity can be executed via two different pathways, one containing the release of lytic granules containing perforin and granzyme and the other via death ligands TNF-related apoptosis-inducing ligand (TRAIL) and FasL (Prager & Watzl, 2019). Both pathways will be described in the following section.

Granules filled with lytic proteins contain the pore-forming molecules perforin and granulysin as well as the serine protease family members granzyme A, B, K, M and H. Granzymes are stored as proenzymes which reach their active form when released

from the acidic granules in pH-neutral surroundings in the synaptic cleft (Griffiths & Isaza, 1993; Krzewski & Coligan, 2012). Ambrose and colleagues suggested granule release as supramolecular attack particles (SMADs), containing a core of granzymes, perforins, serglycan proteoglycans and galectin-I encased by the Ca<sup>2+</sup> binding glycoprotein thrombospondin-1. This mechanism might support the function of the synaptic cleft (Ambrose, Hazime, Worboys, Niembro-Vivanco, & Davis, 2020). When the content of the granules is released, granzymes are received by the target cell through a perforin-dependent mechanism. Perforins are glycoproteins and are able to insert polymerized perforin-pores into bilipid layer membranes in the presence of Ca<sup>2+</sup>. However, two different theories about the granzyme uptake are that there is either a direct uptake via the perforin-pores, or there is a Ca<sup>2+</sup> influx through perforin-micropores in the target cell and rapid dynamin-dependent endocytosis of membrane-bound granzymes (Hay & Slansky, 2022; Keefe et al., 2005; Voskoboinik, Whisstock, & Trapani, 2015). NK-cells do have perforin protecting mechanisms leading to decreased perforin binding, such as the translocation of lysosomal protein CD107a (lysosomal-associated membrane protein 1 (LAMP-1)) to the membrane during degranulation, an increased plasma membrane lipid order and a negatively charged membrane surface caused by phosphatidylserine (Cohnen et al., 2013; Y. Li & Orange, 2021; Rudd-Schmidt et al., 2019). Granzyme B (grzB) is the best researched and most cytotoxic granzyme within the family. Once inside the target cell, grzB has the ability to cleave caspase-3/7, BH3 interacting domain death agonist (BID), inhibitor of caspase-activated DNase (ICAD), Lamin B, DNA-dependent protein kinase (DNA-PK), poly (ADP-ribose) polymerase (PARP),  $\alpha$ -Tubulin and Gasdermin-D (GSDMD), which triggers apoptosis, DNA-degradation, structural integrity and pyroptosis (Andrade et al., 1998; Chowdhury & Lieberman, 2008; Cullen & Martin, 2008; Metkar et al., 2003; Sharif-Askari et al., 2001; Thomas, Du, Xu, Wang, & Ley, 2000; Voskoboinik et al., 2015; D. Zhang, Beresford, Greenberg, & Lieberman, 2001). An overview of all granzymes, substrates and cellular effects are listed in Table 2.

**Table 2** Overview of human granzymes and their substrates. Adapted from (Hay & Slansky, 2022)

Granzyme	Known substrates	
A	Gasdermin B, SET, pro-IL-1 $\beta$ , NDUFS3, histone H1, HMGB2, Apel	Activate and release pro-inflammatory cytokines from target cell, caspase-

		independent cell death, pyroptosis
B	Pro-caspase 3, pro-caspase 7, Pro-caspase 8, Bid, ICAD	Canonical apoptosis
K	SET, $\beta$ -tubulin, APE	Single-stranded DNA-damage, mitochondrial dysfunction, cell membrane damage
M	Nucleophosmin, FADD, surviving, ICAD, $\alpha$ -Tubulin	Caspase-dependent and -independent apoptosis, microtubule disruption
H	ICAD, viral proteins (L. Wang et al., 2012)	Conflicting results are published, but cytotoxic function was observed (Fellows, Gil-Parrado, Jenne, & Kurschus, 2007; Hou et al., 2008)

In addition to the described granzyme-induced target cell death, death receptor pathway can be triggered by NK cell released TRAIL and FasL. FasL is a type II transmembrane protein, but is stored in granules and is therefore dependent on degranulation for surface expression (Bryceson, March, Barber, Ljunggren, & Long, 2005). Degradation leads to a rapid LFA-1 mediated diffusion in the plasma membrane within the immunological synapse (D. Liu et al., 2009). Once expressed on the NK cell surface, FasL binds CD95 of the attached target cell, inducing the intracellular apoptotic cascade (Peter & Krammer, 2003). Just as FasL, TRAIL is stored in granules, however the type of granules as well as the exact trigger inducing expression associated to the synaptic cleft remains unclear (Prager & Watzl, 2019). From the cell surface, TRAIL can also be shed to a soluble form, resulting in the same receptor binding capacity as the membrane bound form. At the target cell, TRAIL can bind to TRAIL-R1/2 resulting in apoptosis signaling, or TRAIL-R3/4 and osteoprotegerin triggering nuclear factor k-light-chain-enhancer of activated B cells (NF- $\kappa$ B) signaling (von Karstedt, Montinaro, & Walczak, 2017).

For the kinetics of the described cytolytic pathways, it is described that granzymes can trigger target cell death within minutes after NK cell contact, while death receptor mediated killing takes about 1-2 hours (J. Li et al., 2014). Explanations could be, either a different timing of surface exposure, or divergent amounts of molecules necessary



for killing (Bryceson et al., 2005; Gwalani & Orange, 2018). Additionally the signaling cascade inside the target cell could differ (Prager & Watzl, 2019).

## Cell death pathways

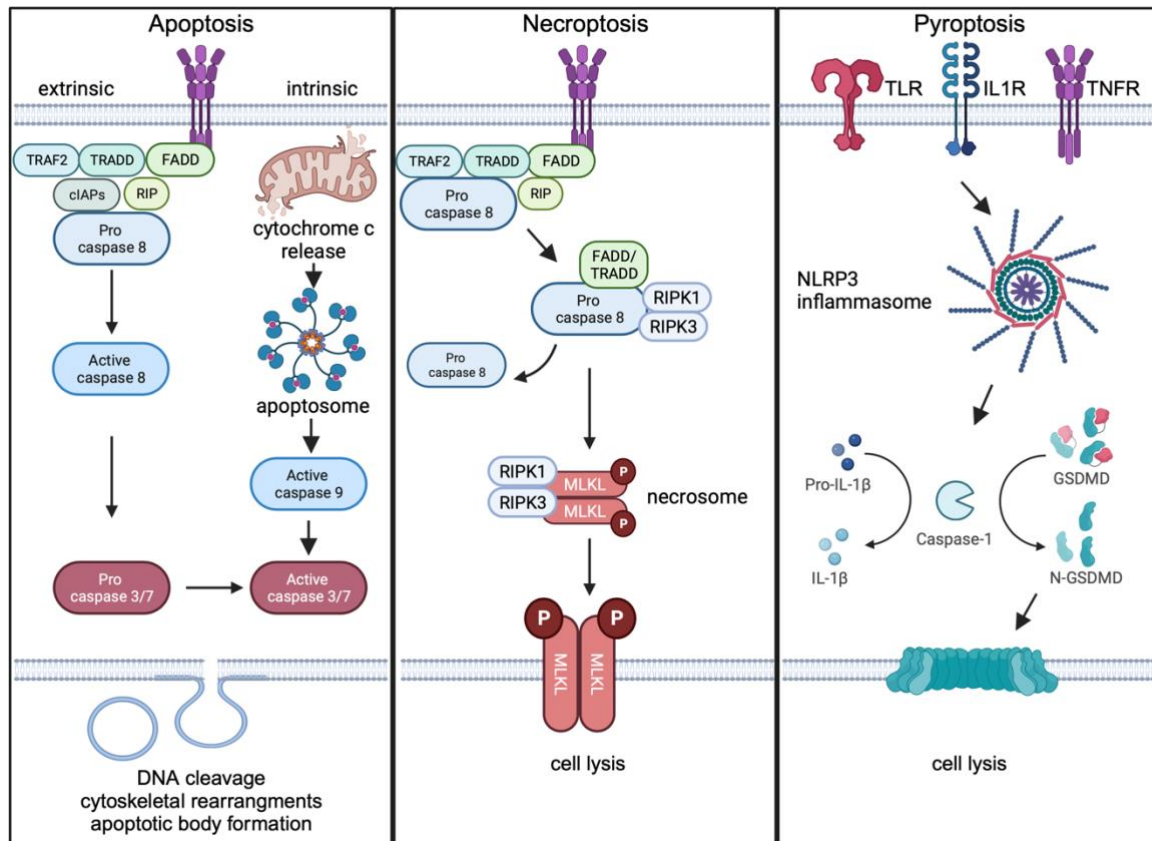


**Figure 4** Overview of characteristic features of the cell death pathways. **Apoptosis:** Extrinsic apoptosis is triggered by activation of a death receptor, which promotes assembly of TRADD, TRAF2/5, cIAP1/2, and ubiquitinated RIPK1, leading to pro-caspase 8 cleavage and activation. Intrinsic apoptosis is defined by the release of cytochrome c from mitochondria, formation of a multiprotein apoptosome, and activation of caspase-9. Caspase-8/9 proteolytically activate caspase-3/7, which promotes cell death. **Necroptosis:** Necroptosis is characterized by activation of a death receptor, and complex formation as in extrinsic apoptosis. Inhibition of pro-caspase-8 activation allows formation of the RIPK1-RIPK3 necrosome, which phosphorylates MLKL. Phospho-MLKL monomers and cell lysis occurs with additional DAMPs released. **Pyroptosis:** Following NLRP3 inflammasome oligomerization and activation, caspase-1 proteolytically processes GSDMD for activation. GSDMD polymerizes into a plasma membrane pore. By osmosis, water enters the cell, causing cellular swelling, and cell lysis.

Adapted from Favor, 2021. Created with BioRender.com.

Cell death in an organized manner is essential for the removal of damaged cells without further damage for the whole organism. Depending on the trigger and intracellular signaling, cells do have various ways of programmed cell death. In the following passage, the pathways for apoptosis, necroptosis and pyroptosis, which can be triggered with NK cell mediated killing will be described (Figure 4).

## Apoptosis

Mechanistically, apoptosis can be triggered by intracellular disbalance, toxic agents or DNA damage, leading to intrinsic apoptosis, or by death receptor ligands for TNFR, Fas or TRAILR, resulting in extrinsic apoptosis (Gon, Gatanaga, & Sendo, 1996; Itoh et al., 1991; X. Liu, Kim, Yang, Jemmerson, & Wang, 1996; Suliman, Lam, Datta, & Srivastava, 2001).

Intrinsic apoptosis is caused by granzyme release inside the cell, which results in mitochondrial outer membrane permeabilization (MOMP) and cytochrome c release. The pro-apoptotic proteins B-cell lymphoma 2 (Bcl-2) family members Bcl-2 homologous antagonist/killer protein (BAK) and Bcl-2-associated X protein (BAX) support cytochrome c release via oligomerized BAX/BAK pores in the mitochondrial membrane with the promotion of further family members BCL2-Like 11 (BIM), BID, p53 upregulated modulator of apoptosis (PUMA), BCL2 associated agonist of cell death (BAD), phorbol-12-myristate-13-acetate-induced protein (NOXA) and BCL2 interacting killer protein (BIK) (Kuwana et al., 2002; Nakano & Vousden, 2001; O'Connor et al., 1998; K. Wang, Yin, Chao, Milliman, & Korsmeyer, 1996). The apoptotic response is fine-tuned with anti-apoptotic proteins BCL-2, B-cell lymphoma-extra large (BCL-XL), myeloid leukemia 1 (MCL-1) (Cheng et al., 2001; Choudhary et al., 2015). MOMP and cytochrome c release additionally lead to formation of the apoptosome, consisting of cytochrome c, dATP, pro-caspase 9 and apoptosis protease activation factor 1 (APAF-1) (Cain, Brown, Langlais, & Cohen, 1999). Upon assembly, pro-caspase 9 is activated by cleavage and causes activation of pro-caspases 3 and 7, creating an amplified apoptosis signaling cascade (P. Li et al., 1997). Regulation can further be executed with caspase 3 inhibition by inhibitors of apoptosis protein 1/2 (IAP1/2) and X-linked inhibitor of apoptosis protein (XIAP), which also tightly regulates the function of caspases 7 and 9 (Bratton et al., 2001).

Extrinsic apoptosis is triggered by ligand binding to the death receptors, leading to receptor oligomerization on the membrane surface (Micheau & Tschopp, 2003; Vanden Berghe et al., 2004). This process recruits the adaptor proteins FAS-associated death domain protein (FADD) and tumor necrosis factor receptor type 1-associated death domain (TRADD), which build the death inducing signaling complex (DISC) together with the activated caspases 8 and 10 (J. Wang, Chun, Wong, Spencer, & Lenardo, 2001). Proteins for the regulation of the process are FADD-like ICE-like Inhibitory Protein (FLIP) and receptor-interacting serine/threonine-protein kinase 1

(RIPK1) and are included in the DISC. During early stages of activation FLIP and RIPK1 limit apoptotic function of the complex, whereas later these regulatory proteins are detached (Schneider-Brachert et al., 2004; Zheng et al., 2006). Subsequently, active caspases 8 and 10 activate downstream executor caspases 3, 6 and 7 and generate positive feedback via BID to promote MOMP (Seol DW, 2001).

### Necroptosis

The necroptosis cell death pathway is triggered by  $\text{TNF}\alpha$  via tumor necrosis receptor (TNFR1), by death receptors or Toll like receptors (TLR3/4) and additional inhibition of caspase 8 (He, Liang, Shao, & Wang, 2011; Holler et al., 2000). Following receptor activation, a complex consisting of FADD, RIPK1, caspase 8/10 is formed and in case of inactive caspase 8, RIPK3 is recruited resulting in the ripoptosome complex (J. Li et al., 2012; Tenev et al., 2011). In this early stage, RIPK1/3 are tightly regulated by ubiquitination via tumor necrosis factor receptor-associated factor 2/5 (TRAF2/5) and IAP/XIAP, which inhibits the cell death function and initiates  $\text{NF}\kappa\text{B}$  dependent pro-inflammatory signaling (Ermolaeva et al., 2008; H. Li, Kobayashi, Blonska, You, & Lin, 2006; Pobeziinskaya et al., 2008). Formation of the ripoptosome leads to the recruitment and activation of mixed lineage kinase domain-like protein (MLKL), building the necroptosome, which includes RIPK1/3 and MLKL (Murphy et al., 2013). With the phosphorylation of MLKL, necroptosomes oligomerize, and assembled MLKL translocate to the cell membrane. In combination with tight junction proteins, small pores are built leading to ion influx, cell swelling and rupture (X. Chen et al., 2014; Samson et al., 2020).

### Pyroptosis

This inflammatory form of cell death is triggered by intracellular sensors (nucleotide-binding domain, leucine rich containing protein (NLR)-family, absent in melanoma 2 (AIM2), pyrin receptors) detecting pathogen/damage-associated molecular patterns (PAMPs, DAMPs), osmotic disbalance, ion influx or membrane disturbance, among others (Bertheloot, Latz, & Franklin, 2021). After activation, the adaptor protein apoptosis-associated speck-like protein containing a CARD (ASC) supports the formation of the NLR Family Pyrin Domain Containing 3 (NLRP3) inflammasome, which is a platform for activation of pro-caspase-1 (Boucher et al., 2018). Caspase 1 processes and activates pro-forms of the cytokines  $\text{IL-1}\beta/\text{IL-18}$  and the pyroptosis

effector gasdermin D (GSDMD). However, GSDMD can also be cleaved by caspases 4/5 and 11 (Shi et al., 2015). Active GSDMD oligomerizes and introduces cell death with pore formation in the cell membrane (X. Liu et al., 2016).

### Crosstalk

Despite describing the cell death pathways independently, an important factor of cell fate determination is the crosstalk between those pathways. Some examples will be described in this section. At different branches of the signaling cascades, other cell death pathways can be triggered or inhibited. For instance, the activation status of caspase 8 in the DISC complex and the ripoptosome is critical for apoptosis and necroptosis, and additionally contributes to the activation of NLRP3 and direct cleavage of GSDMD (Demarco et al., 2020; Fritsch et al., 2019; Gurung et al., 2014). Additionally, inhibition of single proteins during cascades usually lead to a switch towards another cell death pathway. For example, absence of GSDMD leads to a caspase 1 dependent activation of caspase 3/9/BID dependent apoptosis (Tsuchiya et al., 2019). However, those were just some limited examples, the bigger picture might be much more complicated, as even a form of cell death including features of apoptosis, pyroptosis and necroptosis, called PANoptosis was described (Malireddi et al., 2020).

### **NK cells in lung cancer**

In human lungs NK cells make up for about 10% of the lymphocyte population, a value that is comparable to that in peripheral blood (PB) (Dogra et al., 2020). Nevertheless, lung resident NK cells show a less differentiated phenotype and lower cytotoxicity to enable a tight regulation in the tissue. In contrast to NK cells present in PB, lung NK cells are considered as CD16<sup>-</sup>, even despite the fact that express KIR receptors, which are typically absent in CD16<sup>-</sup> NK cells (Brownlie et al., 2021). However, non-residential NK cells show the same phenotypical distribution as the PB NK cells (Marquardt et al., 2017).

The prognostic value of NK cells in lung tumor has not been clarified to date, although it was shown that a NK cell gene signature within the tumor leads to a better overall survival (Habif et al., 2019; Larsen et al., 2014; Takanami et al., 2001). In general lung tumors exhibit a low infiltration of NK cells, which are mainly found at the edges of the tumor, indicating a deficient recruitment (Platonova et al., 2011). Cong et al.

demonstrated the importance of timing, as the depletion of NK cells in a Kras-driven mouse lung cancer model prevented the tumor initiation but did not inhibit tumor progression (Cong et al., 2018). Overall, the importance of NK cells in anti-tumor immunity is indisputable, but during tumor progression cancer cells escape their cytolytic function with various mechanisms.

## **Immune escape of cancer cells**

Several mechanisms can lead to a cancer cell escape of the cytolytic NK cell function. Common strategies are the secretion of factors like transforming growth factor beta (TGF $\beta$ ), prostaglandin E2 (PGE2), Indoleamine-pyrrole 2,3-dioxygenase (IDO) or interleukin 10 (IL-10), which lead to reduced NK cell activity, and the down- or upregulation of NK cell ligands. In this section the focus will be on the changes of ligand expression levels on tumor cells.

Cancer cells commonly downregulate HLA-ABC expression to escape T-cell cytotoxicity (Catalan et al., 2015). However, to additionally inhibit NK cell effector function, MHC-Ib molecules such as HLA-E/-G are frequently upregulated (Andre et al., 2018; da Silva, Montero-Montero, Ferreira, & Quintanilla, 2018). As some tumors also downregulate HLA-ABC to escape T-cells, the mechanisms are potentially adapted to the effector immune cell (Barkal et al., 2018). Additionally, it was shown that decreased MHC-I on tumor cells can induce upregulation of the inhibitory NK cell receptor T cell immunoglobulin and mucin domain-containing protein 3 (TIM3) (Seo et al., 2017). The upregulation of inhibitory ligands (poliovirus receptor (PVR), CD155) for the immunoglobulin superfamily receptors (Table 1) is associated with tumor progression, whereas the blocking of T Cell Immunoreceptor With Ig And ITIM Domains (TIGIT) can promote NK cell cytotoxic effects (Johnston et al., 2014; Q. Zhang et al., 2018). In lung cancer there is typically an overexpression of bromodomain PHD finger transcription factor gene (BPTF) leading to a decrease in cell surface heparan sulfat proteoglycans, which are ligands for the activating NCRs (Buganim et al., 2010; Mayes et al., 2017). An overexpression of galectins was also described as a tumor escape mechanism via different pathways. Galectin-1 can inhibit NK cell recruiting to the tumor, galectin-3 directly inhibits NKp30 and reduces the MHC class I polypeptide-related sequence A (MIC-A) affinity for NKG2A, whereas galectin-9 decreases NK cell cytotoxicity in a TIM3 dependent manner (Baker et al., 2014; W. Wang et al., 2014; Yasinska et al., 2019).

As described, there are multiple unrelated ways for tumor cells to escape NK cell cytotoxicity and understanding and overcoming them is a key challenge in cancer research and therapy.

## Aim

The aim of this work was the establishment of a co-culture system to identify key mechanisms that govern NK-cell - tumor cell interactions. Given the importance of the cell death machinery for NK cell killing of tumor cells I specifically focused on cell death pathways and factors which might contribute to tumor cell vulnerability or resistance.

# Results

## Evaluation of the co-culturing method

For an investigation of NK cell mediated killing of tumor cells, a co-culture system for 2D and 3D was developed (Figure 5A). A heterogeneous panel of lung cancer cell lines (n=19), as well as the established NK cell target lymphoma cell line K562 were used (Pech et al., 2019; X. Song et al., 2020). The cell lines revealed formation of spheroids in ultra-low attachment plates in the time course of 24 hours (h). Histological sections revealed a dense morphology of the tumor spheroids with a structural demarcation. After 4h of tumor cell co-culturing with NK-92, the NK-cells clustered around the tumor spheroid and invasion was observed (Figure 5C). During real time imaging, clustering and invasion were noticed after 1h to 4h.

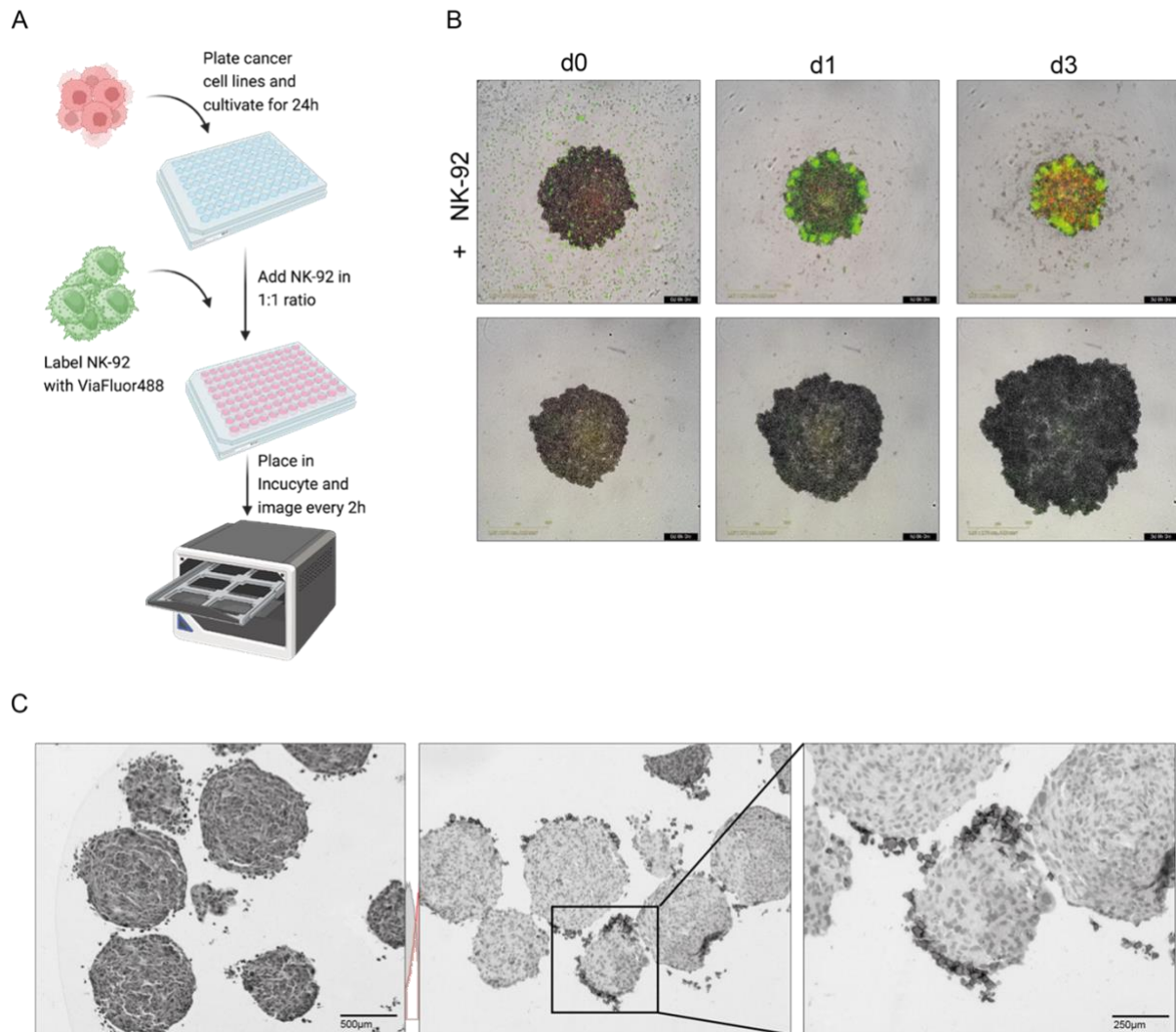


**Figure 5** Characterization of the NK-92/tumor cell co-culture system. A) Schematic overview of the co-culture workflow. B) Spheroids of the PC9 cell line with and without NK-92 cells in a 1:1 ratio at different time points, imaged with the Incucyte. Green: NK-92, red: DRAQ7 labeled dead cells. C) Histological sections of spheroids generated from H1975. Left: H&E staining of the tumor spheroid only. Middle and right: 4h Co-culture, CD56 staining for NK-92 cells (shown in black).



NK-92 cell co-culture led to tumor spheroid shrinkage in 3D, decreased cell numbers in 2D and dead tumor cells, visible after 24h with no further progression after 72h (Figure 5B).

As NK cell invasion and decreased tumor cell growth was observed, the surface expression of the common degranulation marker LAMP-1, as well as secreted factors were analyzed to assess NK cell activation. Indeed, an increase of LAMP-1 was measured after 4h, which was back to baseline levels after 24h (Figure 6A). Amounts of secreted perforin, granzyme B and the pro-inflammatory cytokine IFN $\gamma$  were elevated after 24h of co-culture with the tumor cell line PC9 (Figure 6B).

The short-term ascent of cell-surface LAMP-1 indicated a rapid NK cell activation with decrease overtime, whereas the delayed accumulation of perforin and granzyme B might be caused due accumulation in the supernatant in the course of multiple killing events (Ham, Medlyn, & Billadeau, 2022).

In summary, this data indicated, that during co-culture not only NK cell invaded the tumor spheroid and tumor cell numbers decreased, but also NK cells degranulated granzyme B and perforin.

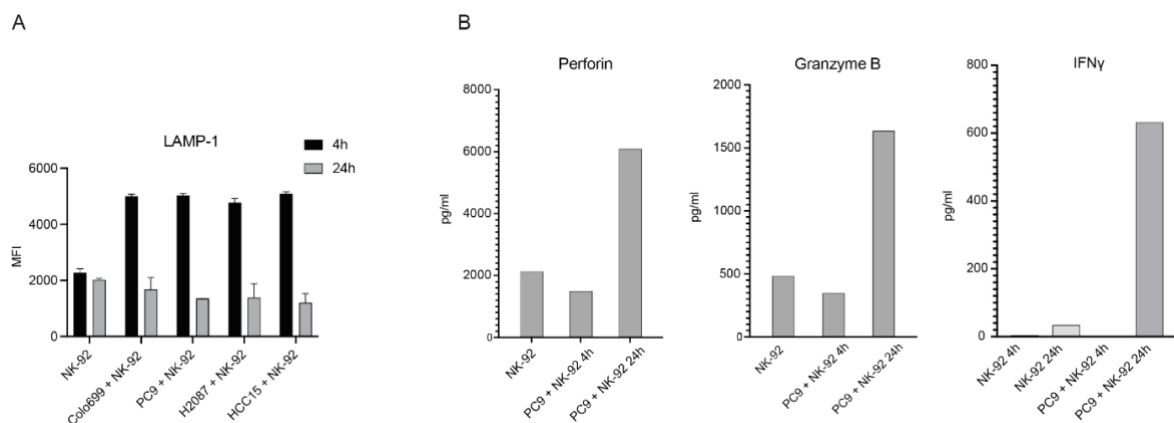


**Figure 6** NK-92 show activation markers during co-culture with human lung cancer cell lines. A) Median fluorescence intensity of LAMP-1 for CD45+ cell population in co-culture (n=3) B) Perforin, granzyme B and IFN $\gamma$  levels in medium supernatant of co-culture (n=1).

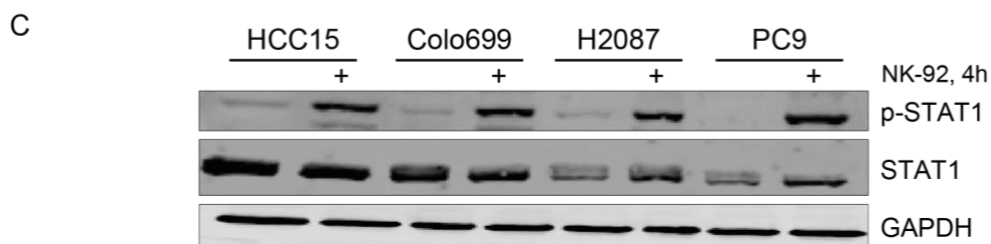
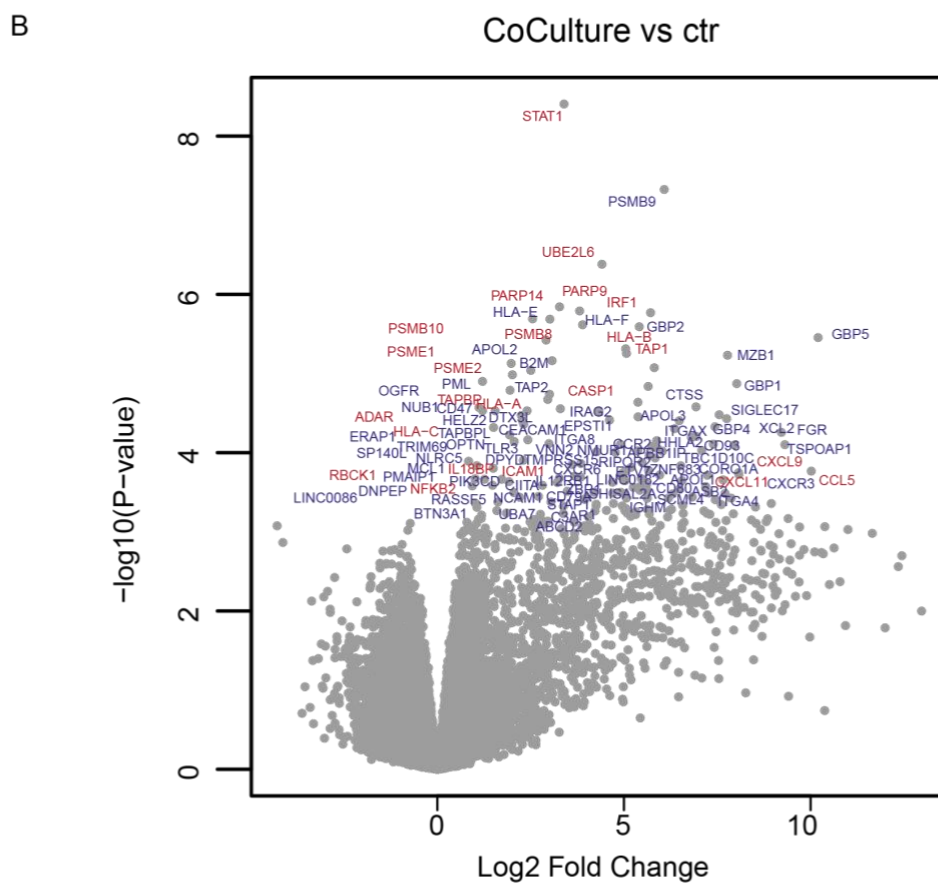
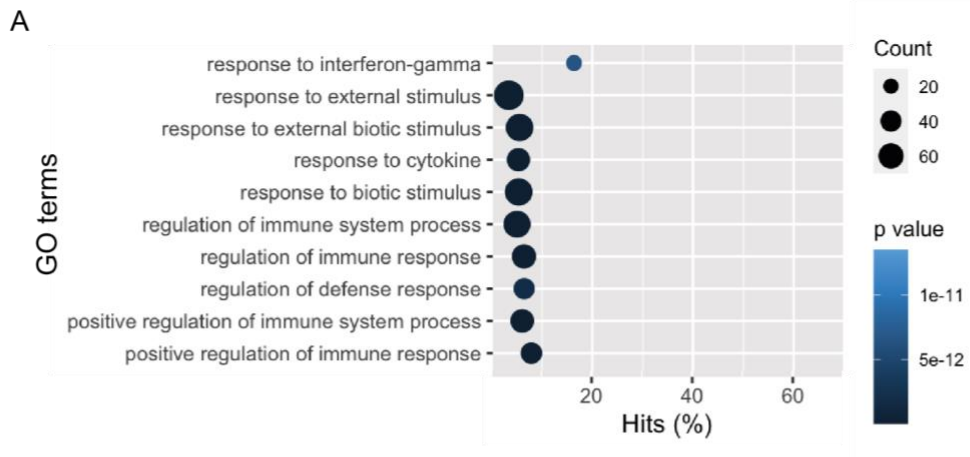
To investigate the overall effect of NK-92 co-culture on the transcriptome of tumor cells, I performed RNA sequencing of co-cultured cancer cell lines PC9 and Colo699. As expected, the sequencing results revealed a strong enrichment of immune response, when co-cultured cell lines were compared with their baseline expression. Of the top 20 enriched GO terms, 15 were directly involved in the innate or adaptive immune response, whereas the remaining 5 were very loosely associated with cellular response to an external stimulus. In the following passages, a few of those upregulated GO terms will be further discussed (Figure 7A).

Upon activation, NK cells secrete IFN $\gamma$  among other cytokines and consequently the response to IFN $\gamma$  and cytokines was enriched in tumor cells (Figure 6B, Figure 7A). Following IFN $\gamma$  release, the pro-inflammatory Janus kinase (JAK)/ signal transducer and activator of transcription (STAT1) pathway is activated in the target cell, which was confirmed via detection of p-STAT1 (Figure 7C) and reflected by the top hit *STAT1* in the list of differentially expressed genes (DE genes), as the feedback loop of STAT1 activation leads to *STAT1* transcription (Figure 7B) (Negishi, Taniguchi, & Yanai, 2018). Despite *STAT1*, several target genes of IFN $\gamma$  signaling were upregulated, such as *guanylate binding protein 2 (GBP2)*, *PARP9* and *proteasome subunit beta type-8 (PSMB8)*. Additionally, the release of cytokines is triggered by IFN $\gamma$ . *CXCL9/11*, which attracts activated T-cells, as well as *CCL5* were indeed upregulated in the tumor cells (Tokunaga et al., 2018). However, also the negative regulator of interferon response *NLRC5* was upregulated.

Upregulation of MHC-I members *HLA-A, B, C, E* and *F* could have adverse effects and might cause immune escape as well as further NK cell activation (Niehrs & Altfeld, 2020).

Moreover, the ligand *ICAM1* was upregulated, which is essential for NK-cell interaction with adhesion protein LFA-1. On the other hand, NK cell inhibiting factors *FGR*, *carcinoembryonic antigen-related cell adhesion molecule (CEACAM1)* and *HERV-H LTR-associating protein 2 (HHLA2)* were upregulated as well. Among them *FGR* acts as a general negative regulator of activating receptors and IFN $\gamma$  production, whereas *CEACAM1* inhibits *NKG2D* and *VAV1* activation and *HHLA2* acts as an inhibitory ligand for *KIR3DL3*.

Some components of cell death pathways were also upregulated upon co-culture. The pro-apoptotic MCL-1 degrader *PSMB8*, which additionally promotes activation of caspases, was upregulated. Interestingly, the expression of the anti-apoptotic counterpart *MCL-1* was increased as well. The upregulated factors *GBP5* and *ZBP1* encoded proteins are essential for the assembly of the pyroptosis-initiating *NLRP3* inflammasome, and act similarly to upregulated *Caspase 1*, as pro-inflammatory effectors. *ZBP1* is not only involved in pyroptosis, but can stimulate *RIPK3* and *RIPK1* dependent caspase 8 activation and is consequently jointly responsible for crosstalk between the cell death pathways (Muendlein et al., 2021; Shenoy et al., 2012).



In summary, co-culture of NK-92 and lung cancer cell lines led to an upregulation of IFN $\gamma$  response and target genes, various receptors with NK cell activating and inhibiting

function (e.g. ICAM1, HHLA2), and of general innate immune response (e.g. STAT1, CXCL9/11).

The increase of mainly apoptotic and pyroptotic pathway members in the list of differentially expressed genes indicated ongoing cell death, which was examined in the next step.

**Figure 7** RNA sequencing of co-cultured cancer cell lines PC9 and Colo699 revealed a strong activation of immune response. A) Top enriched GO terms in co-culture condition versus baseline. B) Differentially expressed genes in co-culture condition versus baseline. Red: genes included in the gene set interferon gamma response. C) Western blot of STAT1 activation in HCC15, Colo699, H2087 and PC9 upon 4h of NK-92 co-culture.

To investigate cancer cell vulnerability towards NK cells, a panel of human lung cancer cell lines and the lymphoma target cell line K562 were co-cultured with NK-92. The observed decrease of tumor cells in co-culture was quantified and revealed sensitivities towards NK-92 mediated killing between 28% and 85% (Figure 8A). In general, cancer cell vulnerability was higher in 2D than in 3D, which could be explained by the better accessibility of target cells in a 2D setting. The average increase between killing in 3D versus 2D was about 28%, but as killing rates significantly correlated for both systems the following experiments were performed in 2D (Figure 8B). However, for both systems, NK-92 revealed cytotoxicity against most of the cell lines and interestingly the sensitivities largely varied between lung cancer cell lines.

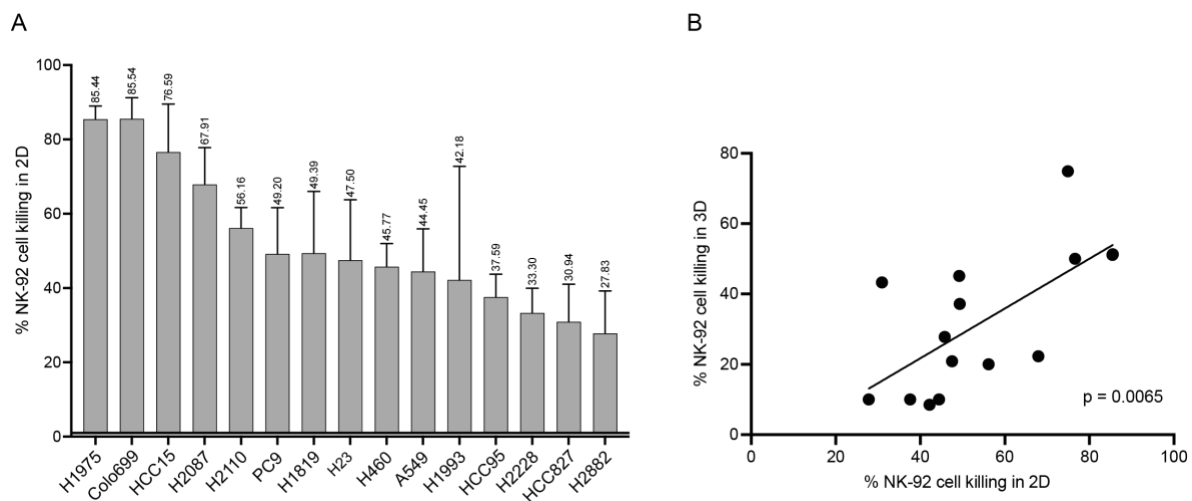


**Figure 8** Sensitivities towards NK-92 cell killing varied largely between cell lines. A) NK-92 cell killing of various lung cancer cell lines (and lymphoma cell line K562) after 72h of co-culture. B) Pearson correlation of NK-92 cell killing of lung cancer cell lines in 2D versus 3D.

## How do tumor cells die?

Shortly after co-culturing of NK-92 and tumor cells, caspase 8 cleavage was observed across cell lines, indicating extrinsic apoptotic signaling (Figure 9A). Cell lines differed in total protein levels for caspase 8, which was not associated with sensitivities. To evaluate the influence of caspase 8 as cell death initiator in co-culture, a caspase 8 knockout was generated for the PC9 cell line (PC9<sup>Casp8ko</sup> cells) (Figure 9B). Interestingly, the caspase 8 knockout did not completely rescue NK cell mediated killing, but decreased it significantly by about 40% (Figure 9C). With a knockdown of the death receptors FAS or TNFR a reduction of cell death between 15% and 50% was reached (Figure 9D).

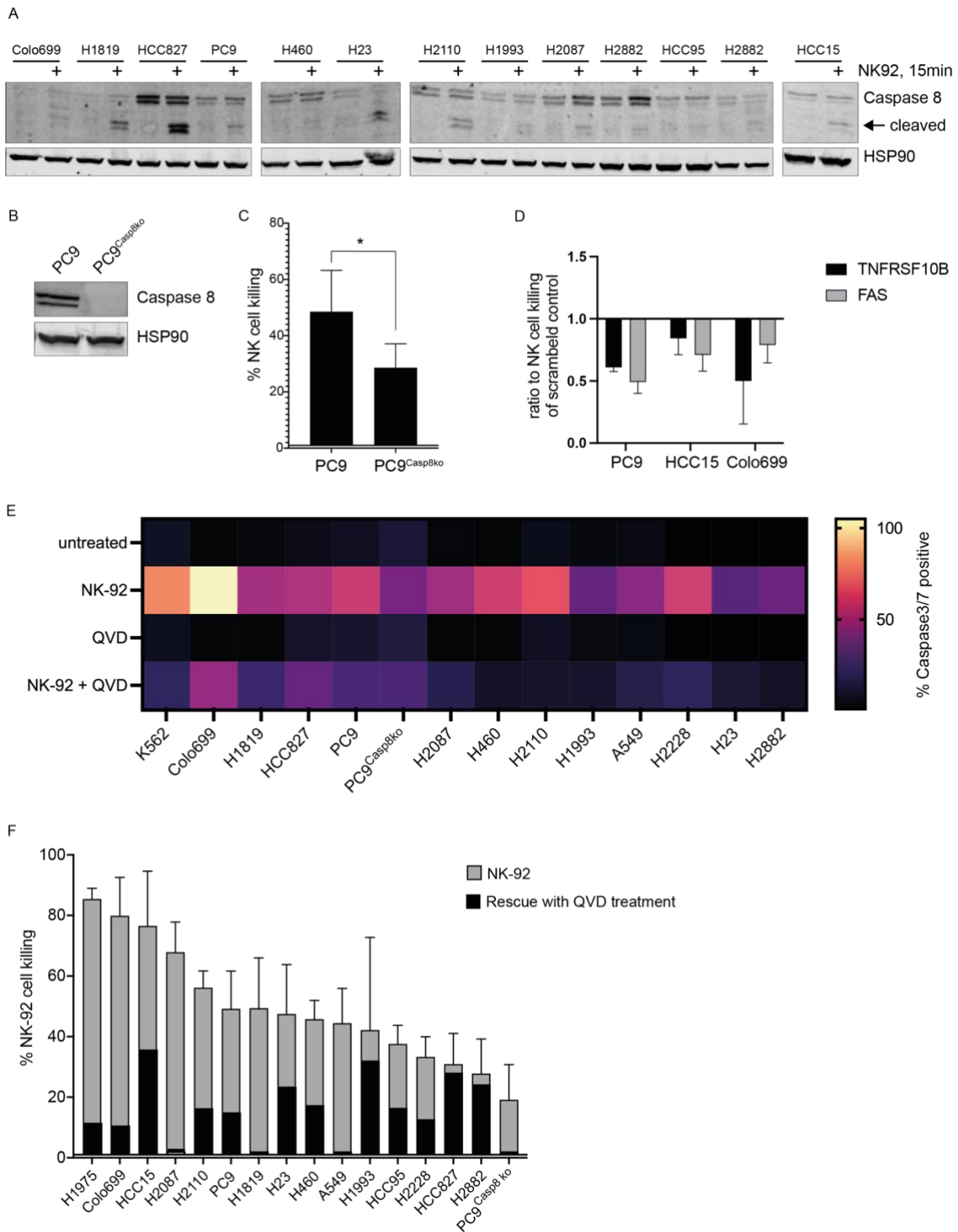


**Figure 9** Lung cancer cell lines undergo apoptosis following NK-92 co-culture with a partial rescue for pan-caspase inhibition. A) Caspase 8 cleavage in lung cancer cell lines after 15min of co-culture with NK-92. B) Verification of caspase 8 knockout in PC9 on protein level. The knockdown decreased NK-92 mediated killing about 40%. C) Knockdown of TNFR or FAS decreased NK cell killing in the cell lines PC9, Colo699 and HCC-15. D) Caspase 3/7 activation upon 24h of co-culture with NK-92 with and without pan-caspase inhibition. E) Grey bars: Percentage of NK-92 mediated killing of the tumor cell line. Black bars: Percentage of rescue with pan-caspase inhibition; remaining grey area shows the remaining killing.

These results highlight the importance of extrinsic apoptosis and the caspase 8 downstream pathway for tumor cell death upon NK cell contact. Following co-culture, not only caspase 8 was cleaved, but downstream effector caspases 3 and 7 were strongly activated as well (Figure 9E). A gradient was observed, the more NK-92 sensitive the cell lines were, the more caspase 3/7 cleavage was detected. Additionally, in the PC9<sup>Casp8ko</sup> cells caspase 3/7 was slightly activated, suggesting ongoing apoptosis despite absent caspase 8.

With the pan-caspase inhibitor Q-VD-OPh (QVD)<sup>1</sup> caspase 3/7 activity was strongly decreased, but not blocked completely in co-culture across different cell lines. Regarding killing effects, QVD treatment limited cell death induction during co-culture, but did not lead to a full rescue for any of the tested cell lines (Figure 9F). The effect of QVD pretreatment in PC9 cells was comparable to the effect of the caspase 8 knockout, whereas the caspase inhibition had no additional effect for the PC9<sup>Casp8ko</sup>. Concurrently, crosstalk with the necroptosis pathway, involvement of pyroptosis or granzyme dependent cleavage of downstream caspases could contribute to the remaining killing events.

To investigate the effect of necroptosis-dependent killing events, the RIPK1 inhibitor Necrostatin1 (Nec1) or RIPK3 inhibitor GSK872, which also blocks RIPK1-independent necroptosis, were used. Those inhibitors only showed minor effects of 5% to 15% of rescue in some cell lines (Figure 10A). However, cell death pathways can rapidly switch to apoptosis in the case of necroptosis blockade. When Nec1 or GSK872 were combined with QVD treatment, for most cell lines there was a small additional effect (1-5%) regarding cell death prevention. However, even upon inhibition of major components of the apoptosis and necroptosis pathway, cell death induction only decreased by 10% to 50%. Interestingly, Nec1 or GSK872 had no effect in the PC9<sup>Casp8ko</sup> cell line. The results indicate that a substantial part of cell death might be executed via pyroptosis or alternative pathways.

Initial cleavage of caspase 8 was not prevented by QVD treatment and as the result of necroptosis inhibition suggested, p-MLKL upon co-culture with NK-92 was only observed for H2087 (Figure 10B). This was also one of the cell lines (H2087, H1819) revealing a stronger additional effect of the QVD and GSK872 combinatory treatment (Figure 10A). Necroptosis did not seem to be a major cell death path for most cell lines, not even to escape pan-caspase inhibition. Caspase 1 activation was observed across

---

<sup>1</sup> QVD is known to inhibit caspases 1, 3, 8 and 9 (Caserta, Smith, Gultice, Reedy, & Brown, 2003)

cell lines, whereas only H2087 showed an increase following QVD treatment (Figure 10B). However, the assessment of additional markers like the pyroptosis effector protein gasdermin D may be helpful to further define cell death pathway distribution. Overall the NK-92 co-cultured cell lines exhibited features of apoptosis and pyroptosis with a few additional components of necroptosis, although in general necroptosis seemed to play a minor role. Nevertheless, the more susceptible cell lines were for NK cell killing, the further the activation of apoptosis effector caspases 3/7 increased. Although on protein level no major differences in activation of caspase 8, 1 or p-MLKL were found.

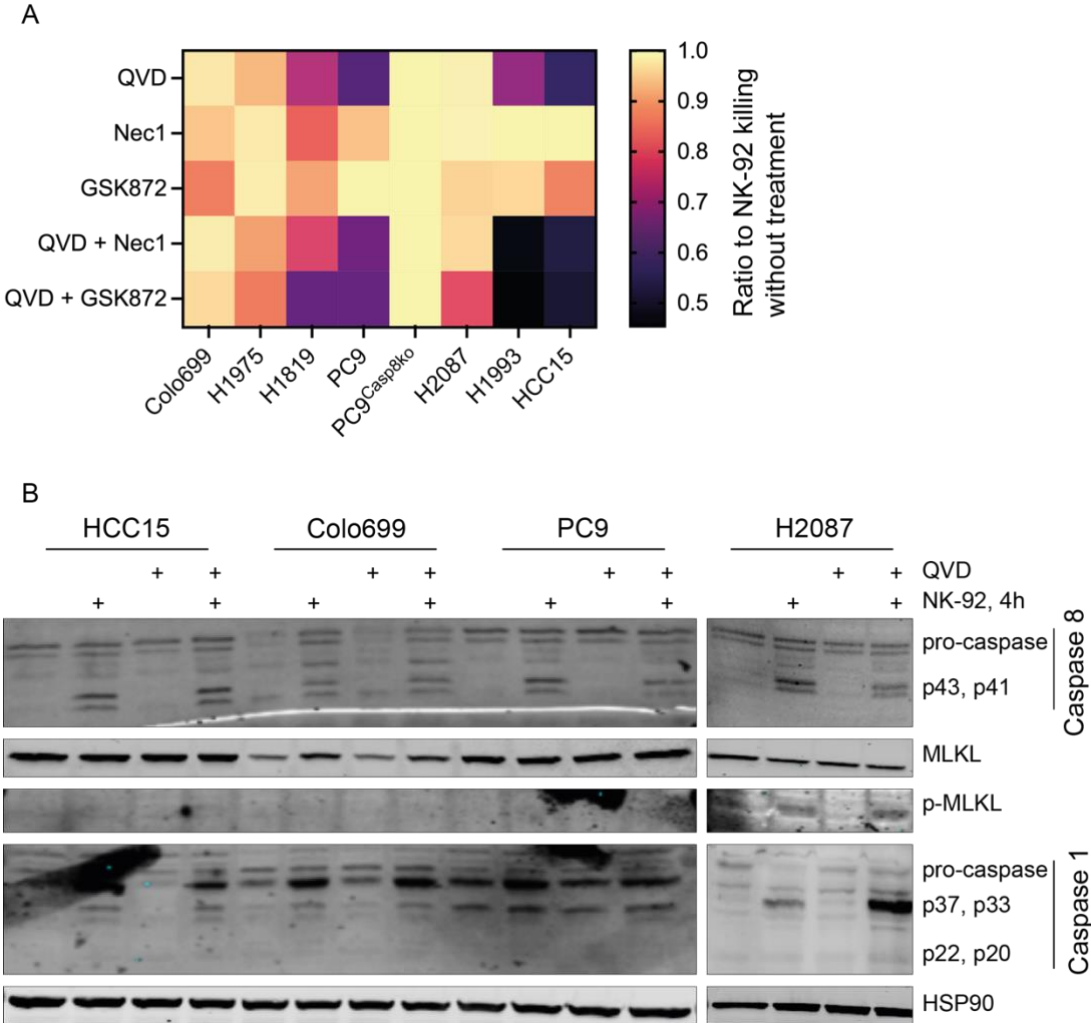


**Figure 10** Cancer cell death upon NK-92 co-culture showed features of apoptosis, pyroptosis and for the cell line H2087 necroptosis as well. A) Effect of pan-caspase-inhibition, RIPK1/3-inhibition and their combination on NK-92 mediated killing of tumor cells. B) Cleavage of caspase 8 and caspase 1 was featured in tested cancer cell lines following 4h of co-culture with NK-92, whereas phosphorylation of MLKL was only observed for H2087.



To further investigate the context of tumor cell vulnerability towards NK-92 and the amount of cell death inhibition with QVD, I compared these parameters using Pearson correlation. Interestingly, the correlation of tumor cell sensitivity towards NK-92 and rescue with QVD treatment was significant ( $p=0.003$ ), so the more sensitive the cell line, the smaller the effect of cell death inhibition with QVD (Figure 11A). Apparently the more susceptible cell lines showed less responsiveness for pan-caspase inhibition or, to put it differently, more sensitive cell lines might have a stronger drive towards apoptosis. For further analysis I decided to divide the cell lines scores in a high and low NK cell sensitivity cluster, based on a cut-off at 50% NK-92 cell killing (Figure 11B). Excitingly, when comparing the RNA-Seq data of the two groups, the low sensitivity cluster showed a significant enrichment for the hallmark of apoptosis gene set ( $p=0.049$ ), as well as enrichment for necrosis and pyroptosis gene sets<sup>2</sup> (Figure 11C).

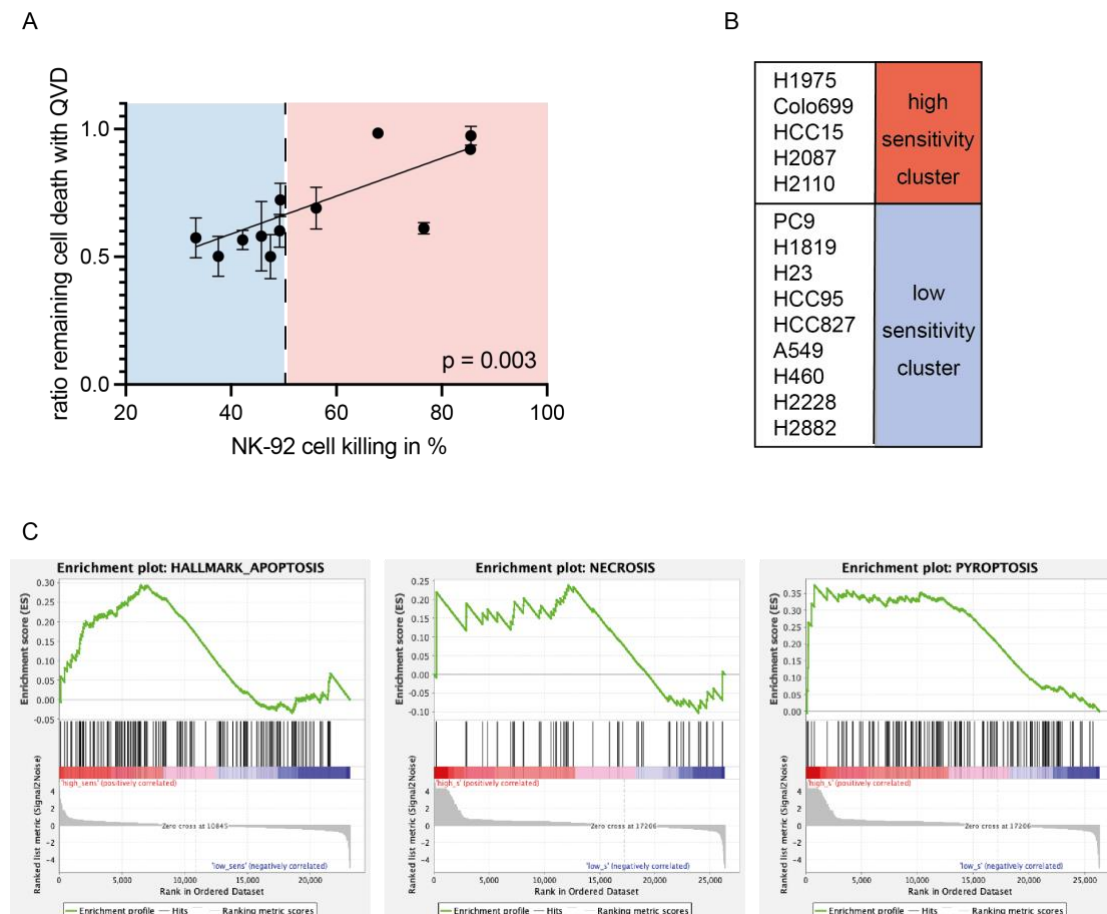


**Figure 11** Cell death gene signatures enriched in highly sensitive cell lines. **A** Pearson correlation of NK-92 cell killing and QVD rescue of cell death was significant with  $p=0,0179$  (two-tailed). Cell lines were divided in sensitivity clusters with high sensitivity over 50% killing (orange) and low sensitivity below 50% killing (blue). **B** List of human lung cancer cell lines in sensitivity clusters. **C** Gene set enrichment analysis of publicly available RNA sequencing data of cell lines listed in **B**. Hallmark apoptosis ( $p=0,049$ ,  $NES=1,38$ ,  $FDR=1$ ), Gene set necrosis ( $p=0,509$ ,  $NES=1,01$ ,  $FDR=0,762$ ), Gene set pyroptosis ( $p=0,39$ ,  $NES=1,1$ ,  $FDR=0,7$ )

<sup>2</sup> Necrosis and pyroptosis gene sets were taken from (Ahluwalia et al., 2021)

## What are the drivers for NK cell killing?

To identify further drivers or pathways, leading to differences in NK-92 cell killing of tumor cells, I investigated common NK cell ligands. The major inhibitory interaction is dependent on MHC I expression on the target cell surface. Allelic mismatch between NK-92 and the cancer cell lines used for this work was found for some of the cell lines (Table 3), which should lead to an increased killing efficiency.

Although, HLA mismatching might not fully determine tumor cell susceptibility towards NK-cell killing, as the highly sensitive cell lines H2087 and H2110 revealed matched HLA alleles.

*Table 3 HLA matching between NK-92 and cancer cell lines*

cell line	HLA-B	HLA-C	HLA matching
NK-92	B*07:02:01,44:03:01	C*07:02:01,16:01:01	
H1975	B*41:01,41:01	C*17:01,17:01	mismatched
Colo699	B*07:02,37:04	C*06:02,07:02	partial mismatch
HCC15	B*15:17,15:17	C*05:01,05:01	mismatched
H2087	B*44:03,44:03	C*16:01,16:01	matched
H2110	B*42:02,57:01	C*08:02,08:02	matched
PC9	B*07:02,55:02	C*03:03,07:02	partial mismatch
H23	B*50:01,50:01	C*06:02,06:02	mismatched
H460	B*35:01,51:01	C*03:03,15:02	partial mismatch
A549	B*18:01:01,20:03:01	C*12:03:01,16:01:01	undefined
HCC95	B*13:02,18:01	C*16:01,16:01	matched
H2228	B*07:02,38:01	C*07:02,12:03	matched
HCC827	B*52:01,51:01	C*12:02,12:02	matched

Furthermore, HLA-ABC expression and tumor cell sensitivities did not correlate at baseline (Figure 12A) or in co-culture conditions (Figure 12B). For a selection of NK cell ligands, the expression did not differ significantly between sensitivity groups at baseline or co-culture conditions (Figure 12C, D).

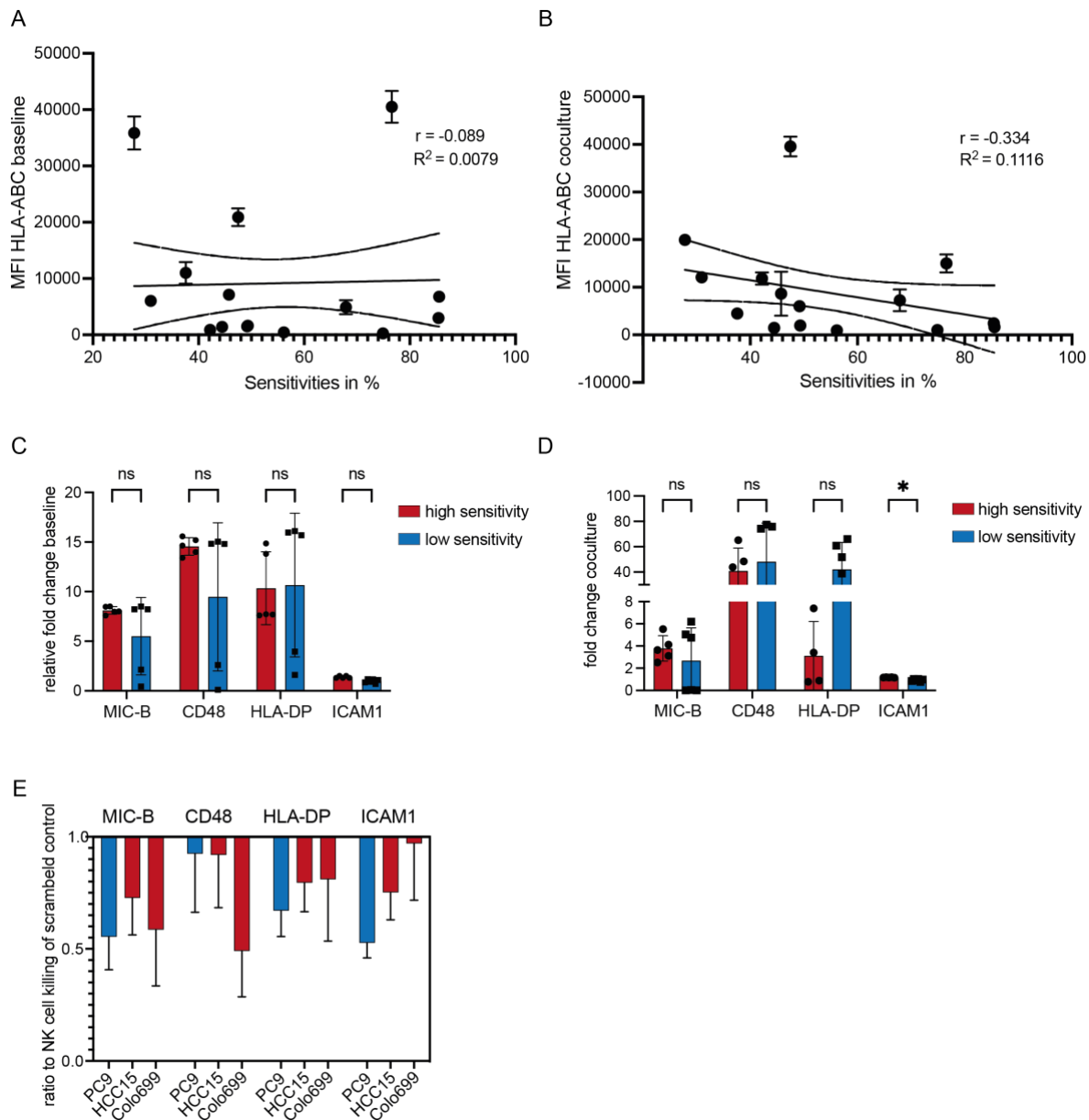


**Figure 12** HLA-expression or NK cell ligands did not define tumor cell sensitivity towards NK cell killing. A) Pearson correlation of tumor cell line sensitivities and median fluorescence intensity of HLA-ABC;  $p=0,7525$ . B) Pearson correlation of tumor cell line sensitivities and median fluorescence intensity of HLA-ABC measured after 24h of coculture;  $p=0,2237$ . C) qPCR measurement of NK-ligands on tumor cells. D) qPCR measurement of NK-ligands on tumor cells after 24h of coculture. ICAM1  $p= 0,0009$  E) siRNA mediated knockdown of NK-cell ligands. Ratio of killing in comparison to the scrambled siRNA control after 72h is shown.

However, ICAM1 was significantly enriched in the high sensitivity group during coculture conditions (Figure 12D). ICAM1 expression has been shown to bind LFA-1 (Urlaub et al., 2017) and therefore might lead to an improved cell-cell adhesion between NK-92 and target cell and result in an increased killing rate. Additionally, at baseline, there was a trend for a higher expression of the activating ligands MIC-B and CD48 in the high sensitivity cluster, whereas the inhibitory ligand HLA-DP was increased in the low sensitivity cluster during coculture. Even though this trend aligned with the observed sensitivities, expression varied widely between cell lines within

clusters. A knockdown of those ligands resulted in a partial rescue of NK-92 cell killing for all tested cell lines, although the effects varied between 5 and 50% (Figure 12E). These results suggested that the NK-cell ligands do influence tumor cell vulnerability, but the exact outcome is most likely a combinatory effect of different ligands.

Therefore, a more unbiased approach was investigated. RNA sequencing analysis of differentially expressed genes between sensitivity clusters revealed the top hit *melanoma-associated antigen 10 (MAGEA10)*, which is regularly upregulated in tumor cells, is involved in cell-cell adhesion and is a known T-cell target (Mendonca et al., 2017; Simister, Border, Vieira, & Pumphrey, 2022) (Figure 13A). Unfortunately, in follow-up experiments none of the top down-regulated genes revealed the expected effect of increased NK cell killing upon knockdown in co-culture across the analyzed cell lines PC9, HCC-15 and Colo699 (Figure 13B).

However, regarding cell death pathways, the cell death associated kinase RIPK3, as well as members of the IFN $\gamma$  pathway such as interferon induced protein with tetratricopeptide repeats 2 (IFIT2), were enriched in the high sensitivity cluster (Figure 13A).

Indeed, besides the upregulation of the hallmark apoptosis gene signature, hallmark peroxisome and interferon gamma response gene sets were increased in the high sensitivity cluster, whereas the hallmark signature hedgehog signaling was significantly increased in the low sensitivity group (Figure 13C, D).

Peroxisomes are closely associated with mitochondria and mainly involved in fatty acid metabolism, redox homeostasis and regulation of intrinsic apoptosis (C. Jiang & Okazaki, 2022).

IFN $\gamma$  is secreted by NK cells upon activation and levels were strongly increased during co-culture (Figure 6B). Downstream signaling in the target cell upon binding of IFN $\gamma$  leads to a pro-inflammatory and pro-apoptotic response and requires the adaptor proteins JAK1/2 and STAT1. A complete activation of STAT1 is reached with phosphorylation via JAK1/2 and PI3K-AKT engagement (Nguyen, Ramana, Bayes, & Stark, 2001). In addition, non-canonical IFN $\gamma$  receptor signaling can be executed via STAT3 instead of STAT1 (Gocher, Workman, & Vignali, 2022). Indeed, STAT1 activation as measured by immunoblotting of p-STAT1, was detected following coculture, whereas p-AKT was slightly induced in the highly sensitive cell lines HCC15 and Colo699, but constitutively active without further increase in the low sensitive cell

line PC9 (Figure 13E). Due to the observed differences of AKT activation, the impact of PI3K was further investigated.

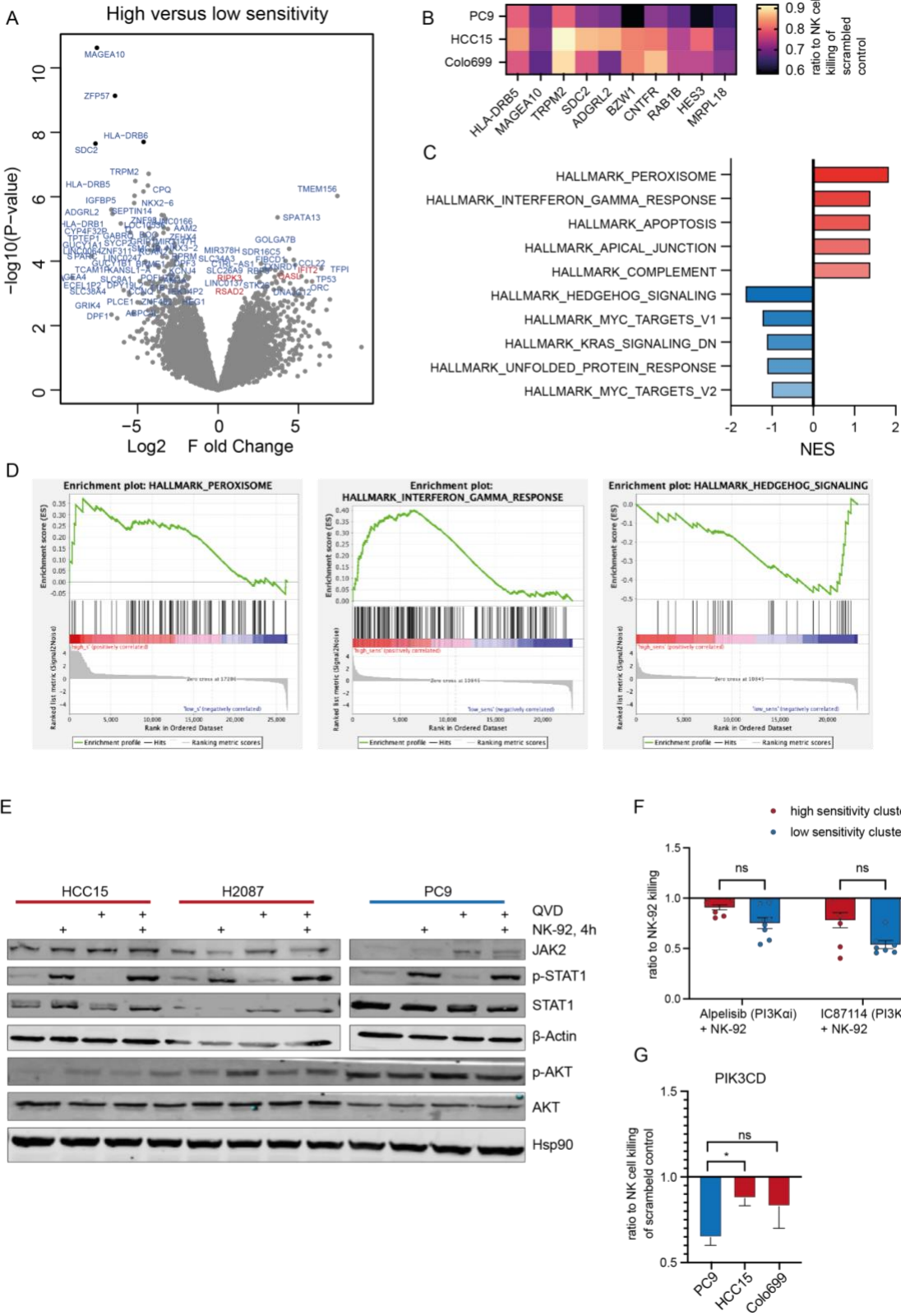


**Figure 13** High sensitivity cluster revealed pro-apoptotic signatures, whereas anti-apoptotic signatures (hedgehog) and activation of the pro-survival AKT pathway were increased in the low sensitivity cluster A) Differentially expressed genes analysis of the high versus low sensitivity cluster. Significantly differentially expressed genes were colored, red: interferon gamma response genes. B) Effect of siRNA mediated knockdown in tumor cell lines during

NK-92 cell co-culture. B) Gene set enrichment analysis high versus low sensitivity. Top 5 enriched gene sets are shown. NES = normalized enrichment score. C) Enrichment plots of the top 2 enriched gene sets and the only significantly enriched gene set hedgehog signaling ( $p= 0.004$ ,  $FDR = 0.26$ ) for the low sensitivity cluster. D) Activation of JAK2, STAT1 and AKT in tumor cells during 4h of co-culture with NK-92. E) Effect of PI3K $\alpha/\delta$  inhibition on NK-92 mediated killing of tumor cells in the high and low sensitivity group. F) Effect of PI3K $\delta$  knockdown on NK-92 mediated killing of tumor cells in PC9, HCC15 ( $p=0.016$ ) and Colo699.

When PI3K was inhibited in tumor cells, NK-92 cell killing was reduced, with a strong trend towards a stronger rescue effect for the low sensitivity cluster (Figure 13F). In addition, also the knockdown of phosphatidylinositol-4,5-bisphosphate 3-kinase catalytic subunit delta (PIK3CD) led to about 40% rescue for PC9, but only 10 to 20% for HCC15 and Colo699 (Figure 13G). Although PI3K/AKT signaling does cause anti-apoptotic effects in general, the inhibition of PI3K $\delta$  led to increased tumor cell survival in NK-92 cell coculture with a stronger impact on the low sensitivity cluster.

On the other hand, the hallmark signature hedgehog signaling was significantly increased in the low sensitivity cluster. The pathway is involved in cell proliferation, as well as inhibition of apoptosis via BCL-2 (Peng et al., 2022).

In summary, pro-apoptotic signatures (apoptosis, IFN $\gamma$  signaling) were enriched in the high sensitivity cluster, whereas anti-apoptotic signatures (hedgehog), as well as activation of the pro-survival AKT pathway were found to be increased in the low sensitivity cluster.

## **Tumor escape mechanisms**

Although this work demonstrated tremendous differences in NK-cell vulnerability of cancer cells, it is well known that tumor cells escape NK cell killing via various mechanisms (Sordo-Bahamonde et al., 2020). In order to demonstrate this in an *in vitro* setting, long term coculture was performed to obtain a NK-cell resistance (cell line<sup>NK-92R</sup>). Indeed, a significant decrease in NK-92 killing was observed for 3 out of 4 cell lines (Figure 14A). With regards to cell death inhibition, the resistant cell lines exhibited similar rescue levels upon QVD treatment as their parental counterparts (Figure 14B). Next, I analyzed the transcriptomes of PC9, Colo699 and their resistant counterparts using RNA-sequencing and primarily found differentially expressed genes between the different cell lines and conditions (Figure 14C). Therefore, parental cell lines and their resistant counterparts were analyzed separately and the top 500 differentially expressed genes were scanned for hits featured in both lists. Eight genes were found to be upregulated and three to be downregulated in both resistant cell lines compared to their parental counterparts (Figure 14D). The upregulated genes are

involved in various common processes as cell-cell adhesion (*bone marrow stromal antigen 2(BST2)*) and signal transduction (*Jagged 1 (JAG1)*) (Mahauad-Fernandez et al., 2018; Qiao et al., 2022).

Ni et al. discovered an upregulation of *plexin cytoplasmic RasGAP domain-containing protein (PLXNC1)* in stomach adenocarcinoma, associated with poor patients outcome and an unfavorable immune signature (Ni et al., 2021). Furthermore,

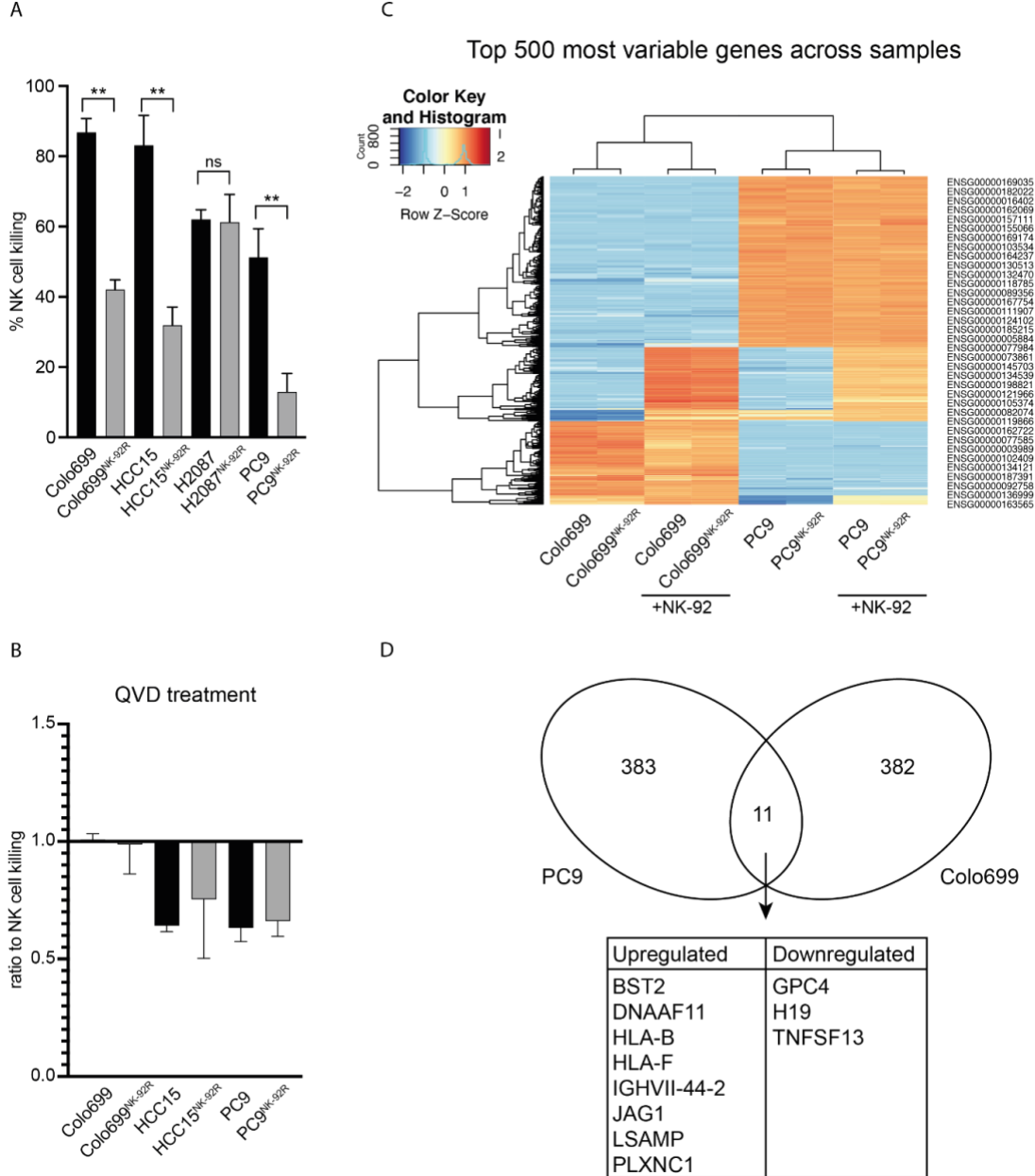


**Figure 14** NK-92 resistant cell lines PC9 and Colo699 revealed minor genetic changes. A) Changes of NK-92 cell killing during 72h of co-culture between parental and resistant cell lines. B) Effect of pan-caspase inhibition on NK-92 mediated killing of tumor cell lines did not differ between parental and resistant cell lines. C) Most variable genes across RNA sequenced cell lines revealed minor changes between parental and resistant cell lines. D) Overlap of up- and down-regulated genes upon resistance between cell lines PC9 and Colo699.

*HLA-B* and *HLA-F* are members of HLA-class I and regulate the threshold for NK-cell killing (Horowitz et al., 2016).

Additionally, upregulation of HLA-class I is a common tumor escape mechanism which seemed to play a role in this setting as well. Among others, *TNFSF13* was downregulated, which might contribute to reduced inflammatory signaling (R. Chen et al., 2021). Even though some hits as JAG1, BST2 and HLA members were already described as pro-tumorigenic factors, those gene list hits need further experimental validation.

General mechanisms which might have led to the resistance phenotype were analyzed via gene set enrichment analysis (Figure 15A). The top enriched pathways angiogenesis is closely related to tumor progression (Lugano, Ramachandran, & Dimberg, 2020).

IL-6/STAT3 signaling was shown to strongly inhibit an anti-tumor immune response and apoptosis via increased expression of MCL-1 (B. Huang, Lang, & Li, 2022). During co-culture, not only an increasing amount of IL-6 accumulated in the supernatant (Figure 15C), but also STAT3 was activated in cancer cells (Figure 15D). A constitutive increase in STAT3 signaling would lead to improved cancer survival despite coculture, as well as further secretion of IL-6 via a positive feedback loop (B. Huang et al., 2022). Another apoptosis associated pathway found to be increased was TNF $\alpha$  signaling via NF $\kappa$ B. TNF signaling can either lead to caspase activation and apoptosis or to NF $\kappa$ B engagement resulting in inflammation and survival (Tang et al., 2017). Besides that, TNF $\alpha$  signaling via NF $\kappa$ B is also involved in epithelial to mesenchymal transition (EMT) (Wu & Zhou, 2010). Some characteristics of EMT are, among others, loss of cell polarity, cell adhesion and cell-cell junctions. TGF $\beta$  has been identified as a key mediator of EMT induction and, was described to be involved in cancer progression, metastasis and therapy resistance (Hao, Baker, & Ten Dijke, 2019). Interestingly, the subsequent top enriched gene sets were TGF $\beta$  signaling and EMT, suggesting an involvement of EMT in the NK-92 resistant phenotype. An EMT phenotype can be induced with long-term treatment of TGF $\beta$ . Indeed, when PC9 were treated with TGF $\beta$  for short- (72h) or long- (3 weeks) term, a trend towards less sensitivity for NK-92 cell killing was observed upon TGF $\beta$  treatment (Figure 15F).

These results suggest an involvement of EMT, as well as the activation of the IL6/STATS3 axis, in lung cancer cell NK cell escape.



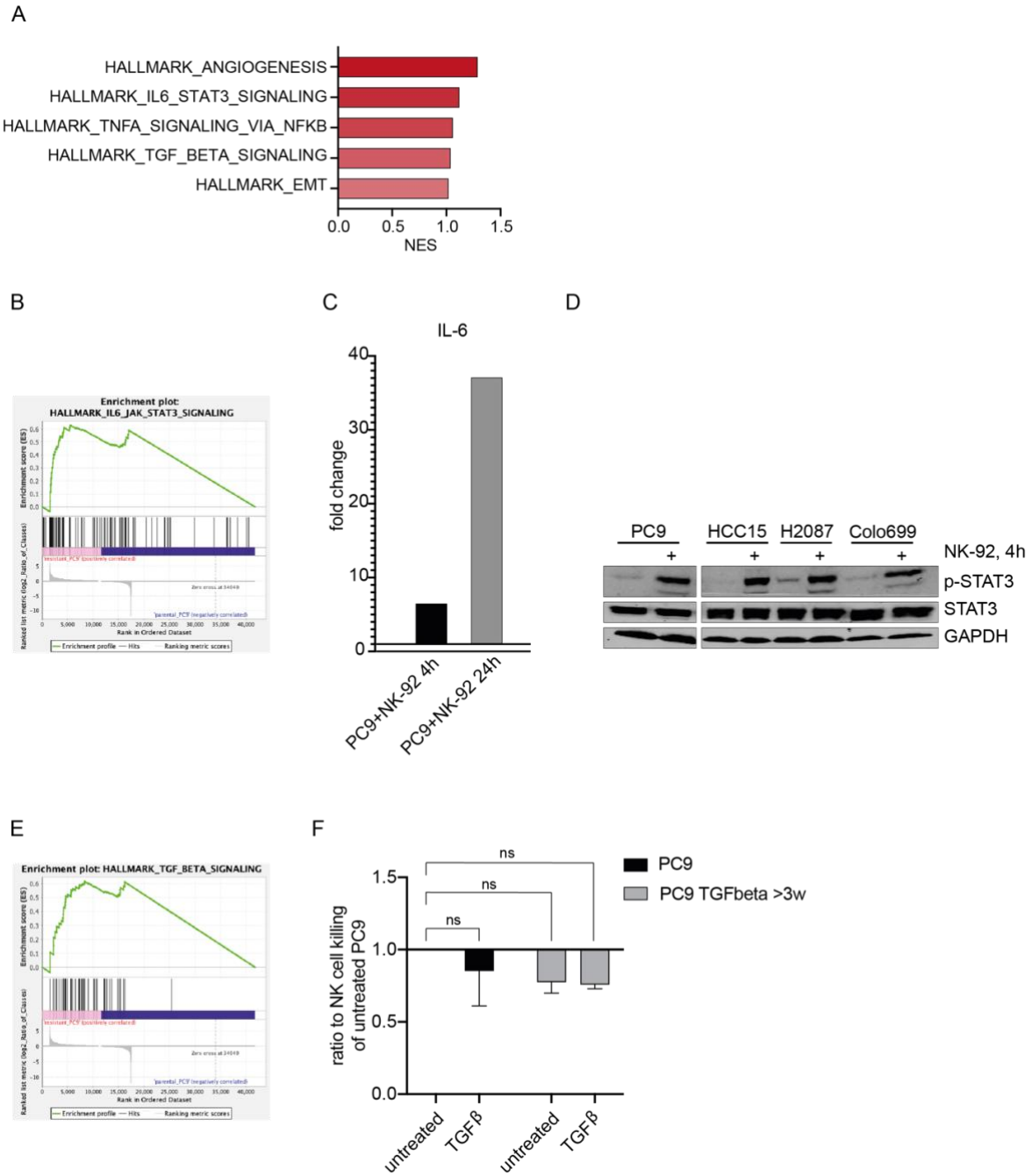


**Figure 15** NK-92 resistant cell lines exhibited survival signaling and epithelial-to-mesenchymal signature enrichment. A) Top 5 hits of gene set enrichment analysis of NK-92 resistant PC9 and Colo699 versus their parental counterparts. B) Enrichment plot of IL-6/JAK/STAT3 signaling ( $p=0.000$ ,  $FDR=0.5$ ). C) Increase of IL-6 in the supernatant of PC9 and NK-92 co-culture over time. ( $n=1$ ) D) Activation of STAT3 in cancer cell lines upon 4h of co-culture with NK-92. E) Enrichment plot of EMT signaling ( $p=0.000$ ,  $FDR=0.5$ ). F) Effect of TGFbeta short- and long-term treatment on NK-92 mediated killing of tumor cells in PC9.

## Summary

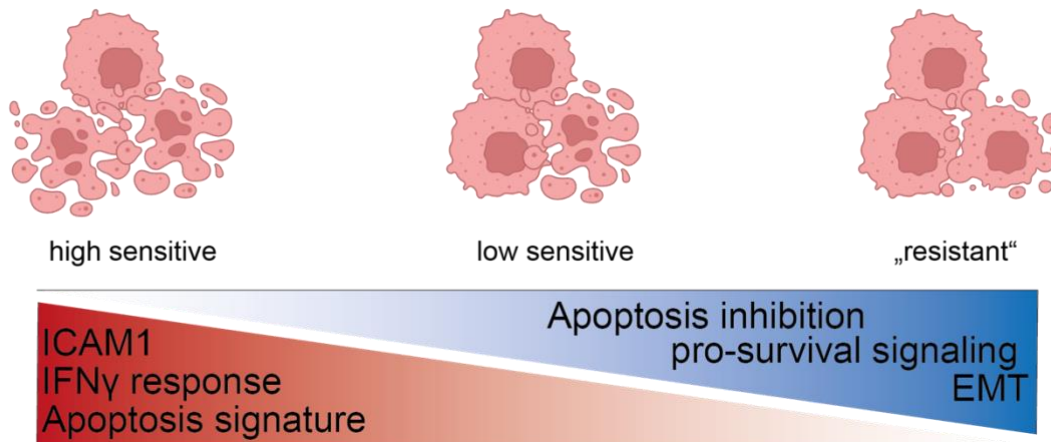


**Figure 16** Summary of results. For more sensitive cell lines towards NK-92 cell killing, ICAM1, IFN $\gamma$  response and apoptosis was upregulated, whereas less sensitive cell lines revealed increased anti-apoptotic and pro-survival signaling, as well as EMT signature, which was strongly associated with an NK-92 resistant cancer cell phenotype.

In summary, NK-92 revealed cytotoxicity against most of the cell lines and interestingly the sensitivities largely varied between lung cancer cell lines. Co-culture of NK-92 and lung cancer cell lines led to an upregulation of IFN $\gamma$  response and target genes, which was more prominently enriched in the high sensitivity cluster. The IFN $\gamma$  downstream pathway JAK/STAT1, leading to pro-apoptotic signaling, was activated across tumor cell lines during coculture. Furthermore, the gene set for apical junctions was upregulated in the high sensitivity group, whereas the data analysis for the NK-92 resistant cell lines showed an upregulation of several hallmarks for EMT. As a trend of less NK-92 cell killing for long-term TGF $\beta$  treated tumor cells, EMT might function as a possible escape mechanism. Additionally, an increased expression of apoptotic and pyroptotic pathway members was observed in the high sensitivity cluster and features of extrinsic apoptosis and pyroptosis were verified across co-cultured tumor cell lines. Interestingly, gene sets for cell death pathways were enriched in the high sensitivity clusters and they exhibited less sensitivity for caspase inhibition. In parallel, the pro-survival hedgehog pathway was enriched in the low sensitivity cluster. (Figure 16)

## Discussion

This research aimed to identify target cell pathways and factors involved in NK cell – target cell killing. Based on the successfully established co-culture system of NK-92 and lung cancer cell lines in 2D and 3D, a broad range of tumor cell susceptibility for NK cells was observed, exhibiting cell death features of apoptosis and pyroptosis. While vulnerable cell lines showed an increased cell death signature and less rescue with cell death inhibition, further investigation of cell death induction via granzymes and intrinsic apoptosis is needed for a better understanding of the process. Bioinformatical analysis did point out increased apoptotic and IFN $\gamma$  signaling in high sensitive cell lines, whereas EMT and pro-survival signaling were increased for less sensitive cell lines.

## EMT

Tumor cell plasticity towards a more metastatic and aggressive phenotype involves several functional and morphological changes, which are included in the process of EMT. The potent EMT inducer TGF $\beta$  is frequently upregulated in cancer and it was shown that an EMT secretory phenotype is associated with decreased survival in NSCLC patients (Kim et al., 1999; Reka et al., 2014). This phenotypical switching can contribute to therapy resistance and immune escape (Zavadil, Haley, Kalluri, Muthuswamy, & Thompson, 2008). Prior publication showed that NK cells caused an induction of EMT in melanoma cells after 72h of co-culture, dependent on the secretion of IFN $\gamma$  and TNF $\alpha$  (Huergo-Zapico et al., 2018). Interestingly, Chockley et al demonstrated an increased susceptibility for cancer cells towards NK cells following EMT transition, which was explained with the downregulation of the inhibitory ligand e-cadherin and upregulation of NKG2D ligand cell adhesion molecule 1 (CADM1) upon co-culture. However, there seemed to be a short timeframe for increased NK cell killing between the transition and metastatic events as the tumor cells vulnerability was especially increased at the beginning of the metastatic process (Chockley et al., 2018). This work did not further investigate short-term induction of EMT in lung cancer cell lines, although EMT associated gene sets were increased as a possible mechanism of NK cell escape. Moreover, triggering of EMT via TGF $\beta$  did decrease tumor cell death in PC9 in 72h of NK cell co-culture. Further investigation of the NK-resistant cell lines is needed to measure markers of EMT and potential changes of NK cell ligand

expression. Another point of interest would be to determine the main drivers of EMT induction during long-term NK cell co-culture, which might be IFN $\gamma$  and TNF $\alpha$ , as this mechanism was already described for melanoma (Huergo-Zapico et al., 2018). Additionally, the time course of EMT development and NK cell susceptibility could be further analyzed with the co-culture system established in this thesis.

## Increased IFN $\gamma$ signature

Among others, NK cell cytotoxic effects are mediated by the production of IFN $\gamma$ , triggered by IL-2 and IL-15 and reinforced by TNF $\alpha$  (Almishri et al., 2016). Additionally, IFN $\gamma$  secretion can recruit further inflammatory immune cells and a negative correlation was found between the cancer stage and IFN $\gamma$  production (Lee et al., 2017; Reefman et al., 2010). In cancer cells, IFN $\gamma$  can drive immune-activating, as well as suppressing signaling (Strieter et al., 1995). Downstream signaling following IFN $\gamma$  binding is driven by JAK1/2 and STAT1 homodimerization, which translocate to the nucleus to bind co-activating proteins and initiate transcription of multiple genes (Negishi et al., 2018). Although, studies showed an IFN $\gamma$  concentration dependent signaling, for low doses the activation of the anti-apoptotic PI3K-AKT pathway results in increased stemness (M. Song et al., 2019). Gao and colleagues demonstrated strong cross-talk between JAK/STAT1 and PI3K-AKT pathways, with evidence of pro-apoptotic signaling for PI3K inhibition, dependent on PD-L1 expression (Gao et al., 2018). Surprisingly, this work showed increased survival of cancer cells during NK-cell co-culture with PI3K $\delta$  inhibition or knockdown, especially for the low sensitivity cluster. The PI3K-AKT pathway was described as a regulatory response signaling upon IFN $\gamma$ , as well as a factor for complete activation of STAT1 (Gocher et al., 2022). For the function as a STAT1 activator, an inhibition might lead to decreased pro-apoptotic STAT1 signaling and consequently to less cell death upon NK cell co-culture. However, further experiments are necessary to investigate this the influence of PI3K-Akt activation on STAT1 signaling.

In the high sensitivity cluster, IFN $\gamma$  signaling in general was found to be upregulated, as well as the differentially expressed genes *interferon induced protein with tetratricopeptide repeats 2 (IFIT2)*, *radical S-adenosyl methionine domain-containing protein 2 (RSAD2)*, *Oligoadenylate synthase-like (OASL)*. IFIT2 is negatively associated with cancer progression and is strongly involved in the promotion of

apoptosis in different types of cancer via BCL-2 regulation (Stawowczyk, Van Scoy, Kumar, & Reich, 2011). Moreover, Lai et al. demonstrated increased rates of metastasis with reduced levels of IFIT2, as well as an induction of EMT upon IFIT2 knockdown in oral squamous cell carcinoma (OSCC) (Lai, Liu, Chang, & Lee, 2013). The role of RSAD2 in cancer is not fully established, although its activation increases glycolysis and lipogenesis, proposing an increased metabolism and pro-tumorigenic function (Weinstein, Godet, & Gilkes, 2022). For OASL a recent study demonstrated a positive correlation with effector immune cell infiltration and patient's outcome in cervical cancer under immune checkpoint therapy (C. H. Huang et al., 2023). However, for a non-treatment setting, OASL upregulation was mostly associated with an unfavorable cancer progression (C. Zhang et al., 2021; Zhao et al., 2023). Taken together, further experiments like RNA sequencing of co-cultured or IFN $\gamma$  treated tumor cells might be necessary to characterize the effects of an enriched IFN $\gamma$  signature in the high sensitivity cluster.

## **Cell death**

The importance of a functional extrinsic apoptosis pathway for NK cell tumor surveillance was shown in various studies, demonstrating increased tumor development and growth in both humans and mice with deficiencies in extrinsic apoptosis initiation and execution (Price et al., 2014; Sedger et al., 2002). However, malignant cells can develop several mechanisms to evade immune cell killing. Systematic evidence linking tumor cell vulnerability towards NK cells to cell death mechanisms still needs to be investigated. This work did not only demonstrate the relevance of extrinsic apoptosis in NK cell killing in the context of patient derived lung cancer models, but also the involvement of apoptotic predisposition for tumor cells sensitivity for NK cell killing. Gene set enrichment for the cell death pathways apoptosis, pyroptosis and necrosis was demonstrated in the high sensitivity cluster, although similar expression levels of death receptors or protein levels of caspase 1 or 8 were found. However, the apoptosis effector caspases 3 and 7 increased according to the cell line sensitivity towards NK-92 induction during co-culture.

### Efficiency of pan-caspase inhibition

Interestingly, pan-caspase inhibition did not completely rescue NK cell killing and the effects were negatively correlated with cancer cell killing. Either the more vulnerable cell lines are less dependent on apoptosis due to increased crosstalk with other cell death pathways, or caspase inhibition is less efficient.

The pan-caspase inhibitor QVD inhibits key components of the apoptotic machinery, but as characteristics of pyroptosis upon co-culture of tumor cells and NK-92 were observed, this might not be sufficient for cell death prevention. Additionally, QVD function depends on irreversible binding of the caspases catalytic site, which might be disrupted by mutations (Caserta et al., 2003). However, mutations in caspase genes were extremely rare and mainly found in gastric carcinoma (Ghavami et al., 2009). Therefore, mutated binding sites in the analyzed lung cancer cell panel are unlikely and might not explain the observed differences in pan-caspase inhibition response.

### Effect of granzymes

Another factor is the effect of granzymes during co-culture of cancer cells and NK-92. As pointed out in the introduction, granzymes target several proteins involved in different stages of the cell death pathways, as well as in the inflammatory response (Metkar et al., 2008). Probably the more sensitive the cell lines are, the more vulnerable they are for granzyme-dependent cleavage, which could level out pan-caspase inhibition. As granzyme B level were shown to predict lung cancer patients outcome, granzyme sensitivity of tumor cells would be of great interest for therapy prediction and improvement (Hurkmans et al., 2020). For further investigation, the effects of single types of granzymes on different lung cancer cell lines need to be studied.

### Cell death signatures as prognostic factor

In the recent years the data collection of apoptotic gene signatures in cancer is gaining increasing importance for prognostic implications and therapy prediction in cancer (Ahluwalia et al., 2021; Y. Wang et al., 2022; Zhong, Zhang, Huang, Lin, & Huang, 2021; R. Zou, Zhao, Xiao, & Lu, 2022; X. Zou, He, Zhang, & Yan, 2022). These studies demonstrated an association of apoptosis-related genes and decreased survival and increased immune infiltration in lung adenocarcinoma, breast cancer, renal cell cancer and bladder cancer. In lung cancer, a high apoptosis or cell death related gene signature was found to predict decreased patients survival, but an increased cytotoxic

T-cell infiltration in combination with inhibitory checkpoints on tumor cells. According to that, a higher efficacy for immunotherapy alone or in combination with chemotherapy is eminent in patients with a high apoptosis or cell death related gene signature (Ahluwalia et al., 2021; X. Zou et al., 2022). In contrast, my work demonstrated an increased killing of tumor cells with an apoptosis-related gene signature. Although, when gene set enrichment analyses were performed for the slightly different cell sensitivity clusters based on the 3D co-culture model of NK-92 and tumor cells, the combined cell death index (developed by Ahluwalia et al., 2021) was increased in the low sensitivity group. Those results suggest, that the cancer cells vulnerability towards NK cell killing is shaped by susceptibility for apoptosis, but the additional complexity of structure and tumor microenvironment does strongly influence the reachability of tumor cells by NK cells. That would support the suggestion of Zou et al. to use cell death gene signatures for therapy prediction, which might apply to NK cell-based therapy options as well. However, a comprehensive analysis of NK cell effects in the context of cell death related signature in patients was not performed so far and would be necessary for an improved understanding. Furthermore, a gene signature score tailored to NK cell killing in patients would be useful to support the emerging options of NK cell-based therapies.

## Concluding remarks

This work established and characterized an *in vitro* co-culture system for further analysis of NK-cell - tumor cell interactions. Given the importance of successful killing of tumor cells during NK cell tumor surveillance, the focus was set on the execution of cell death pathways in tumor cells. I have argued throughout this work, that more susceptible cancer cell lines revealed an increased tendency to undergo apoptosis, considering the increased apoptotic signature and decreased sensitivity for pan-caspase inhibition. Acknowledging the highly dynamic nature of NK cell – tumor cell interaction, leading to immune escape of tumor cells as a key challenge in cancer research and therapy, I successfully developed NK cell resistant lung cancer cell lines in long-term co-culture, reflecting known escape mechanisms like HLA dysregulation. These results, as well as the method to study immune escape could form the basis for future experiments.

As with the majority of studies, the design of the current study is subject to limitations. The co-culture system was established in 3D for a better reflection of physiological conditions in the tumor microenvironment. In the course of the project, effects on cell death pathways were compared in 2D versus 3D and classified as comparable results. Therefore, for follow up experiments the 2D environment was chosen due to feasibility. However, for the aspect of apoptotic gene signatures, cancer cell receptor repertoire and their impact on NK cell interaction, as well as immune escape results gathered in 3D would be more physiological relevant. Furthermore, this study did capture several aspects of NK cell – tumor cell interaction. An increased amount of functional data as a follow up of bioinformatical analysis could have been gathered by focusing on less facets.

However, this project contributed to the understanding of the complex interplay between NK cells and patient derived lung cancer models with a systematic capture of tumor cell susceptibility towards NK cells in 2D and 3D, the discovery of extrinsic apoptosis in tumor cells triggered by NK cells and the verification of EMT and specifically TGF $\beta$  involvement in cancer NK cell escape in this *in vitro* model.

Taken together, in this doctoral thesis work I identified several targets and pathways, which are involved in lung tumor cell susceptibility towards NK cells. This data, as well as the established co-culture system may therefore build a basis for future functional studies to determine the specific effects of individual cell death and inflammatory signaling components in the context of NK cell mediated killing of cancer cells.



## Methods

### Cell culture

Cells were cultured in a humidified atmosphere containing 5% CO<sub>2</sub> at 37 °C. Human lung cancer cell lines K562, Colo699, H1975, H3122, H1819, HCC827, PC9, HCC4006, H3255, H2087, H460, H23, H2110, H1993, H1581, H2882, HCC95, A549 and HCC15 were maintained in RPMI medium supplemented with 10% fetal bovine serum (FBS) and 1% penicillin/streptomycin (Pen/Strep). The human natural killer cell line NK-92 (purchased from Leibniz-Institut DSMZ-Deutsche Sammlung von Mikroorganismen und Zellkulturen GmbH) was maintained in alpha-MEM supplemented with L-Glutamine, Ribonucleosides, Deoxyribonucleosides, 2.2g/L NaHCO<sub>2</sub>, 10ng/ml IL2, 12,5% FBS and 12,5% horse serum (HS).

### Inhibitor treatment

For inhibition experiments the dedicated inhibitor was added to the tumor cells 60min prior to the start of co-culture. For the condition without NK-92 cells, the inhibitor was added at the same time point. All inhibitors were solved in DMSO and for non-treatment conditions DMSO was added in the same amount as inhibitor in the treatment condition.

*Table 4 Table of inhibitors*

Inhibitor	Concentration used in experiment (if not further labeled in results)	Company, product number
Alpelisib	50nM	MedChemExpress, HY-15244
IC-87114	1µM	MedChemExpress, HY-10110
QVD-OPH	20µM	MedChemExpress, HY-12305
Necrostatin-1	5µM	MedChemExpress, HY-15760
GSK-843	3µM	MedChemExpress, HY-125402

### Co-Culture

#### 2D

To assess NK-92 killing of tumor cells a co-culture system was developed. Tumor cells were cultivated in 96 well plate (5000 cells per well) for 24h. The NK-92 cell line and

optional treatments were added in a 1:1 ratio in 100µl alpha-MEM. Analysis was performed after 72h of Coculture with a crystal violet staining.

### 3D

Tumor cells were cultivated (10,000 cells per well) in 96 ultra low attachment well plate (Corning® 96-well Clear Round Bottom Ultra-Low Attachment Microplate, #7007) until they formed stable spheroids after 24h. The NK-92 cell line was labeled with ViaFluor488. Therefore, the cell line was centrifuged at 200g for 5min and resuspended in 500µl PBS including 1µl ViaFluor. Following incubation at 37°C for 10min 500µl alphaMEM was added for 10min at 37°C. Labeled cells were then centrifuged and adjusted to 10,000 cells/100µl, including IL2 as 2x concentration. The NK-92 cell line, DRAQ7 (300nM) and optional treatments were added in a 1:1 ratio in 100µl alpha-MEM. For continuously observation the plate was placed in the Incucyte and analyzed with the spheroid module using following parameters:

Brightfield: segmentation sensitivity 100%, cleanup hole fill 22µm<sup>2</sup>, minimum area filter 5000µm<sup>2</sup>, maximum eccentricity 0.98.

Green: top-hat segmentation: radius 20µm, threshold 0.6 GCU.

Red: top-hat segmentation: radius 50µm, threshold 1 RCU.

### **Caspase 3/7 assay**

For the detection of caspase 3/7 activation, the CellEvent™ Caspase-3/7 Green Flow Cytometry Assay Kit (Invitrogen, # C10427) was used. When NK cells were added to the tumor cell culture, the caspase 3/7 detection solution was added in a dilution of 1:1000 to the co-culture and control condition. For continuously observation the plate was placed in the Incucyte and analyzed with the spheroid module using following parameters:

Brightfield: segmentation sensitivity 100%, cleanup hole fill 22µm<sup>2</sup>, minimum area filter 5000µm<sup>2</sup>, maximum eccentricity 0.98.

Green: top-hat segmentation: radius 20µm, threshold 0.6 GCU.

### **NK cell expansion PBMCs**

Isolation of PBMCs

PBMCs were isolated from buffy coats received from Blutspendezentrale Uniklinik Köln (Ethikantrag 21-1532). The blood was transferred into 50ml falcons and diluted with equal amount of PBS. For density gradient cell separation 20ml Ficoll-Paque™ PLUS was over layered with 30ml blood dilution. Next the sample was centrifuged at room temperature at 760g for 20min with the brakes switched off. After centrifugation the top layer containing plasma was discarded and the second layer with PBMCs was transferred into a new tube. Next, collected PBMCs were washed with PBS three times and centrifuged at 350xg for 8min. For paletes removal the samples were centrifuges at 200xg for 10min. After the last wash cells were counted with the Invitrogen Countess 3 cell counter (Thermo Fisher).

#### NK cell expansion

Freshly isolated PBMCs were cultivated in NK MACS medium (Miltenyi Biotech, #130-114-429), supplemented with IL-2 (10ng/ml, Peprotech, # 200-02) and IL-15 (10ng/ml, Peprotech, #200-15). At day 14 cells were analyzed via FACS for viability and their content of NKp46 positive cells.

#### **Long term Co-culture**

To reach a decreased sensitivity for tumor cell lines towards NK-92 cells long term co-culture was used. Therefore, tumor cell lines were seeded in a cell culture T-75 flask. When a confluency of about 70% was reached,  $2 \times 10^6$  NK-92 cells were added. After 72h medium and NK-92 cells were discarded, confluent cells were washed with PBS and left in medium until they grew back to 70% confluency. Co-culture was repeated for 5 cycles and tumor cell sensitivity towards NK-92 cells was measured in 2D and 3D assay.

#### **Cytokine analysis**

Cytokine analysis was performed by EveTechnology. According to their protocol, 1ml supernatant was collected after dedicated time points of cell culture and sent to the company.

#### **Spheroid embedding**

A schematic overview for the workflow of tumor spheroid embedding is shown in Figure 17. Tumor cells were cultivated (10,000 cells per well) in a 96 ultra low attachment well

plate (Corning® 96-well Clear Round Bottom Ultra-Low Attachment Microplate, #7007) for 7 days with change of medium every 72h. For co-culture conditions NK-92 were added in a 1:1 ratio 4h prior the fixation step. After 7 days the spheroids of each cell line were pooled, washed with PBS once and fixed in 4% formaldehyde (ROTI®Histofix) for 60min. Following the fixation step, spheroids were washed three times with PBS. The pooled spheroids of each cell lines were then carefully resuspended in 200µl pre-warmed 2% agarose gel and filled in small prepared glass tubes to achieve the formation of cylinder-shaped agarose pieces. Once the gel solidified after 30min, the agarose was removed from the tubes and added to a histology cassette (VWR® histology cassette, #18000-240). Further processing was performed at the department of pathology. Imaging was performed at the CECAD imaging facility, using Evos FL Auto2 (Thermo Fisher Scientific).

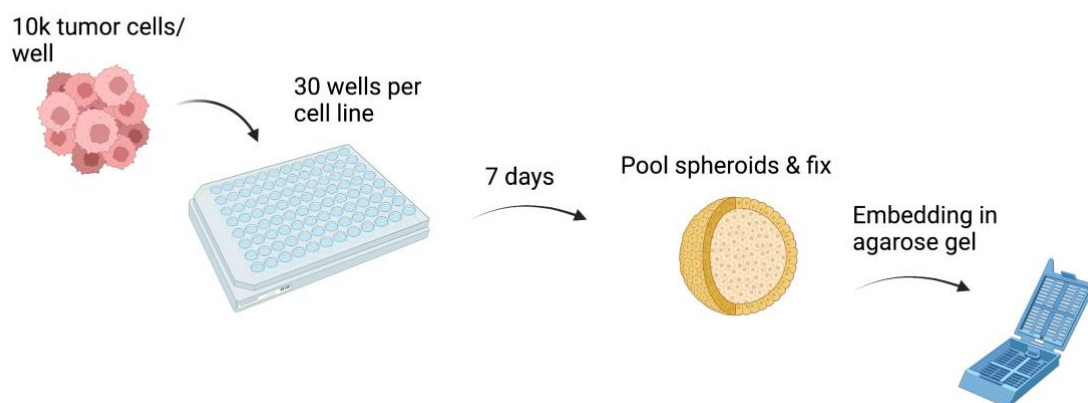


*Figure 17* Workflow of the embedding of tumor spheroids.

## Western Blotting

### Protein Extraction / Preparation of cell lysates

To extract proteins out of the cells the medium was aspirated and cells were washed with 1 ml ice-cold PBS. Afterwards the cells were harvested in 40 µl ice-cold cell RIPA buffer by scratching. Cell lysates were then collected in a 1.5 ml tube and incubated on ice for 30 min. Subsequently the cells were centrifuged for 10 min at 4 °C and 20,000 x g. Supernatant of each tube was transferred into a new tube and the pellets were discarded. The protein concentration was determined via BCA assay.

### Determination of total protein concentration

The Pierce™ BCA Protein Assay Kit was used to determine total protein concentration. In a 96-well plate 2µl of each lysate was applied, supplemented with a standard of 0, 0.25, 0.5, 1 and 2 µg/ml BSA to calculate the total protein concentration. Afterwards 200 µl of 1x Dye Reagent was added. Subsequently the plate was incubated for 30 min at 37 °C. For analysis the absorbance of the standards and samples was measured in a spectrophotometer (Tecan plate reader) at 595 nm. Each sample was diluted to 1 µg/µl, mixed with 1:3 Laemmli-buffer and denatured at 96 °C for 5min.

#### SDS Polyacrylamide gel electrophoresis (SDS PAGE)

Lysates were shortly centrifuged and 20 µg protein of each sample were loaded on a 4-20% Tris-Glycine Mini Gel (15 wells). The Plus Prestained Protein Ladder was used as a marker. Proteins in the gel were separated with a voltage of 120 V for 1.5 hours.

#### Immunoblotting

Afterwards the separated proteins were transferred to a polyvinylidene difluoride (PVDF) membrane by using the iBlot2 program: 20 V for 30 s, 23 V for 1:45 min, 25 V for 45 s. Subsequently the membrane was blocked for 1 hour in a blocking solution containing 2% gelatin from cold water fish skin in TBST to prevent non-specific binding of antibodies. The membrane was then incubated with primary antibodies (Table 5) diluted in TBST (dilution 1:1000) at 4°C overnight. The membrane was washed again three times for 5 min in TBST and then incubated with secondary antibodies (Table 6) diluted in TBST and 0.01% SDS-TBS for 1h at room temperature. Afterwards the membrane was washed three times for 5min in TBST and proteins were detected by using the Odyssey CLx Imaging System.

**Table 5** List of primary western blot antibodies

<b>antibody</b>	<b>species</b>	<b>Company, product number</b>
STAT1	rabbit	Cell signaling, #9172
p-STAT1	rabbit	Cell signaling, #CS9177S
STAT3	rabbit	Cell signaling, #9132
p-STAT3	rabbit	Cell signaling, #CS9131S
GAPDH	rabbit	Cell signaling, #2118
Caspase 8	mouse	Cell signaling, #9746

Caspase 1	rabbit	Cell signaling, #83383
Cleaved caspase 1	rabbit	Cell signaling, #4199
MLKL	rabbit	Cell signaling, #14993
p-MLKL	rabbit	Cell signaling, #91689
JAK2	mouse	Cell signaling, #74987
Actin	mouse	Santa cruz, #sc-47778
AKT	mouse	Cell signaling, #2920
p-AKT	rabbit	Cell signaling, #CS4060
HSP90	rabbit	Cell signaling, #4877

**Table 6** List of secondary western blot antibodies

antibody	Company, product number
IRDye® 800CW Goat anti-Mouse IgG	Li-Cor, # 926-32210
IRDye® 680CW Goat anti-Mouse IgG	Li-Cor, # 926-68070
IRDye® 800CW Goat anti-Rabbit IgG	Li-Cor, #926-32211
IRDye® 680CW Goat anti-Rabbit IgG	Li-Cor, # 926-68071

### Fluorescence-activated cell sorting (FACS)

For FACS analysis cells were detached, centrifuged at 200g for 5 min and resuspended in FACS buffer (2 mM EDTA, 2% FCS, PBS). Cells were counted and adjusted to  $5 \times 10^6$  cells/ml. For each staining 100 $\mu$ l/well were transferred to a V-bottom 96 well plate and an appropriated amount of antibody was added for incubation for 30min at room temperature. Following incubation cells were centrifuged for 3min at 500g, washed with PBS, centrifuged again and resuspended in 200 $\mu$ l FACS buffer. Samples were measured with the FACS machine MACSQuant 16 (Miltenyi). Analysis was performed with FlowJo.

**Table 7** FACS antibodies

antibody	label	Company, product number
HLA-ABC	PE	Biolegend, #311406
LAMP-1	APC	Biolegend, # 328620
CD45	FITC	Miltenyi, #130-110-631

### Crystal violet assay

Medium and NK-92 cells were aspirated and the wells were gently washed with tap water twice. After washing any remaining liquid was removed and the cells were incubated with 4% formaldehyde (ROTI®Histofix) for 20min at room temperature on a bench rocker to fix the monolayer. ROTI®Histofix was removed and the wells were washed with tap water twice. After the remaining liquid was removed and the plate was air dried, 50 µL of 0.5% crystal violet staining solution (for 100ml: 75ml H<sub>2</sub>O, 25ml methanol (Roth, #8388.1), 500mg crystal violet (Roth, #T123.3)) was added to each well and incubated for 20min at room temperature on a bench rocker. Following the staining, washing steps with tap water were repeated and the plate was air dried for at least 2h. To dissolve the staining 200µl methanol were added to each well and incubated for 20min at room temperature on a bench rocker. Optical density of each well was measured at 570nm by using the TECAN plate reader (TECAN, Infinite®200Pro).

### Quantitative reverse transcription polymerase chain reaction (RT-qPCR)

RNA-isolation was performed using the RNeasy-Mini Kit (Qiagen, Cat. No./ID:74104), following the manufacturers protocol “Purification of Total RNA from Animal Cells using Spin Technology”. Next, remaining genomic DNA was removed with incubation of reaction 1 (**Table 8**) for 2min at 42°C.

*Table 8 Reaction 1*

RNA	700ng
4x gDNA wiper mix	4µl
H <sub>2</sub> O	Up to 16µl

For reverse transcription reaction 2 was incubated for 15min at 37°C and 5sec at 85°C.

*Table 9 Reaction 2*

Reaction 1	8µl
5x HiScript III Enzyme Mix	4µl
H <sub>2</sub> O	8µl

For RT-qPCR reaction 2 was diluted 1:5 and 1:10 primer mix of forward and reverse primer (**Table 12**) in H<sub>2</sub>O was prepared for each target. The reaction was prepared in

384 well plates with 2µl reaction 2 and 8µl reaction 3 per well. Each sample-target combination was performed as triplicates.

**Table 10** Reaction 3

Primer mix	0.6µl
2x ChamQ Universal SYBR qPCR Master Mix	5µl
H <sub>2</sub> O	2.4µl

After sealing and centrifugation, the plate was placed in the QuantStudio5 System with following parameters for the QuantStudio Design & Analysis desktop software:

Block type: 384-well block

Experiment type: comparative C<sub>T</sub> ( $\Delta\Delta C_T$ )

Chemistry: SYBR Green reagents

Run mode: standard

**Table 11** RT-qPCR program QuantStudio5

50°C	2min	} 40x
95°C	10min	
95°C	15s	
50°C	1min	

Data was analyzed with the  $\Delta\Delta C_T$  method.

**Table 12** List of qPCR primers

Gene	Primer sequence forward	Primer sequence reverse
GAPDH	AGGTGAAGGTCGGAGTCAAC	AGTTGAGGTCAATGAAGGGG
MIC-B	CGCCTAAAGTCTGCGAGGA	CCCTGACTGCACAGATCCAT
CD48	CTGGGGGTCCTATTCAGCCT	CCCCACGAAGTTGAGGTAA
HLA-DP	AGGCAGCATTCAAGTCCGAT	GGGGGTCATTTCCAGCATCA
ICAM1	TCTTCCTCGGCCTTCCATA	AGGTACCATGGCCCCAAATG

### HLA-typing analysis

HLA-matching between NK-92 and tumor target cell lines was reviewed with publicly available cell line information (<https://www.cellosaurus.org/index.html>) and tested with the KIR ligand calculator of EMBL (<https://www.ebi.ac.uk/ipd/kir/matching/ligand/>).



## **RNA sequencing**

### RNA-isolation

RNA-isolation was performed in the pre-PCR area using the RNeasy-Mini Kit (Qiagen, Cat. No./ID:74104), following the manufacturers protocol “Purification of Total RNA from Animal Cells using Spin Technology”. Following quality control measurement with the TapeStation, Lexogen QuantSeq 3' mRNA-Seq was performed in the Cologne Center for Genomics (CCG).

### Analysis

RNA sequencing baseline data of cancer cells were downloaded from the European Molecular Biology Laboratory – European Bioinformatics Institute (EMBL-EBI) as counts per million (CPM) (Barretina et al., 2012; Ghandi et al., 2019). Further data processing was accomplished with R Studio (R 4.2.1), using the R packages “limma”, “edgeR”, “Glimma”, “org.Hs.eg.db”, “gplots” (Law et al., 2016). First, the counts for all samples and genes were stored and converted to a DGEList object. The information about high or low sensitivity towards NK-92 cell killing was also included as group information. Next, gene name information was added with “org.Hs.eg.db”. Lowly expressed genes were filtered with a threshold of 0.5 CPM followed by conversion to log<sub>2</sub> counts per million for normalization. For hierarchical clustering the “heatmap.2” function was used to calculate a matrix of euclidean distances from the log<sub>2</sub> CPM for the 500 most variable genes. Trimmed Mean of M (TMM) normalization for composition bias was calculated with the “calcNormFactors” function and implemented in the DGEList object. To assess differentially expressed genes between sensitivity groups a design matrix for the groups was created and the data was voom transformed to adjust the library size according to the calculated normalization (Law, Chen, Shi, & Smyth, 2014). Using the “lmer” function a linear model for each gene was fitted (Ritchie et al., 2015). The group comparison was specified with the “makeContrast” function and stored as contrast matrix. With the “contrast.fit” function the generated contrast matrix was applied and with the “eBayes” function calculated empirical Bayes shrinkage on the variances, and estimated moderate t-statistics and p-values. Results were visualized with the “vulcanoplot” function. Further analysis included gene ontology (GO) enrichment using the “goana” function.

## **Gene set enrichment analysis (GSEA)**

GSEA was performed using the desktop application GSEA 4.3.2<sup>3</sup>. Expression data of cell lines was applied as normalized data and prepared according to the GSEA user guide. Phenotype labels of cell lines were set according to sensitivity clusters. As gene set files, the gene set files H.all.v2023.1.Hs.symbols.gmt, as well as the lists in **Table 13** were used. Other than that, standard parameters were used to automatically run the GSEA. (Mootha et al., 2003; Subramanian et al., 2005)

*Table 13 Additional gene sets used for GSEA (Ahluwalia et al., 2021)*

necrosis	apoptosis	pyroptosis
BAX	AIFM1	TIGAR
BIRC2	AKT1	PRKACB
BIRC3	AKT2	PDCD4
CASP8	AKT3	RHEB
CFLAR	APAF1	TYK2
FADD	ATM	STAT1
FAS	BAD	CASP4
FASLG	BAX	NLRP1
RIPK1	BCL2	RELB
TNF	BCL2L1	P2RX4
TP53	BID	SENP6
TRAF2	BIRC2	IFI16
ALKBH7	BIRC3	IRF8
ARHGEF2	CAPN1	GBP2
BNIP3	CAPN2	SARM1
BOK	CASP10	IRAK4
CAV1	CASP3	DDX58
CD14	CASP6	IFNG
CYLD	CASP7	TP53
DNM1L	CASP8	RIPK3
FZD9	CASP9	BRD4
GSDME	CFLAR	ZBP1
HEBP2	CHP1	BAX
IPMK	CHP2	NEDD4
IRF3	CHUK	NOD2
ITPK1	CSF2RB	MAP3K7
LY96	CYCS	TNFRSF4
MAP3K5	DFFA	CLEC4E
MLKL	DFFB	MAPK8
MT_CO2	ENDOD1	SOD1
MT3	ENDOG	DPP8

<sup>3</sup> Downloaded from <https://www.gsea-msigdb.org/gsea/index.jsp>

MTCO2P12	EXOG	ADCY4
PELI1	FADD	CTSB
PGAM5	FAS	BRCC3
PPIF	FASLG	NLRC5
PYGL	IKBKB	DDX3X
RBCK1	IKBKG	PTGER2
RIPK3	IL1A	GSDMA
SLC25A4	IL1B	TICAM1
SPATA2	IL1R1	HIF1A
TICAM1	IL1RAP	HSPA12A
TICAM2	IL3	HDAC6
TLR3	IL3RA	ADRA2B
TLR4	IRAK1	POP1
TMEM123	IRAK2	NLRP9
TRPM7	IRAK3	CARD8
TSPO	MAP3K14	NEK7
UCN	MYD88	HMOX1
YBX3	NFKB1	HK1
	NFKBIA	BNIP3
	NGF	NLRC4
	NTRK1	NFKB2
	PIK3CA	TLR2
	PIK3CB	IRGM
	PIK3CD	KCNK6
	PIK3CG	FADD
	PIK3R1	RELA
	PIK3R2	PRKACA
	PIK3R3	GZMA
	PIK3R5	FOXO1
	PPP3CA	AOAH
	PPP3CB	NLRP2
	PPP3CC	LDLR
	PPP3R1	RIPK1
	PPP3R2	GSDMD
	PRKACA	ATG7
	PRKACB	CYCS
	PRKACG	SERPINB1
	PRKAR1A	AIM2
	PRKAR1B	IRF1
	PRKAR2A	MAPK1
	PRKAR2B	NFKB1
	PRKX	CASP9
	RELA	DAPK3

	RIPK1	NAIP
	TNF	PYDC2
	TNFRSF10A	CASP6
	TNFRSF10B	GBP3
	TNFRSF10C	PRKAA1
	TNFRSF10D	PDCD6IP
	TNFRSF1A	TRAF6
	TNFSF10	GSDMB
	TP53	SDHB
	TRADD	GSDMC
	TRAF2	PELI2
	XIAP	IL18
		P2RX7
		IRF2
		IRAK1
		TOMM20
		TNF
		NLRP3
		IL1b
		PCSK9
		EP300
		DHX9
		TXNIP
		CD63
		NFE2L2
		MEFV
		MUL1
		SEN7
		CAMP
		MALT1
		GPX4
		IL13
		KLF2
		TLR3
		PRKACG
		PANX1
		PYCARD
		NLRX1
		JOSD2
		IRF3
		NLRP12
		NOS2
		RHOA

		REL
		TLR4
		CASP5
		JAK1
		NLRP7
		CASP3
		TNFRSF1A
		CD274
		PDE8A
		MAPK14
		KAT2B
		GBP4
		NR1H2
		CDC37
		GZMB
		CASP1
		BTK
		SYK
		GBP1
		HMGB1
		MYD88
		STAT3
		DPP9
		CYLD
		PTGER4
		NLRP6
		CASP8

### **Silencing RNA screen**

siRNAs for siRNA-mediated gene silencing were purchased at Horizon Discovery Ltd.. Lyophilized siRNAs were diluted in siRNA buffer as a stock solution of 100µM and incubated for 30min on a bench rocker. Transfection reagent LipofectaminRNAiMAX was diluted 1:100 in OptiMEM and for each well (96 well plate) 25µl transfection reagent with a final siRNA concentration of 25nM was added. For each siRNA quadruplicates were plated. After 30min of incubation 7000 cells per well were plated in 100µl RPMI supplemented with 10% FBS. NK-92 cells for co-culture conditions were added in a 1:1 ration in 100µl alphaMEM (supplemented as described in ...) to 2 wells

of each siRNA, the 2 remaining control wells were filled with 100µl supplemented alphaMEM. The plates were placed in the Incucyte and observed for 72h. Incucyte analysis was performed with basic analyzer using following parameters:

PC9: segmentation adjustment 1, minimum area filter 500µm<sup>2</sup>

HCC15: segmentation adjustment 0.7, minimum area filter 550µm<sup>2</sup>

H1819: segmentation adjustment 1.1, minimum area filter 1200µm<sup>2</sup>

*Table 14 siRNA sequences*

Gene Symbol	GENE ID	Gene Accession	Sequence
HLA-DRB5	3127	NM_002125	CUGCUUGGCUCUUAUUCUU
HLA-DRB5	3127	NM_002125	CGUGAGCUGAAGUGCAGAU
HLA-DRB5	3127	NM_002125	CAGAAAUGUCCAUCUUG
HLA-DRB5	3127	NM_002125	ACCUGGCUCCAAAGACAAA
MAGEA10	4109	NM_021048	AGUGCAAGUUCUAGCGCUA
MAGEA10	4109	NM_021048	GGUAAAUGGGAGUGAUCCA
MAGEA10	4109	NM_021048	GGUCUUUGGCAUUGAUGUA
MAGEA10	4109	NM_021048	CAAAGGAGGAGAGUCCAA
TRPM2	7226	NM_003307	AGACGGAGUUCUGAUCUA
TRPM2	7226	NM_003307	CGGCAACAAUGACAAGCAA
TRPM2	7226	NM_003307	UCGAGGACAUCAGCAAUAA
TRPM2	7226	NM_003307	GACAAUGCCUGGAUCGAGA
PIK3CD	5293	NM_005026	ACGAUGAGCUGUCCAGUA
PIK3CD	5293	NM_005026	CCAAAGACAACAGGCAGUA
PIK3CD	5293	NM_005026	GCGUGGGCAUCAUCUUUAA
PIK3CD	5293	NM_005026	CGAGUGAAGUUUAACGAAG
STAT3	6774	NM_213662	GAGAUUGACCAGCAGUAUA
STAT3	6774	NM_213662	CAACAUGUCAUUUGCUGAA
STAT3	6774	NM_213662	CCAACAAUCCCAAGAAUGU
STAT3	6774	NM_213662	CAACAGAUUGCCUGCAUUG
C8orf4	56892	NM_020130	GUAAGAAAGCCGUGGGCAA
C8orf4	56892	NM_020130	GGAGAGAGCCAAGAUCAUU
C8orf4	56892	NM_020130	GAAACUCUGGAGACAAGAA
C8orf4	56892	NM_020130	GAAAACGCGUGCCUGAUG
BZW1	9689	NM_014670	GCAGAUGACAUGAUGCGUA
BZW1	9689	NM_014670	CAGCAAAGCCAACGCUAU
BZW1	9689	NM_014670	CGUAAUGGAGUUUGAGUAA
BZW1	9689	NM_014670	GCUUCGUUCUCUUAUAUA
CNTFR	1271	NM_001842	CCGGGAAGGAGUACAUUAU
CNTFR	1271	NM_001842	CUGCAUGGCUCCAAAAUUA
CNTFR	1271	NM_001842	GGACUGAGGAACCGCGACA
CNTFR	1271	NM_001842	UACAAGGUCUCCAUAAGUG
RAB1B	81876	NM_030981	UGCAGGAGAUUGACCGCUA
RAB1B	81876	NM_030981	CCAGCGAGAACGUCAAUAA
RAB1B	81876	NM_030981	CGGUGGGAUUCUGAGUAUAU
RAB1B	81876	NM_030981	GAAUAUGACUACCUGUUUA
HES3	390992	NM_001024598	CCUAUUUGGUCUCGCGACA
HES3	390992	NM_001024598	CGGAAGCGCAAUUGGAGA

HES3	390992	NM_001024598	GGGGAUGACCUGAACUGAA
HES3	390992	NM_001024598	AUCCUGGAGUUGAGCGUGA
MRPL18	29074	NM_014161	UGGCACAGGUUGCGAGUUA
MRPL18	29074	NM_014161	GCAAGUCAGAAGUUGUUUA
MRPL18	29074	NM_014161	GAUGCUUAGAGGCGGGAAU
MRPL18	29074	NM_014161	UUGUGAGAGUAUAGGACGA
CD48	962	NM_001778	GAAACUGUCAUGUGUGAUA
CD48	962	NM_001778	GGAGUAGAAUGGAUUGCAA
CD48	962	NM_001778	GCACCUACAUCAUGAGGGU
CD48	962	NM_001778	CUAAGUACUUUGAAUCCAA
CD58	965	NM_001779	UAACUUGUGCAUUGACUAA
CD58	965	NM_001779	GAAGUUCUUUCUUUAUGUG
CD58	965	NM_001779	GCACUUUAACCCAUACCAU
CD58	965	NM_001779	CGCCAAAUUUACUGAUAC
MICB	4277	NM_005931	GCUAUGAACGUCACAAAUU
MICB	4277	NM_005931	GACAGACUUUCCAUAUGUU
MICB	4277	NM_005931	GCUACUGGGUCCACUGGUU
MICB	4277	NM_005931	CUGCUGCUAUGCCAUGUUU
SDC2	6383	NM_002998	CAAAGAGCCUGUCGAUGA
SDC2	6383	NM_002998	GAAACCACGACGCUGAAUA
SDC2	6383	NM_002998	GACUGGUGUUAAUGAGUAU
SDC2	6383	NM_002998	CAAGAUACCUGCUCAGACA
TMEM156	80008	NM_024943	GAUCAACAAUCAUGGAGGA
TMEM156	80008	NM_024943	GAGGAAGUGAUUCGGAGAA
TMEM156	80008	NM_024943	AGCAAGGAGAAAUCGAUAA
TMEM156	80008	NM_024943	UGAGAUCAAUAUACACGAA
ADGRL2	23266	NM_012302	CGACAAACGUGCCGCAUCA
ADGRL2	23266	NM_012302	GAGGAAAGACUGAUAU CGA
ADGRL2	23266	NM_012302	ACAGAACAAUGGAAUGAUA
ADGRL2	23266	NM_012302	AAAUUUGACUUGAGGACUA
IGFBP5	3488	NM_000599	CGCAAAGGAUUCUACAAGA
IGFBP5	3488	NM_000599	GAAAGAAGCUGACCCAGUC
IGFBP5	3488	NM_000599	GAUCAUCUCUGCACCUGAG
IGFBP5	3488	NM_000599	GCAGGGAACGCAUGAUUCA
ICAM1	3383	NM_000201	GGUAGCAGCCGCAGUCAUA
ICAM1	3383	NM_000201	GAGCCAAGGUGACGCUGAA
ICAM1	3383	NM_000201	CGGCUGACGUGUGCAGUAA
ICAM1	3383	NM_000201	GAAGAUAGCCAACCAAUGU
FAS	355	NM_152876	GAACAUGGAAUCAUCAAGG
FAS	355	NM_152876	UGGAAGGCCUGCAUCAUGA
FAS	355	NM_152876	UGAGGAAGACUGUUACUAC
FAS	355	NM_152876	GCGUAUGACACAUUGAUUA
TNFRSF10B	8795	NM_147187	GCAAAUAUGGACAGGACUA
TNFRSF10B	8795	NM_147187	GCAAGUCUUUACUGUGGAA
TNFRSF10B	8795	NM_147187	CAAGGUCGGUGAUUGUACA
TNFRSF10B	8795	NM_147187	UCAUGUAUCUJAGAAGGUAA
HLA-B	3106	NM_005514	GGACCAAACUCAGGACACU
HLA-B	3106	NM_005514	CAUCGGAGCUGUGGUCGCU
HLA-B	3106	NM_005514	ACACCCAGUUCGUGAGGUU

HLA-B	3106	NM_005514	UGGAGAACGGGAAGGACAA
HLA-DPA1	3113	NM_033554	CGGACCAUGUGUCAACUUA
HLA-DPA1	3113	NM_033554	UAAAGUCUCUGCGUUCUGG
HLA-DPA1	3113	NM_033554	GAUUACAGCUUCCACAAGU
HLA-DPA1	3113	NM_033554	GAAAUACUGUAAAGGUGAC
ON-TARGETplus Non-targeting Control	0		UGGUUUACAUGUCGACUAA
ON-TARGETplus Non-targeting Control	0		UGGUUUACAUGUUGUGUGA
ON-TARGETplus Non-targeting Control	0		UGGUUUACAUGUUUUCUGA
ON-TARGETplus Non-targeting Control	0		UGGUUUACAUGUUUCCUA
ON-TARGETplus Cyclophilin Control	0		ACAGCAAUCCAUCGUGU
ON-TARGETplus Cyclophilin Control	0		GAAAGAGCAUCUACGGUGA
ON-TARGETplus Cyclophilin Control	0		GAAAGGAUUUGGCUACAAA
ON-TARGETplus Cyclophilin Control	0		GGAAAGACUGUCCAAAAA



## List of figures

Figure 1 Balancing inhibitory and activation signal in NK cell - tumor cell interaction..	8
Figure 2 Schematic overview of NK cell receptor downstream signaling and crosstalk .....	12
Figure 3 Overview of NK cell mediated target cell lysis.....	13
Figure 4 Overview of characteristic features of the cell death pathways.....	17
Figure 5 Characterization of the NK-92/tumor cell co-culture system.....	24
Figure 6 NK-92 show activation markers during co-culture with human lung cancer cell lines .....	25
Figure 7 RNA sequencing of co-cultured cancer cell lines PC9 and Colo699 revealed a strong activation of immune response .....	28
Figure 8 Sensitivities towards NK-92 cell killing varied largely between cell lines .....	28
Figure 9 Lung cancer cell lines undergo apoptosis following NK-92 co-culture with a partial rescue for pan-caspase inhibition .....	30
Figure 10 Cancer cell death upon NK-92 co-culture showed features of apoptosis, pyroptosis and for the cell line H2087 necroptosis as well .....	32
Figure 11 Cell death gene signatures enriched in highly sensitive cell lines.....	33
Figure 12 HLA-expression or NK cell ligands did not define tumor cell sensitivity towards NK cell killing .....	35
Figure 13 High sensitivity cluster revealed pro-apoptotic signatures, whereas anti- apoptotic signatures (hedgehog) and activation of the pro-survival AKT pathway were increased in the low sensitivity cluster.....	37
Figure 14 NK-92 resistant cell lines PC9 and Colo699 revealed minor genetical changes .....	39
Figure 15 NK-92 resistant cell lines exhibited survival signaling and epithelial-to- mesenchymal signature enrichment .....	41
Figure 16 Summary of results .....	42
Figure 17 Workflow of the embedding of tumor spheroids.....	52

## List of tables

Table 1 Natural Killer cell receptors and their ligands .....	9
Table 2 Overview of human granzymes and their substrates .....	15
Table 3 HLA matching between NK-92 and cancer cell lines .....	34
Table 4 Table of inhibitors .....	49
Table 5 List of primary western blot antibodies .....	53
Table 6 List of secondary western blot antibodies.....	54
Table 7 FACS antibodies.....	54
Table 8 Reaction 1 .....	55
Table 9 Reaction 2.....	55
Table 10 Reaction 3.....	56
Table 11 RT-qPCR program QuantStudio5.....	56
Table 12 List of qPCR primers .....	56
Table 13 Additional gene sets used for GSEA (Ahluwalia et al., 2021) .....	58
Table 14 siRNA sequences .....	62

## List of abbreviations

2D	two-dimensional
3BP2	c-Abl Src homology 3 domain-binding protein-2
3D	three-dimensional
AIM2	absent in menaloma 2
alpha-MEM	alpha Modified Eagle Medium
APAF-1	apoptosis protease activation factor 1
APE1	DNA (apurinic/aprimidinic site) endonuclease 1
ASC	adaptor protein apoptosis-associated speck-like protein containing a CARD
B7-H6	HHLA2
BAD	BCL2 associated agonist of cell death
BAK	Bcl-2 homologous antagonist/killer protein
BAX	Bcl-2-associated X protein
BCA	Bicinchoninic acid
BCL-2	B-cell lymphoma 2
BCL-XL	B-cell lymphoma extra large
BID	BH3 interacting domain death agonist
BIK	BCL2 Interacting Killer
BIM	BCL2-Like 11
BPTF	bromodomain PHD finger transcription factor gene
BST2	bone marrow stromal antigen 2
Ca <sup>2+</sup>	Calcium ion
CADM1	Cell Adhesion Molecule 1
CARD	caspase activation and recruitment domains
Casp8ko	caspase 8 knockout
CCL	chemokine (C-C motif) ligand
CD	Cluster of differentiation
CEACAM	carcinoembryonic antigen-related cell adhesion molecule
CECAD	Cellular Stress Responses in Aging-Associated Diseases
ciAP	cellular inhibitor of apoptosis proteins
CO <sub>2</sub>	Carbon dioxide
CRK	CT10-regulated kinase
CXCL	C-X-C Motif Chemokine Ligand
DAMP	damage-associated molecular pattern
DNA	Deoxyribonucleic acid
DNA-PK	DNA-dependent protein kinase
DAP	Death-associated protein
dATP	Deoxyadenosine triphosphate
DISC	death inducing signaling complex
DMSO	Dimethyl sulfoxide
DNAM-1	DNAX-accessory molecule
EAT-2	SH2 domain-containing protein 1B

EDTA	Ethylenediaminetetraacetic acid
EMT	epithelial-mesenchymal transition
ERK	Extracellular-signal regulated kinases
ERT	Ethylene-responsive transcriptional coactivator-like protein
F-actin	fibrous actin
FACS	Fluorescence-activated cell sorting
FADD	FAS-associated death domain protein
FasL	FAS-ligand
FBS	fetal bovine serum
FLIP	FADD-like ICE-like Inhibitory Protein
G-actin	globular actin
GBP2	guanylate binding protein 2
GCU	green Object Integrated Intensity
GO terms	gene ontology terms
GRB2	Growth factor receptor-bound protein 2
grzB	Ganzyme B
GSDMD	Gasdermin D
GSEA	gene set enrichment analysis
h	hours
HHLA2	HERV-H LTR-Associating Protein 2
HLA	human leukocyte antigen
HMGB2	High Mobility Group Box 2
IAP	Inhibitors of apoptosis
ICAD	Inhibitor of Caspase-activated DNase
ICAM1	Intercellular Adhesion Molecule 1
IDO	Indoleamine-pyrrole 2,3-dioxygenase
IFIT2	interferon induced protein with tetratricopeptide repeats 2
IFNgamma	interferon gamma
IL	Interleukin
ILT2	inhibitory receptors Ig-like transcript 2
ITAM	immunoreceptor tyrosine activation motif
ITIM	immunoreceptor tyrosin-based inhibitory motif
ITSM	immunoreceptor tyrosine based switch motif
JAG1	Jagged 1
JAK	Janus kinase
KIR	killer-immunoglobulin-like receptor
KLRG1	Killer cell lectin-like receptor subfamily G member 1
KRAS	Kirsten rat sarcoma virus
LAG-3	Lymphocyte-activation gene 3
LAIR	Leukocyte-associated immunoglobulin-like receptor
LAMP-1	Lysosomal-associated membrane protein 1
LAT	Linker for activation of T cells
LFA1	Lymphocyte function associated antigen 1

MAGEA10	Melanoma-associated antigen 10
MCL-1	Myeloid leukemia 1
Mg+	Magnesium ion
MHC	major histocompatibility complex
MIC	MHC class I polypeptide-related sequence
min	minutes
MLKL	mixed lineage kinase domain-like
Mn+	manganese ions
MOMP	mitochondrial outer membrane permeabilization
MTOC	microtubule organization center
MUNCH13-4	member of the Unc13 protein family
NCR	NK cell receptor
NDUFS3	Nicotinamide adenine dinucleotide dehydrogenase [ubiquinone] iron-sulfur protein 3
Nec1	Necrostatin 1
NF- $\kappa$ B	nuclear factor k-light-chain-enhancer of activated B cells
NK	Natural killer
NKG2A	natural-killer group 2, member A
NKG2C	natural-killer group 2, member C
NKG2D	natural-killer group 2, member D
NKp	Natural cytotoxicity triggering receptor
NLR	nucleotide-binding domain, leucine rich containing protein
NLRC5	NOD-like receptor family CARD domain containing 5
NLRP3	NLR Family Pyrin Domain Containing 3
nN	nano newton
NOD	nucleotide oligomerization domain-containing protein
NOXA	PMAIP1
NTAL	Non-T cell activation linker
OASL	Oligoadenylate synthase-like
ORAI1	calcium release-activated calcium modulator 1
OSCC	oral squamous cell carcinoma
p-	phosphorylated-
PAMP	pathogen-associated molecular pattern
PARP	Poly (ADP-ribose) polymerase
PB	peripheral blood
PBMC	Peripheral blood mononuclear cells
PBS	Phosphate-buffered Saline
PCNA	Proliferating cell nuclear antigen
PD-L1	Programmed death-ligand 1
Pen/Strep	penicillin/streptomycin
PGE2	prostaglandin E2
PI3CD	Phosphatidylinositol-4,5-Bisphosphate 3-Kinase Catalytic Subunit Delta
PI3K	Phosphoinositide 3-kinases

PLCg	Phospholipase C, gamma
PLXNC1	Plexin cytoplasmic RasGAP domain-containing protein
PMAIP	Phorbol-12-myristate-13-acetate-induced protein
PSMB8	Proteasome subunit beta type-8
PUMA	p53 upregulated modulator of apoptosis
PVDF	polyvinylidene difluoride
PVR	poliovirus receptor
PVRL2	Poliovirus receptor-related 2
PYK2	Protein Tyrosine Kinase 2 Beta
QVD	Q-VD-OPh
RAB	Ras-associated binding protein
RAP27a	Ras-related protein Rab-27A
RAS	Rat sarcoma virus
RCU	Red Object Integrated Intensity
RHO	Ras homologous
RIPA	Radioimmunoprecipitation assay buffer
RIPK	Receptor-interacting serine/threonine-protein kinase
RNA	Ribonucleic acid
RPMI	Roswell Park Memorial Institute
RSAD2	Radical S-adenosyl methionine domain-containing protein 2
SAP	serum amyloid P component
SDS	sodium dodecyl sulfate
SDS PAGE	SDS Polyacrylamide gel electrophoresis
SH2	Src Homology 2
SHP	small heterodimer partner
siRNA	silencing RNA
SLAM	signaling lymphocytic activation molecule
SLP76	Lymphocyte cytosolic protein 2
SMAD	supramolecular attack particle
STAT	signal transducer and activator of transcription
SYK	spleen tyrosine kinase
t-SNAREs	target synaptosome-associated protein receptor
TBS	tris-buffered saline
TBST	tris-buffered saline tween20
TCR	T cell receptor
TGFbeta	Transforming growth factor beta
TIGIT	T Cell Immunoreceptor With Ig And ITIM Domains
TIM3	T cell immunoglobulin and mucin domain-containing protein 3
TLR	Toll like receptor
TNFalpha	Tumor necrosis factor alpha
TNFSF13	TNF super family 13
TRADD	Tumor necrosis factor receptor type 1-associated DEATH domain
TRAF	Tumor necrosis factor receptor-associated factor

TRAIL	TNF-related apoptosis-inducing ligand
TRAIL-R	TRAIL receptor
ULBP	UL16-binding proteins
v-SNARE	vesicle synaptosome-associated protein receptor
VAMP7	VAMP7 vesicle associated membrane protein 7
VAV1	vav guanine nucleotide exchange factor 1
WASP	Wiskott–Aldrich Syndrome protein
XIAP	X-linked inhibitor of apoptosis protein
ZAP70	Zeta Chain Of T Cell Receptor Associated Protein Kinase 70

## Literature

- Ahluwalia, P., Ahluwalia, M., Mondal, A. K., Sahajpal, N., Kota, V., Rojiani, M. V., . . . Kolhe, R. (2021). Immunogenomic Gene Signature of Cell-Death Associated Genes with Prognostic Implications in Lung Cancer. *Cancers (Basel)*, 13(1). doi:10.3390/cancers13010155
- Aldemir, H., Prod'homme, V., Dumaurier, M. J., Retiere, C., Poupon, G., Cazareth, J., . . . Braud, V. M. (2005). Cutting edge: lectin-like transcript 1 is a ligand for the CD161 receptor. *J Immunol*, 175(12), 7791-7795. doi:10.4049/jimmunol.175.12.7791
- Almishri, W., Santodomingo-Garzon, T., Le, T., Stack, D., Mody, C. H., & Swain, M. G. (2016). TNFalpha Augments Cytokine-Induced NK Cell IFNgamma Production through TNFR2. *J Innate Immun*, 8(6), 617-629. doi:10.1159/000448077
- Ambrose, A. R., Hazime, K. S., Worboys, J. D., Niembro-Vivanco, O., & Davis, D. M. (2020). Synaptic secretion from human natural killer cells is diverse and includes supramolecular attack particles. *Proc Natl Acad Sci U S A*, 117(38), 23717-23720. doi:10.1073/pnas.2010274117
- Andrade, F., Roy, S., Nicholson, D., Thornberry, N., Rosen, A., & Casciola-Rosen, L. (1998). Granzyme B directly and efficiently cleaves several downstream caspase substrates: implications for CTL-induced apoptosis. *Immunity*, 8(4), 451-460. doi:10.1016/s1074-7613(00)80550-6
- Andre, P., Denis, C., Soulas, C., Bourbon-Caillet, C., Lopez, J., Arnoux, T., . . . Vivier, E. (2018). Anti-NKG2A mAb Is a Checkpoint Inhibitor that Promotes Anti-tumor Immunity by Unleashing Both T and NK Cells. *Cell*, 175(7), 1731-1743 e1713. doi:10.1016/j.cell.2018.10.014
- Arneson, L. N., Brickshawana, A., Segovis, C. M., Schoon, R. A., Dick, C. J., & Leibson, P. J. (2007). Cutting edge: syntaxin 11 regulates lymphocyte-mediated secretion and cytotoxicity. *J Immunol*, 179(6), 3397-3401. doi:10.4049/jimmunol.179.6.3397
- Baker, G. J., Chockley, P., Yadav, V. N., Doherty, R., Ritt, M., Sivaramakrishnan, S., . . . Lowenstein, P. R. (2014). Natural killer cells eradicate galectin-1-deficient glioma in the absence of adaptive immunity. *Cancer Res*, 74(18), 5079-5090. doi:10.1158/0008-5472.CAN-14-1203
- Barkal, A. A., Weiskopf, K., Kao, K. S., Gordon, S. R., Rosental, B., Yiu, Y. Y., . . . Maute, R. L. (2018). Engagement of MHC class I by the inhibitory receptor LILRB1 suppresses macrophages and is a target of cancer immunotherapy. *Nat Immunol*, 19(1), 76-84. doi:10.1038/s41590-017-0004-z
- Barretina, J., Caponigro, G., Stransky, N., Venkatesan, K., Margolin, A. A., Kim, S., . . . Garraway, L. A. (2012). The Cancer Cell Line Encyclopedia enables predictive modelling of anticancer drug sensitivity. *Nature*, 483(7391), 603-607. doi:10.1038/nature11003
- Beldi-Ferchiou, A., & Caillat-Zucman, S. (2017). Control of NK Cell Activation by Immune Checkpoint Molecules. *Int J Mol Sci*, 18(10). doi:10.3390/ijms18102129
- Bertheloot, D., Latz, E., & Franklin, B. S. (2021). Necroptosis, pyroptosis and apoptosis: an intricate game of cell death. *Cell Mol Immunol*, 18(5), 1106-1121. doi:10.1038/s41423-020-00630-3
- Bhatt, R. S., Berjts, A., Konge, J. C., Mahoney, K. M., Klee, A. N., Freeman, S. S., . . . Freeman, G. J. (2021). KIR3DL3 Is an Inhibitory Receptor for HHLA2 that



- Mediates an Alternative Immunoinhibitory Pathway to PD1. *Cancer Immunol Res*, 9(2), 156-169. doi:10.1158/2326-6066.CIR-20-0315
- Bloch-Queyrat, C., Fondaneche, M. C., Chen, R., Yin, L., Relouzat, F., Veillette, A., . . . Latour, S. (2005). Regulation of natural cytotoxicity by the adaptor SAP and the Src-related kinase Fyn. *J Exp Med*, 202(1), 181-192. doi:10.1084/jem.20050449
- Blokhuis, J. H., Hilton, H. G., Guethlein, L. A., Norman, P. J., Nemat-Gorgani, N., Nakimuli, A., . . . Parham, P. (2017). KIR2DS5 allotypes that recognize the C2 epitope of HLA-C are common among Africans and absent from Europeans. *Immun Inflamm Dis*, 5(4), 461-468. doi:10.1002/iid3.178
- Boucher, D., Monteleone, M., Coll, R. C., Chen, K. W., Ross, C. M., Teo, J. L., . . . Schroder, K. (2018). Caspase-1 self-cleavage is an intrinsic mechanism to terminate inflammasome activity. *J Exp Med*, 215(3), 827-840. doi:10.1084/jem.20172222
- Boyington, J. C., Motyka, S. A., Schuck, P., Brooks, A. G., & Sun, P. D. (2000). Crystal structure of an NK cell immunoglobulin-like receptor in complex with its class I MHC ligand. *Nature*, 405(6786), 537-543. doi:10.1038/35014520
- Bratton, S. B., Walker, G., Srinivasula, S. M., Sun, X. M., Butterworth, M., Alnemri, E. S., & Cohen, G. M. (2001). Recruitment, activation and retention of caspases-9 and -3 by Apaf-1 apoptosome and associated XIAP complexes. *EMBO J*, 20(5), 998-1009. doi:10.1093/emboj/20.5.998
- Brownlie, D., Scharenberg, M., Mold, J. E., Hard, J., Kekalainen, E., Buggert, M., . . . Michaelsson, J. (2021). Expansions of adaptive-like NK cells with a tissue-resident phenotype in human lung and blood. *Proc Natl Acad Sci U S A*, 118(11). doi:10.1073/pnas.2016580118
- Bruder, C., Bulliard, J. L., Germann, S., Konzelmann, I., Bochud, M., Leyvraz, M., & Chiolero, A. (2018). Estimating lifetime and 10-year risk of lung cancer. *Prev Med Rep*, 11, 125-130. doi:10.1016/j.pmedr.2018.06.010
- Bryceson, Y. T., March, M. E., Barber, D. F., Ljunggren, H. G., & Long, E. O. (2005). Cytolytic granule polarization and degranulation controlled by different receptors in resting NK cells. *J Exp Med*, 202(7), 1001-1012. doi:10.1084/jem.20051143
- Buganim, Y., Goldstein, I., Lipson, D., Milyavsky, M., Polak-Charcon, S., Mardoukh, C., . . . Rotter, V. (2010). A novel translocation breakpoint within the BPTF gene is associated with a pre-malignant phenotype. *PLoS One*, 5(3), e9657. doi:10.1371/journal.pone.0009657
- Burnell, S. E. A., Capitani, L., MacLachlan, B. J., Mason, G. H., Gallimore, A. M., & Godkin, A. (2022). Seven mysteries of LAG-3: a multi-faceted immune receptor of increasing complexity. *Immunother Adv*, 2(1), ltab025. doi:10.1093/immadv/ltab025
- Cain, K., Brown, D. G., Langlais, C., & Cohen, G. M. (1999). Caspase activation involves the formation of the aposome, a large (approximately 700 kDa) caspase-activating complex. *J Biol Chem*, 274(32), 22686-22692. doi:10.1074/jbc.274.32.22686
- Campbell, K. S., & Purdy, A. K. (2011). Structure/function of human killer cell immunoglobulin-like receptors: lessons from polymorphisms, evolution, crystal structures and mutations. *Immunology*, 132(3), 315-325. doi:10.1111/j.1365-2567.2010.03398.x
- Cancer Stat Facts: Lung and Bronchus Cancer. Retrieved from <https://seer.cancer.gov/statfacts/html/lungb.html>

- Caserta, T. M., Smith, A. N., Gultice, A. D., Reedy, M. A., & Brown, T. L. (2003). Q-VD-OPh, a broad spectrum caspase inhibitor with potent antiapoptotic properties. *Apoptosis*, 8(4), 345-352. doi:10.1023/a:1024116916932
- Casey, T. M., Meade, J. L., & Hewitt, E. W. (2007). Organelle proteomics: identification of the exocytic machinery associated with the natural killer cell secretory lysosome. *Mol Cell Proteomics*, 6(5), 767-780. doi:10.1074/mcp.M600365-MCP200
- Catalan, E., Charni, S., Jaime, P., Aguilo, J. I., Enriquez, J. A., Naval, J., . . . Anel, A. (2015). MHC-I modulation due to changes in tumor cell metabolism regulates tumor sensitivity to CTL and NK cells. *Oncoimmunology*, 4(1), e985924. doi:10.4161/2162402X.2014.985924
- Chen, R., Relouzat, F., Roncagalli, R., Aoukaty, A., Tan, R., Latour, S., & Veillette, A. (2004). Molecular dissection of 2B4 signaling: implications for signal transduction by SLAM-related receptors. *Mol Cell Biol*, 24(12), 5144-5156. doi:10.1128/MCB.24.12.5144-5156.2004
- Chen, R., Wang, X., Dai, Z., Wang, Z., Wu, W., Hu, Z., . . . Cheng, Q. (2021). TNFSF13 Is a Novel Onco-Inflammatory Marker and Correlates With Immune Infiltration in Gliomas. *Front Immunol*, 12, 713757. doi:10.3389/fimmu.2021.713757
- Chen, X., Allan, D. S. J., Krzewski, K., Ge, B., Kopcow, H., & Strominger, J. L. (2006). CD28-stimulated ERK2 phosphorylation is required for polarization of the microtubule organizing center and granules in YTS NK cells. *Proc Natl Acad Sci U S A*, 103(27), 10346-10351. doi:10.1073/pnas.0604236103
- Chen, X., Li, W., Ren, J., Huang, D., He, W. T., Song, Y., . . . Han, J. (2014). Translocation of mixed lineage kinase domain-like protein to plasma membrane leads to necrotic cell death. *Cell Res*, 24(1), 105-121. doi:10.1038/cr.2013.171
- Cheng, E. H., Wei, M. C., Weiler, S., Flavell, R. A., Mak, T. W., Lindsten, T., & Korsmeyer, S. J. (2001). BCL-2, BCL-X(L) sequester BH3 domain-only molecules preventing BAX- and BAK-mediated mitochondrial apoptosis. *Mol Cell*, 8(3), 705-711. doi:10.1016/s1097-2765(01)00320-3
- Chockley, P. J., Chen, J., Chen, G., Beer, D. G., Standiford, T. J., & Keshamouni, V. G. (2018). Epithelial-mesenchymal transition leads to NK cell-mediated metastasis-specific immunosurveillance in lung cancer. *J Clin Invest*, 128(4), 1384-1396. doi:10.1172/JCI97611
- Choudhary, G. S., Tat, T. T., Misra, S., Hill, B. T., Smith, M. R., Almasan, A., & Mazumder, S. (2015). Cyclin E/Cdk2-dependent phosphorylation of Mcl-1 determines its stability and cellular sensitivity to BH3 mimetics. *Oncotarget*, 6(19), 16912-16925. doi:10.18632/oncotarget.4857
- Chowdhury, D., & Lieberman, J. (2008). Death by a thousand cuts: granzyme pathways of programmed cell death. *Annu Rev Immunol*, 26, 389-420. doi:10.1146/annurev.immunol.26.021607.090404
- Claus, M., Urlaub, D., Fasbender, F., & Watzl, C. (2019). SLAM family receptors in natural killer cells - Mediators of adhesion, activation and inhibition via cis and trans interactions. *Clin Immunol*, 204, 37-42. doi:10.1016/j.clim.2018.10.011
- Cohnen, A., Chiang, S. C., Stojanovic, A., Schmidt, H., Claus, M., Saftig, P., . . . Watzl, C. (2013). Surface CD107a/LAMP-1 protects natural killer cells from degranulation-associated damage. *Blood*, 122(8), 1411-1418. doi:10.1182/blood-2012-07-441832

- Colucci, F., Schweighoffer, E., Tomasello, E., Turner, M., Ortaldo, J. R., Vivier, E., . . . Di Santo, J. P. (2002). Natural cytotoxicity uncoupled from the Syk and ZAP-70 intracellular kinases. *Nat Immunol*, 3(3), 288-294. doi:10.1038/ni764
- Cong, J., Wang, X., Zheng, X., Wang, D., Fu, B., Sun, R., . . . Wei, H. (2018). Dysfunction of Natural Killer Cells by FBP1-Induced Inhibition of Glycolysis during Lung Cancer Progression. *Cell Metab*, 28(2), 243-255 e245. doi:10.1016/j.cmet.2018.06.021
- Cullen, S. P., & Martin, S. J. (2008). Mechanisms of granule-dependent killing. *Cell Death Differ*, 15(2), 251-262. doi:10.1038/sj.cdd.4402244
- da Silva, I. L., Montero-Montero, L., Ferreira, E., & Quintanilla, M. (2018). New Insights Into the Role of Qa-2 and HLA-G Non-classical MHC-I Complexes in Malignancy. *Front Immunol*, 9, 2894. doi:10.3389/fimmu.2018.02894
- Demarco, B., Grayczyk, J. P., Bjanes, E., Le Roy, D., Tonnus, W., Assenmacher, C. A., . . . Broz, P. (2020). Caspase-8-dependent gasdermin D cleavage promotes antimicrobial defense but confers susceptibility to TNF-induced lethality. *Sci Adv*, 6(47). doi:10.1126/sciadv.abc3465
- Deuss, F. A., Watson, G. M., Fu, Z., Rossjohn, J., & Berry, R. (2019). Structural Basis for CD96 Immune Receptor Recognition of Nectin-like Protein-5, CD155. *Structure*, 27(2), 219-228 e213. doi:10.1016/j.str.2018.10.023
- Dogra, P., Rancan, C., Ma, W., Toth, M., Senda, T., Carpenter, D. J., . . . Farber, D. L. (2020). Tissue Determinants of Human NK Cell Development, Function, and Residence. *Cell*, 180(4), 749-763 e713. doi:10.1016/j.cell.2020.01.022
- Ermolaeva, M. A., Michallet, M. C., Papadopoulou, N., Utermohlen, O., Kranidioti, K., Kollias, G., . . . Paspaparakis, M. (2008). Function of TRADD in tumor necrosis factor receptor 1 signaling and in TRIF-dependent inflammatory responses. *Nat Immunol*, 9(9), 1037-1046. doi:10.1038/ni.1638
- Fellows, E., Gil-Parrado, S., Jenne, D. E., & Kurschus, F. C. (2007). Natural killer cell-derived human granzyme H induces an alternative, caspase-independent cell-death program. *Blood*, 110(2), 544-552. doi:10.1182/blood-2006-10-051649
- Fritsch, M., Gunther, S. D., Schwarzer, R., Albert, M. C., Schorn, F., Werthenbach, J. P., . . . Kashkar, H. (2019). Caspase-8 is the molecular switch for apoptosis, necroptosis and pyroptosis. *Nature*, 575(7784), 683-687. doi:10.1038/s41586-019-1770-6
- Gao, Y., Yang, J., Cai, Y., Fu, S., Zhang, N., Fu, X., & Li, L. (2018). IFN-gamma-mediated inhibition of lung cancer correlates with PD-L1 expression and is regulated by PI3K-AKT signaling. *Int J Cancer*, 143(4), 931-943. doi:10.1002/ijc.31357
- Garcia-Beltran, W. F., Holzemer, A., Martrus, G., Chung, A. W., Pacheco, Y., Simoneau, C. R., . . . Altfeld, M. (2016). Open conformers of HLA-F are high-affinity ligands of the activating NK-cell receptor KIR3DS1. *Nat Immunol*, 17(9), 1067-1074. doi:10.1038/ni.3513
- Garrity, D., Call, M. E., Feng, J., & Wucherpfennig, K. W. (2005). The activating NKG2D receptor assembles in the membrane with two signaling dimers into a hexameric structure. *Proc Natl Acad Sci U S A*, 102(21), 7641-7646. doi:10.1073/pnas.0502439102
- Ghandi, M., Huang, F. W., Jane-Valbuena, J., Kryukov, G. V., Lo, C. C., McDonald, E. R., 3rd, . . . Sellers, W. R. (2019). Next-generation characterization of the Cancer Cell Line Encyclopedia. *Nature*, 569(7757), 503-508. doi:10.1038/s41586-019-1186-3

- Ghavami, S., Hashemi, M., Ande, S. R., Yeganeh, B., Xiao, W., Eshraghi, M., . . . Los, M. (2009). Apoptosis and cancer: mutations within caspase genes. *J Med Genet*, *46*(8), 497-510. doi:10.1136/jmg.2009.066944
- Giurisato, E., Cella, M., Takai, T., Kurosaki, T., Feng, Y., Longmore, G. D., . . . Shaw, A. S. (2007). Phosphatidylinositol 3-kinase activation is required to form the NKG2D immunological synapse. *Mol Cell Biol*, *27*(24), 8583-8599. doi:10.1128/MCB.01477-07
- Gocher, A. M., Workman, C. J., & Vignali, D. A. A. (2022). Interferon-gamma: teammate or opponent in the tumour microenvironment? *Nat Rev Immunol*, *22*(3), 158-172. doi:10.1038/s41577-021-00566-3
- Gon, S., Gatanaga, T., & Sendo, F. (1996). Involvement of two types of TNF receptor in TNF-alpha induced neutrophil apoptosis. *Microbiol Immunol*, *40*(6), 463-465. doi:10.1111/j.1348-0421.1996.tb01095.x
- Gong, J. H., Maki, G., & Klingemann, H. G. (1994). Characterization of a human cell line (NK-92) with phenotypical and functional characteristics of activated natural killer cells. *Leukemia*, *8*(4), 652-658. Retrieved from <https://www.ncbi.nlm.nih.gov/pubmed/8152260>
- Graham, D. B., Cella, M., Giurisato, E., Fujikawa, K., Miletic, A. V., Kloepfel, T., . . . Swat, W. (2006). Vav1 controls DAP10-mediated natural cytotoxicity by regulating actin and microtubule dynamics. *J Immunol*, *177*(4), 2349-2355. doi:10.4049/jimmunol.177.4.2349
- Griffiths, G. M., & Isaaz, S. (1993). Granzymes A and B are targeted to the lytic granules of lymphocytes by the mannose-6-phosphate receptor. *J Cell Biol*, *120*(4), 885-896. doi:10.1083/jcb.120.4.885
- Gurung, P., Anand, P. K., Malireddi, R. K., Vande Walle, L., Van Opdenbosch, N., Dillon, C. P., . . . Kanneganti, T. D. (2014). FADD and caspase-8 mediate priming and activation of the canonical and noncanonical Nlrp3 inflammasomes. *J Immunol*, *192*(4), 1835-1846. doi:10.4049/jimmunol.1302839
- Gutierrez-Guerrero, A., Mancilla-Herrera, I., Maravillas-Montero, J. L., Martinez-Duncker, I., Veillette, A., & Cruz-Munoz, M. E. (2022). SLAMF7 selectively favors degranulation to promote cytotoxicity in human NK cells. *Eur J Immunol*, *52*(1), 62-74. doi:10.1002/eji.202149406
- Gwalani, L. A., & Orange, J. S. (2018). Single Degranulations in NK Cells Can Mediate Target Cell Killing. *J Immunol*, *200*(9), 3231-3243. doi:10.4049/jimmunol.1701500
- Habif, G., Crinier, A., Andre, P., Vivier, E., & Narni-Mancinelli, E. (2019). Targeting natural killer cells in solid tumors. *Cell Mol Immunol*, *16*(5), 415-422. doi:10.1038/s41423-019-0224-2
- Ham, H., Medlyn, M., & Billadeau, D. D. (2022). Locked and Loaded: Mechanisms Regulating Natural Killer Cell Lytic Granule Biogenesis and Release. *Front Immunol*, *13*, 871106. doi:10.3389/fimmu.2022.871106
- Hao, Y., Baker, D., & Ten Dijke, P. (2019). TGF-beta-Mediated Epithelial-Mesenchymal Transition and Cancer Metastasis. *Int J Mol Sci*, *20*(11). doi:10.3390/ijms20112767
- Hay, Z. L. Z., & Slansky, J. E. (2022). Granzymes: The Molecular Executors of Immune-Mediated Cytotoxicity. *Int J Mol Sci*, *23*(3). doi:10.3390/ijms23031833
- He, S., Liang, Y., Shao, F., & Wang, X. (2011). Toll-like receptors activate programmed necrosis in macrophages through a receptor-interacting kinase-3-mediated pathway. *Proc Natl Acad Sci U S A*, *108*(50), 20054-20059. doi:10.1073/pnas.1116302108

- Hoffmann, S. C., Cohnen, A., Ludwig, T., & Watzl, C. (2011). 2B4 engagement mediates rapid LFA-1 and actin-dependent NK cell adhesion to tumor cells as measured by single cell force spectroscopy. *J Immunol*, *186*(5), 2757-2764. doi:10.4049/jimmunol.1002867
- Holler, N., Zaru, R., Micheau, O., Thome, M., Attinger, A., Valitutti, S., . . . Tschopp, J. (2000). Fas triggers an alternative, caspase-8-independent cell death pathway using the kinase RIP as effector molecule. *Nat Immunol*, *1*(6), 489-495. doi:10.1038/82732
- Horowitz, A., Djaoud, Z., Nemat-Gorgani, N., Blokhuis, J., Hilton, H. G., Beziat, V., . . . Parham, P. (2016). Class I HLA haplotypes form two schools that educate NK cells in different ways. *Sci Immunol*, *1*(3). doi:10.1126/sciimmunol.aag1672
- Hosomi, S., Chen, Z., Baker, K., Chen, L., Huang, Y. H., Olszak, T., . . . Blumberg, R. S. (2013). CEACAM1 on activated NK cells inhibits NKG2D-mediated cytolytic function and signaling. *Eur J Immunol*, *43*(9), 2473-2483. doi:10.1002/eji.201242676
- Hou, Q., Zhao, T., Zhang, H., Lu, H., Zhang, Q., Sun, L., & Fan, Z. (2008). Granzyme H induces apoptosis of target tumor cells characterized by DNA fragmentation and Bid-dependent mitochondrial damage. *Mol Immunol*, *45*(4), 1044-1055. doi:10.1016/j.molimm.2007.07.032
- Huang, B., Lang, X., & Li, X. (2022). The role of IL-6/JAK2/STAT3 signaling pathway in cancers. *Front Oncol*, *12*, 1023177. doi:10.3389/fonc.2022.1023177
- Huang, C. H., Huang, Y. C., Xu, J. K., Chen, S. Y., Tseng, L. C., Huang, J. L., & Lin, C. S. (2023). ATM Inhibition-Induced ISG15/IFI27/OASL Is Correlated with Immunotherapy Response and Inflamed Immunophenotype. *Cells*, *12*(9). doi:10.3390/cells12091288
- Huergo-Zapico, L., Parodi, M., Cantoni, C., Lavarello, C., Fernandez-Martinez, J. L., Petretto, A., . . . Vitale, M. (2018). NK-cell Editing Mediates Epithelial-to-Mesenchymal Transition via Phenotypic and Proteomic Changes in Melanoma Cell Lines. *Cancer Res*, *78*(14), 3913-3925. doi:10.1158/0008-5472.CAN-17-1891
- Hurkmans, D. P., Basak, E. A., Schepers, N., Oomen-De Hoop, E., Van der Leest, C. H., El Bouazzaoui, S., . . . Mathijssen, R. H. J. (2020). Granzyme B is correlated with clinical outcome after PD-1 blockade in patients with stage IV non-small-cell lung cancer. *J Immunother Cancer*, *8*(1). doi:10.1136/jitc-2020-000586
- Imai, K., Matsuyama, S., Miyake, S., Suga, K., & Nakachi, K. (2000). Natural cytotoxic activity of peripheral-blood lymphocytes and cancer incidence: an 11-year follow-up study of a general population. *Lancet*, *356*(9244), 1795-1799. doi:10.1016/S0140-6736(00)03231-1
- Islami, F., Torre, L. A., & Jemal, A. (2015). Global trends of lung cancer mortality and smoking prevalence. *Transl Lung Cancer Res*, *4*(4), 327-338. doi:10.3978/j.issn.2218-6751.2015.08.04
- Itoh, N., Yonehara, S., Ishii, A., Yonehara, M., Mizushima, S., Sameshima, M., . . . Nagata, S. (1991). The polypeptide encoded by the cDNA for human cell surface antigen Fas can mediate apoptosis. *Cell*, *66*(2), 233-243. doi:10.1016/0092-8674(91)90614-5
- Jandus, C., Boligan, K. F., Chijioke, O., Liu, H., Dahlhaus, M., Demoulins, T., . . . von Gunten, S. (2014). Interactions between Siglec-7/9 receptors and ligands influence NK cell-dependent tumor immunosurveillance. *J Clin Invest*, *124*(4), 1810-1820. doi:10.1172/JCI65899

- Jiang, C., & Okazaki, T. (2022). Control of mitochondrial dynamics and apoptotic pathways by peroxisomes. *Front Cell Dev Biol*, *10*, 938177. doi:10.3389/fcell.2022.938177
- Jiang, W., Li, F., Jiang, Y., Li, S., Liu, X., Xu, Y., . . . Zheng, C. (2022). Tim-3 Blockade Elicits Potent Anti-Multiple Myeloma Immunity of Natural Killer Cells. *Front Oncol*, *12*, 739976. doi:10.3389/fonc.2022.739976
- Johnston, R. J., Comps-Agrar, L., Hackney, J., Yu, X., Huseni, M., Yang, Y., . . . Grogan, J. L. (2014). The immunoreceptor TIGIT regulates antitumor and antiviral CD8(+) T cell effector function. *Cancer Cell*, *26*(6), 923-937. doi:10.1016/j.ccell.2014.10.018
- Joyce, M. G., & Sun, P. D. (2011). The structural basis of ligand recognition by natural killer cell receptors. *J Biomed Biotechnol*, *2011*, 203628. doi:10.1155/2011/203628
- Keefe, D., Shi, L., Feske, S., Massol, R., Navarro, F., Kirchhausen, T., & Lieberman, J. (2005). Perforin triggers a plasma membrane-repair response that facilitates CTL induction of apoptosis. *Immunity*, *23*(3), 249-262. doi:10.1016/j.immuni.2005.08.001
- Khan, M., Arooj, S., & Wang, H. (2020). NK Cell-Based Immune Checkpoint Inhibition. *Front Immunol*, *11*, 167. doi:10.3389/fimmu.2020.00167
- Kim, W. S., Park, C., Jung, Y. S., Kim, H. S., Han, J., Park, C. H., . . . Park, K. (1999). Reduced transforming growth factor-beta type II receptor (TGF-beta RII) expression in adenocarcinoma of the lung. *Anticancer Res*, *19*(1A), 301-306. Retrieved from <https://www.ncbi.nlm.nih.gov/pubmed/10226558>
- Koch, J., Steinle, A., Watzl, C., & Mandelboim, O. (2013). Activating natural cytotoxicity receptors of natural killer cells in cancer and infection. *Trends Immunol*, *34*(4), 182-191. doi:10.1016/j.it.2013.01.003
- Krzewski, K., & Coligan, J. E. (2012). Human NK cell lytic granules and regulation of their exocytosis. *Front Immunol*, *3*, 335. doi:10.3389/fimmu.2012.00335
- Kuwana, T., Mackey, M. R., Perkins, G., Ellisman, M. H., Latterich, M., Schneiter, R., . . . Newmeyer, D. D. (2002). Bid, Bax, and lipids cooperate to form supramolecular openings in the outer mitochondrial membrane. *Cell*, *111*(3), 331-342. doi:10.1016/s0092-8674(02)01036-x
- Lai, K. C., Liu, C. J., Chang, K. W., & Lee, T. C. (2013). Depleting IFIT2 mediates atypical PKC signaling to enhance the migration and metastatic activity of oral squamous cell carcinoma cells. *Oncogene*, *32*(32), 3686-3697. doi:10.1038/onc.2012.384
- Larsen, S. K., Gao, Y., & Basse, P. H. (2014). NK cells in the tumor microenvironment. *Crit Rev Oncog*, *19*(1-2), 91-105. doi:10.1615/critrevoncog.2014011142
- Law, C. W., Alhamdoosh, M., Su, S., Dong, X., Tian, L., Smyth, G. K., & Ritchie, M. E. (2016). RNA-seq analysis is easy as 1-2-3 with limma, Glimma and edgeR. *F1000Res*, *5*. doi:10.12688/f1000research.9005.3
- Law, C. W., Chen, Y., Shi, W., & Smyth, G. K. (2014). voom: Precision weights unlock linear model analysis tools for RNA-seq read counts. *Genome Biol*, *15*(2), R29. doi:10.1186/gb-2014-15-2-r29
- Lee, J., Park, K. H., Ryu, J. H., Bae, H. J., Choi, A., Lee, H., . . . Oh, E. J. (2017). Natural killer cell activity for IFN-gamma production as a supportive diagnostic marker for gastric cancer. *Oncotarget*, *8*(41), 70431-70440. doi:10.18632/oncotarget.19712
- Li, C., Ge, B., Nicotra, M., Stern, J. N., Kopcow, H. D., Chen, X., & Strominger, J. L. (2008). JNK MAP kinase activation is required for MTOC and granule

- polarization in NKG2D-mediated NK cell cytotoxicity. *Proc Natl Acad Sci U S A*, 105(8), 3017-3022. doi:10.1073/pnas.0712310105
- Li, H., Kobayashi, M., Blonska, M., You, Y., & Lin, X. (2006). Ubiquitination of RIP is required for tumor necrosis factor alpha-induced NF-kappaB activation. *J Biol Chem*, 281(19), 13636-13643. doi:10.1074/jbc.M600620200
- Li, J., Figueira, S. K., Vrazo, A. C., Binkowski, B. F., Butler, B. L., Tabata, Y., . . . Risma, K. A. (2014). Real-time detection of CTL function reveals distinct patterns of caspase activation mediated by Fas versus granzyme B. *J Immunol*, 193(2), 519-528. doi:10.4049/jimmunol.1301668
- Li, J., McQuade, T., Siemer, A. B., Napetschnig, J., Moriwaki, K., Hsiao, Y. S., . . . Wu, H. (2012). The RIP1/RIP3 necrosome forms a functional amyloid signaling complex required for programmed necrosis. *Cell*, 150(2), 339-350. doi:10.1016/j.cell.2012.06.019
- Li, P., Nijhawan, D., Budihardjo, I., Srinivasula, S. M., Ahmad, M., Alnemri, E. S., & Wang, X. (1997). Cytochrome c and dATP-dependent formation of Apaf-1/caspase-9 complex initiates an apoptotic protease cascade. *Cell*, 91(4), 479-489. doi:10.1016/s0092-8674(00)80434-1
- Li, Y., Hofmann, M., Wang, Q., Teng, L., Chlewicki, L. K., Pircher, H., & Mariuzza, R. A. (2009). Structure of natural killer cell receptor KLRG1 bound to E-cadherin reveals basis for MHC-independent missing self recognition. *Immunity*, 31(1), 35-46. doi:10.1016/j.immuni.2009.04.019
- Li, Y., & Orange, J. S. (2021). Degranulation enhances presynaptic membrane packing, which protects NK cells from perforin-mediated autolysis. *PLoS Biol*, 19(8), e3001328. doi:10.1371/journal.pbio.3001328
- Liu, D., Bryceson, Y. T., Meckel, T., Vasiliver-Shamis, G., Dustin, M. L., & Long, E. O. (2009). Integrin-dependent organization and bidirectional vesicular traffic at cytotoxic immune synapses. *Immunity*, 31(1), 99-109. doi:10.1016/j.immuni.2009.05.009
- Liu, X., Kim, C. N., Yang, J., Jemmerson, R., & Wang, X. (1996). Induction of apoptotic program in cell-free extracts: requirement for dATP and cytochrome c. *Cell*, 86(1), 147-157. doi:10.1016/s0092-8674(00)80085-9
- Liu, X., Zhang, Z., Ruan, J., Pan, Y., Magupalli, V. G., Wu, H., & Lieberman, J. (2016). Inflammasome-activated gasdermin D causes pyroptosis by forming membrane pores. *Nature*, 535(7610), 153-158. doi:10.1038/nature18629
- Lou, Z., Jevremovic, D., Billadeau, D. D., & Leibson, P. J. (2000). A balance between positive and negative signals in cytotoxic lymphocytes regulates the polarization of lipid rafts during the development of cell-mediated killing. *J Exp Med*, 191(2), 347-354. doi:10.1084/jem.191.2.347
- Lu, W., Gong, D., Bar-Sagi, D., & Cole, P. A. (2001). Site-specific incorporation of a phosphotyrosine mimetic reveals a role for tyrosine phosphorylation of SHP-2 in cell signaling. *Mol Cell*, 8(4), 759-769. doi:10.1016/s1097-2765(01)00369-0
- Lugano, R., Ramachandran, M., & Dimberg, A. (2020). Tumor angiogenesis: causes, consequences, challenges and opportunities. *Cell Mol Life Sci*, 77(9), 1745-1770. doi:10.1007/s00018-019-03351-7
- Mahauad-Fernandez, W. D., Naushad, W., Panzner, T. D., Bashir, A., Lal, G., & Okeoma, C. M. (2018). BST-2 promotes survival in circulation and pulmonary metastatic seeding of breast cancer cells. *Sci Rep*, 8(1), 17608. doi:10.1038/s41598-018-35710-y
- Malireddi, R. K. S., Gurung, P., Kesavardhana, S., Samir, P., Burton, A., Mummareddy, H., . . . Kanneganti, T. D. (2020). Innate immune priming in the absence of TAK1 drives RIPK1 kinase activity-independent pyroptosis,

- apoptosis, necroptosis, and inflammatory disease. *J Exp Med*, 217(3). doi:10.1084/jem.20191644
- Marcet-Palacios, M., Odemuyiwa, S. O., Coughlin, J. J., Garofoli, D., Ewen, C., Davidson, C. E., . . . Moqbel, R. (2008). Vesicle-associated membrane protein 7 (VAMP-7) is essential for target cell killing in a natural killer cell line. *Biochem Biophys Res Commun*, 366(3), 617-623. doi:10.1016/j.bbrc.2007.11.079
- Marquardt, N., Kekalainen, E., Chen, P., Kvedaraite, E., Wilson, J. N., Ivarsson, M. A., . . . Michaelsson, J. (2017). Human lung natural killer cells are predominantly comprised of highly differentiated hypofunctional CD69(-)CD56(dim) cells. *J Allergy Clin Immunol*, 139(4), 1321-1330 e1324. doi:10.1016/j.jaci.2016.07.043
- Maul-Pavicic, A., Chiang, S. C., Rensing-Ehl, A., Jessen, B., Fauriat, C., Wood, S. M., . . . Ehl, S. (2011). ORA1-mediated calcium influx is required for human cytotoxic lymphocyte degranulation and target cell lysis. *Proc Natl Acad Sci U S A*, 108(8), 3324-3329. doi:10.1073/pnas.1013285108
- Mayes, K., Elsayed, Z., Alhazmi, A., Waters, M., Alkhatib, S. G., Roberts, M., . . . Landry, J. W. (2017). BPTF inhibits NK cell activity and the abundance of natural cytotoxicity receptor co-ligands. *Oncotarget*, 8(38), 64344-64357. doi:10.18632/oncotarget.17834
- McCann, F. E., Eissmann, P., Onfelt, B., Leung, R., & Davis, D. M. (2007). The activating NKG2D ligand MHC class I-related chain A transfers from target cells to NK cells in a manner that allows functional consequences. *J Immunol*, 178(6), 3418-3426. doi:10.4049/jimmunol.178.6.3418
- Ménager, M. M., Ménasché, G., Romao, M., Knapnougel, P., Ho, C.-H., Garfa, M., . . . de Saint Basile, G. (2007). Secretory cytotoxic granule maturation and exocytosis require the effector protein hMunc13-4. *Nature Immunology*, 8(3), 257-267. doi:10.1038/ni1431
- Mendonca, B. D. S., Agostini, M., Aquino, I. G., Dias, W. B., Bastos, D. C., & Rumjanek, F. D. (2017). Suppression of MAGE-A10 alters the metastatic phenotype of tongue squamous cell carcinoma cells. *Biochem Biophys Rep*, 10, 267-275. doi:10.1016/j.bbrep.2017.04.009
- Metkar, S. S., Mena, C., Pardo, J., Wang, B., Wallich, R., Freudenberg, M., . . . Froelich, C. J. (2008). Human and mouse granzyme A induce a proinflammatory cytokine response. *Immunity*, 29(5), 720-733. doi:10.1016/j.immuni.2008.08.014
- Metkar, S. S., Wang, B., Ebbs, M. L., Kim, J. H., Lee, Y. J., Raja, S. M., & Froelich, C. J. (2003). Granzyme B activates procaspase-3 which signals a mitochondrial amplification loop for maximal apoptosis. *J Cell Biol*, 160(6), 875-885. doi:10.1083/jcb.200210158
- Micheau, O., & Tschopp, J. (2003). Induction of TNF receptor I-mediated apoptosis via two sequential signaling complexes. *Cell*, 114(2), 181-190. doi:10.1016/s0092-8674(03)00521-x
- Mizrahi, S., Markel, G., Porgador, A., Bushkin, Y., & Mandelboim, O. (2007). CD100 on NK cells enhance IFN $\gamma$  secretion and killing of target cells expressing CD72. *PLoS One*, 2(9), e818. doi:10.1371/journal.pone.0000818
- Mootha, V. K., Lindgren, C. M., Eriksson, K. F., Subramanian, A., Sihag, S., Lehar, J., . . . Groop, L. C. (2003). PGC-1 $\alpha$ -responsive genes involved in oxidative phosphorylation are coordinately downregulated in human diabetes. *Nat Genet*, 34(3), 267-273. doi:10.1038/ng1180



- Moretta, L., Bottino, C., Pende, D., Castriconi, R., Mingari, M. C., & Moretta, A. (2006). Surface NK receptors and their ligands on tumor cells. *Semin Immunol*, 18(3), 151-158. doi:10.1016/j.smim.2006.03.002
- Moretta, L., & Moretta, A. (2004). Unravelling natural killer cell function: triggering and inhibitory human NK receptors. *EMBO J*, 23(2), 255-259. doi:10.1038/sj.emboj.7600019
- Muendlein, H. I., Connolly, W. M., Magri, Z., Smirnova, I., Ilyukha, V., Gautam, A., . . . Poltorak, A. (2021). ZBP1 promotes LPS-induced cell death and IL-1beta release via RHIM-mediated interactions with RIPK1. *Nat Commun*, 12(1), 86. doi:10.1038/s41467-020-20357-z
- Murphy, J. M., Czabotar, P. E., Hildebrand, J. M., Lucet, I. S., Zhang, J. G., Alvarez-Diaz, S., . . . Alexander, W. S. (2013). The pseudokinase MLKL mediates necroptosis via a molecular switch mechanism. *Immunity*, 39(3), 443-453. doi:10.1016/j.immuni.2013.06.018
- Nakano, K., & Vousden, K. H. (2001). PUMA, a novel proapoptotic gene, is induced by p53. *Mol Cell*, 7(3), 683-694. doi:10.1016/s1097-2765(01)00214-3
- Negishi, H., Taniguchi, T., & Yanai, H. (2018). The Interferon (IFN) Class of Cytokines and the IFN Regulatory Factor (IRF) Transcription Factor Family. *Cold Spring Harb Perspect Biol*, 10(11). doi:10.1101/cshperspect.a028423
- Nguyen, H., Ramana, C. V., Bayes, J., & Stark, G. R. (2001). Roles of phosphatidylinositol 3-kinase in interferon-gamma-dependent phosphorylation of STAT1 on serine 727 and activation of gene expression. *J Biol Chem*, 276(36), 33361-33368. doi:10.1074/jbc.M105070200
- Ni, Z., Huang, C., Zhao, H., Zhou, J., Hu, M., Chen, Q., . . . Huang, Q. (2021). PLXNC1: A Novel Potential Immune-Related Target for Stomach Adenocarcinoma. *Front Cell Dev Biol*, 9, 662707. doi:10.3389/fcell.2021.662707
- Niehhs, A., & Altfeld, M. (2020). Regulation of NK-Cell Function by HLA Class II. *Front Cell Infect Microbiol*, 10, 55. doi:10.3389/fcimb.2020.00055
- O'Connor, L., Strasser, A., O'Reilly, L. A., Hausmann, G., Adams, J. M., Cory, S., & Huang, D. C. (1998). Bim: a novel member of the Bcl-2 family that promotes apoptosis. *EMBO J*, 17(2), 384-395. doi:10.1093/emboj/17.2.384
- Orange, J. S. (2008). Formation and function of the lytic NK-cell immunological synapse. *Nat Rev Immunol*, 8(9), 713-725. doi:10.1038/nri2381
- Orange, J. S., Ramesh, N., Remold-O'Donnell, E., Sasahara, Y., Koopman, L., Byrne, M., . . . Strominger, J. L. (2002). Wiskott-Aldrich syndrome protein is required for NK cell cytotoxicity and colocalizes with actin to NK cell-activating immunologic synapses. *Proc Natl Acad Sci U S A*, 99(17), 11351-11356. doi:10.1073/pnas.162376099
- Pech, M. F., Fong, L. E., Villalta, J. E., Chan, L. J., Kharbanda, S., O'Brien, J. J., . . . Settleman, J. (2019). Systematic identification of cancer cell vulnerabilities to natural killer cell-mediated immune surveillance. *Elife*, 8. doi:10.7554/eLife.47362
- Peng, Z. P., Huang, S. F., Li, J. J., Tang, X. K., Wang, X. Y., & Li, H. M. (2022). The Effects of Hedgehog Signaling Pathway on the Proliferation and Apoptosis of Melanoma Cells. *J Oncol*, 2022, 4984866. doi:10.1155/2022/4984866
- Perez-Quintero, L. A., Roncagalli, R., Guo, H., Latour, S., Davidson, D., & Veillette, A. (2014). EAT-2, a SAP-like adaptor, controls NK cell activation through phospholipase Cgamma, Ca<sup>++</sup>, and Erk, leading to granule polarization. *J Exp Med*, 211(4), 727-742. doi:10.1084/jem.20132038

- Peter, M. E., & Krammer, P. H. (2003). The CD95(APO-1/Fas) DISC and beyond. *Cell Death Differ*, *10*(1), 26-35. doi:10.1038/sj.cdd.4401186
- Peterson, M. E., & Long, E. O. (2008). Inhibitory receptor signaling via tyrosine phosphorylation of the adaptor Crk. *Immunity*, *29*(4), 578-588. doi:10.1016/j.immuni.2008.07.014
- Platonova, S., Cherfils-Vicini, J., Damotte, D., Crozet, L., Vieillard, V., Validire, P., . . . Cremer, I. (2011). Profound coordinated alterations of intratumoral NK cell phenotype and function in lung carcinoma. *Cancer Res*, *71*(16), 5412-5422. doi:10.1158/0008-5472.CAN-10-4179
- Pobezinskaya, Y. L., Kim, Y. S., Choksi, S., Morgan, M. J., Li, T., Liu, C., & Liu, Z. (2008). The function of TRADD in signaling through tumor necrosis factor receptor 1 and TRIF-dependent Toll-like receptors. *Nat Immunol*, *9*(9), 1047-1054. doi:10.1038/ni.1639
- Prager, I., & Watzl, C. (2019). Mechanisms of natural killer cell-mediated cellular cytotoxicity. *J Leukoc Biol*, *105*(6), 1319-1329. doi:10.1002/JLB.MR0718-269R
- Price, S., Shaw, P. A., Seitz, A., Joshi, G., Davis, J., Niemela, J. E., . . . Lenardo, M. J. (2014). Natural history of autoimmune lymphoproliferative syndrome associated with FAS gene mutations. *Blood*, *123*(13), 1989-1999. doi:10.1182/blood-2013-10-535393
- Qiao, X., Ma, B., Sun, W., Zhang, N., Liu, Y., Jia, L., & Liu, C. (2022). JAG1 is associated with the prognosis and metastasis in breast cancer. *Sci Rep*, *12*(1), 21986. doi:10.1038/s41598-022-26241-8
- Raulet, D. H., & Vance, R. E. (2006). Self-tolerance of natural killer cells. *Nat Rev Immunol*, *6*(7), 520-531. doi:10.1038/nri1863
- Reefman, E., Kay, J. G., Wood, S. M., Offenhauser, C., Brown, D. L., Roy, S., . . . Stow, J. L. (2010). Cytokine secretion is distinct from secretion of cytotoxic granules in NK cells. *J Immunol*, *184*(9), 4852-4862. doi:10.4049/jimmunol.0803954
- Regunathan, J., Chen, Y., Kutlesa, S., Dai, X., Bai, L., Wen, R., . . . Malarkannan, S. (2006). Differential and nonredundant roles of phospholipase Cgamma2 and phospholipase Cgamma1 in the terminal maturation of NK cells. *J Immunol*, *177*(8), 5365-5376. doi:10.4049/jimmunol.177.8.5365
- Reka, A. K., Chen, G., Jones, R. C., Amunugama, R., Kim, S., Karnovsky, A., . . . Keshamouni, V. G. (2014). Epithelial-mesenchymal transition-associated secretory phenotype predicts survival in lung cancer patients. *Carcinogenesis*, *35*(6), 1292-1300. doi:10.1093/carcin/bgu041
- Ritchie, M. E., Phipson, B., Wu, D., Hu, Y., Law, C. W., Shi, W., & Smyth, G. K. (2015). limma powers differential expression analyses for RNA-sequencing and microarray studies. *Nucleic Acids Res*, *43*(7), e47. doi:10.1093/nar/gkv007
- Rudd-Schmidt, J. A., Hodel, A. W., Noori, T., Lopez, J. A., Cho, H. J., Verschoor, S., . . . Voskoboinik, I. (2019). Lipid order and charge protect killer T cells from accidental death. *Nat Commun*, *10*(1), 5396. doi:10.1038/s41467-019-13385-x
- Samson, A. L., Zhang, Y., Geoghegan, N. D., Gavin, X. J., Davies, K. A., Mlodzianoski, M. J., . . . Murphy, J. M. (2020). MLKL trafficking and accumulation at the plasma membrane control the kinetics and threshold for necroptosis. *Nat Commun*, *11*(1), 3151. doi:10.1038/s41467-020-16887-1
- Sancho, D., Nieto, M., Llano, M., Rodriguez-Fernandez, J. L., Tejedor, R., Avraham, S., . . . Sanchez-Madrid, F. (2000). The tyrosine kinase PYK-2/RAFTK regulates natural killer (NK) cell cytotoxic response, and is translocated and

- activated upon specific target cell recognition and killing. *J Cell Biol*, 149(6), 1249-1262. doi:10.1083/jcb.149.6.1249
- Santoni, G., Amantini, C., Santoni, M., Maggi, F., Morelli, M. B., & Santoni, A. (2021). Mechanosensation and Mechanotransduction in Natural Killer Cells. *Front Immunol*, 12, 688918. doi:10.3389/fimmu.2021.688918
- Schneider-Brachert, W., Tchikov, V., Neumeyer, J., Jakob, M., Winoto-Morbach, S., Held-Feindt, J., . . . Schutze, S. (2004). Compartmentalization of TNF receptor 1 signaling: internalized TNF receptors as death signaling vesicles. *Immunity*, 21(3), 415-428. doi:10.1016/j.immuni.2004.08.017
- Sedger, L. M., Glaccum, M. B., Schuh, J. C., Kanaly, S. T., Williamson, E., Kayagaki, N., . . . Gliniak, B. (2002). Characterization of the in vivo function of TNF- $\alpha$ -related apoptosis-inducing ligand, TRAIL/Apo2L, using TRAIL/Apo2L gene-deficient mice. *Eur J Immunol*, 32(8), 2246-2254. doi:10.1002/1521-4141(200208)32:8<2246::AID-IMMU2246>3.0.CO;2-6
- Seo, H., Jeon, I., Kim, B. S., Park, M., Bae, E. A., Song, B., . . . Kang, C. Y. (2017). IL-21-mediated reversal of NK cell exhaustion facilitates anti-tumour immunity in MHC class I-deficient tumours. *Nat Commun*, 8, 15776. doi:10.1038/ncomms15776
- Seol DW, L. J., Seol MH, Park SY, Talanian RV, Billiar TR. (2001). Signaling events triggered by tumor necrosis factor-related apoptosis-inducing ligand (TRAIL): caspase-8 is required for TRAIL-induced apoptosis. *Cancer Res*, 2001 Feb 1(61(3)), 1138-1143.
- Sharif-Askari, E., Alam, A., Rheaume, E., Beresford, P. J., Scotto, C., Sharma, K., . . . Sekaly, R. P. (2001). Direct cleavage of the human DNA fragmentation factor-45 by granzyme B induces caspase-activated DNase release and DNA fragmentation. *EMBO J*, 20(12), 3101-3113. doi:10.1093/emboj/20.12.3101
- Shaver, K. A., Croom-Perez, T. J., & Copik, A. J. (2021). Natural Killer Cells: The Linchpin for Successful Cancer Immunotherapy. *Front Immunol*, 12, 679117. doi:10.3389/fimmu.2021.679117
- Shenoy, A. R., Wellington, D. A., Kumar, P., Kassa, H., Booth, C. J., Cresswell, P., & MacMicking, J. D. (2012). GBP5 promotes NLRP3 inflammasome assembly and immunity in mammals. *Science*, 336(6080), 481-485. doi:10.1126/science.1217141
- Shi, J., Zhao, Y., Wang, K., Shi, X., Wang, Y., Huang, H., . . . Shao, F. (2015). Cleavage of GSDMD by inflammatory caspases determines pyroptotic cell death. *Nature*, 526(7575), 660-665. doi:10.1038/nature15514
- Simister, P. C., Border, E. C., Vieira, J. F., & Pumphrey, N. J. (2022). Structural insights into engineering a T-cell receptor targeting MAGE-A10 with higher affinity and specificity for cancer immunotherapy. *J Immunother Cancer*, 10(7). doi:10.1136/jitc-2022-004600
- Snyder, K. M., Hullsiek, R., Mishra, H. K., Mendez, D. C., Li, Y., Rogich, A., . . . Walcheck, B. (2018). Expression of a Recombinant High Affinity IgG Fc Receptor by Engineered NK Cells as a Docking Platform for Therapeutic mAbs to Target Cancer Cells. *Front Immunol*, 9, 2873. doi:10.3389/fimmu.2018.02873
- Song, M., Ping, Y., Zhang, K., Yang, L., Li, F., Zhang, C., . . . Zhang, Y. (2019). Low-Dose IFN $\gamma$  Induces Tumor Cell Stemness in Tumor Microenvironment of Non-Small Cell Lung Cancer. *Cancer Res*, 79(14), 3737-3748. doi:10.1158/0008-5472.CAN-19-0596

- Song, X., Xu, C., Wu, X., Zhao, X., Fan, J., & Meng, S. (2020). The potential markers of NK-92 associated to cytotoxicity against K562 cells. *Biologicals*, 68, 46-53. doi:10.1016/j.biologicals.2020.08.009
- Sordo-Bahamonde, C., Lorenzo-Herrero, S., Payer, A. R., Gonzalez, S., & Lopez-Soto, A. (2020). Mechanisms of Apoptosis Resistance to NK Cell-Mediated Cytotoxicity in Cancer. *Int J Mol Sci*, 21(10). doi:10.3390/ijms21103726
- Stanietsky, N., Simic, H., Arapovic, J., Toporik, A., Levy, O., Novik, A., . . . Mandelboim, O. (2009). The interaction of TIGIT with PVR and PVRL2 inhibits human NK cell cytotoxicity. *Proc Natl Acad Sci U S A*, 106(42), 17858-17863. doi:10.1073/pnas.0903474106
- Stawowczyk, M., Van Scoy, S., Kumar, K. P., & Reich, N. C. (2011). The interferon stimulated gene 54 promotes apoptosis. *J Biol Chem*, 286(9), 7257-7266. doi:10.1074/jbc.M110.207068
- Stebbins, C. C., Watzl, C., Billadeau, D. D., Leibson, P. J., Burshtyn, D. N., & Long, E. O. (2003). Vav1 dephosphorylation by the tyrosine phosphatase SHP-1 as a mechanism for inhibition of cellular cytotoxicity. *Mol Cell Biol*, 23(17), 6291-6299. doi:10.1128/MCB.23.17.6291-6299.2003
- Stinchcombe, J. C., Barral, D. C., Mules, E. H., Booth, S., Hume, A. N., Machesky, L. M., . . . Griffiths, G. M. (2001). Rab27a is required for regulated secretion in cytotoxic T lymphocytes. *J Cell Biol*, 152(4), 825-834. doi:10.1083/jcb.152.4.825
- Strieter, R. M., Polverini, P. J., Kunkel, S. L., Arenberg, D. A., Burdick, M. D., Kasper, J., . . . et al. (1995). The functional role of the ELR motif in CXC chemokine-mediated angiogenesis. *J Biol Chem*, 270(45), 27348-27357. doi:10.1074/jbc.270.45.27348
- Subramanian, A., Tamayo, P., Mootha, V. K., Mukherjee, S., Ebert, B. L., Gillette, M. A., . . . Mesirov, J. P. (2005). Gene set enrichment analysis: a knowledge-based approach for interpreting genome-wide expression profiles. *Proc Natl Acad Sci U S A*, 102(43), 15545-15550. doi:10.1073/pnas.0506580102
- Suliman, A., Lam, A., Datta, R., & Srivastava, R. K. (2001). Intracellular mechanisms of TRAIL: apoptosis through mitochondrial-dependent and -independent pathways. *Oncogene*, 20(17), 2122-2133. doi:10.1038/sj.onc.1204282
- Sung, H., Ferlay, J., Siegel, R. L., Laversanne, M., Soerjomataram, I., Jemal, A., & Bray, F. (2021). Global Cancer Statistics 2020: GLOBOCAN Estimates of Incidence and Mortality Worldwide for 36 Cancers in 185 Countries. *CA Cancer J Clin*, 71(3), 209-249. doi:10.3322/caac.21660
- Takanami, I., Takeuchi, K., & Giga, M. (2001). The prognostic value of natural killer cell infiltration in resected pulmonary adenocarcinoma. *J Thorac Cardiovasc Surg*, 121(6), 1058-1063. doi:10.1067/mtc.2001.113026
- Tam, Y. K., Maki, G., Miyagawa, B., Hennemann, B., Tonn, T., & Klingemann, H. G. (1999). Characterization of genetically altered, interleukin 2-independent natural killer cell lines suitable for adoptive cellular immunotherapy. *Hum Gene Ther*, 10(8), 1359-1373. doi:10.1089/10430349950018030
- Tang, D., Tao, D., Fang, Y., Deng, C., Xu, Q., & Zhou, J. (2017). TNF-Alpha Promotes Invasion and Metastasis via NF-Kappa B Pathway in Oral Squamous Cell Carcinoma. *Med Sci Monit Basic Res*, 23, 141-149. doi:10.12659/msmbr.903910
- Tenev, T., Bianchi, K., Darding, M., Broemer, M., Langlais, C., Wallberg, F., . . . Meier, P. (2011). The Ripoptosome, a signaling platform that assembles in response to genotoxic stress and loss of IAPs. *Mol Cell*, 43(3), 432-448. doi:10.1016/j.molcel.2011.06.006

- Thomas, D. A., Du, C., Xu, M., Wang, X., & Ley, T. J. (2000). DFF45/ICAD can be directly processed by granzyme B during the induction of apoptosis. *Immunity*, *12*(6), 621-632. doi:10.1016/s1074-7613(00)80213-7
- Tokunaga, R., Zhang, W., Naseem, M., Puccini, A., Berger, M. D., Soni, S., . . . Lenz, H. J. (2018). CXCL9, CXCL10, CXCL11/CXCR3 axis for immune activation - A target for novel cancer therapy. *Cancer Treat Rev*, *63*, 40-47. doi:10.1016/j.ctrv.2017.11.007
- Treanor, B., Lanigan, P. M., Kumar, S., Dunsby, C., Munro, I., Auksoorius, E., . . . Davis, D. M. (2006). Microclusters of inhibitory killer immunoglobulin-like receptor signaling at natural killer cell immunological synapses. *J Cell Biol*, *174*(1), 153-161. doi:10.1083/jcb.200601108
- Tsuchiya, K., Nakajima, S., Hosojima, S., Thi Nguyen, D., Hattori, T., Manh Le, T., . . . Suda, T. (2019). Caspase-1 initiates apoptosis in the absence of gasdermin D. *Nat Commun*, *10*(1), 2091. doi:10.1038/s41467-019-09753-2
- Upshaw, J. L., Arneson, L. N., Schoon, R. A., Dick, C. J., Billadeau, D. D., & Leibson, P. J. (2006). NKG2D-mediated signaling requires a DAP10-bound Grb2-Vav1 intermediate and phosphatidylinositol-3-kinase in human natural killer cells. *Nat Immunol*, *7*(5), 524-532. doi:10.1038/ni1325
- Urlaub, D., Hofer, K., Muller, M. L., & Watzl, C. (2017). LFA-1 Activation in NK Cells and Their Subsets: Influence of Receptors, Maturation, and Cytokine Stimulation. *J Immunol*, *198*(5), 1944-1951. doi:10.4049/jimmunol.1601004
- Van Laethem, F., Donaty, L., Tchernonog, E., Lacheretz-Szablewski, V., Russello, J., Buthiau, D., . . . Bret, C. (2022). LAIR1, an ITIM-Containing Receptor Involved in Immune Disorders and in Hematological Neoplasms. *Int J Mol Sci*, *23*(24). doi:10.3390/ijms232416136
- Vanden Berghe, T., van Loo, G., Saelens, X., Van Gurp, M., Brouckaert, G., Kalai, M., . . . Vandenabeele, P. (2004). Differential signaling to apoptotic and necrotic cell death by Fas-associated death domain protein FADD. *J Biol Chem*, *279*(9), 7925-7933. doi:10.1074/jbc.M307807200
- Vivier, E., Artis, D., Colonna, M., Diefenbach, A., Di Santo, J. P., Eberl, G., . . . Spits, H. (2018). Innate Lymphoid Cells: 10 Years On. *Cell*, *174*(5), 1054-1066. doi:10.1016/j.cell.2018.07.017
- von Karstedt, S., Montinaro, A., & Walczak, H. (2017). Exploring the TRAILs less travelled: TRAIL in cancer biology and therapy. *Nat Rev Cancer*, *17*(6), 352-366. doi:10.1038/nrc.2017.28
- Voskoboinik, I., Whisstock, J. C., & Trapani, J. A. (2015). Perforin and granzymes: function, dysfunction and human pathology. *Nat Rev Immunol*, *15*(6), 388-400. doi:10.1038/nri3839
- Wang, J., Chun, H. J., Wong, W., Spencer, D. M., & Lenardo, M. J. (2001). Caspase-10 is an initiator caspase in death receptor signaling. *Proc Natl Acad Sci U S A*, *98*(24), 13884-13888. doi:10.1073/pnas.241358198
- Wang, K., Yin, X. M., Chao, D. T., Milliman, C. L., & Korsmeyer, S. J. (1996). BID: a novel BH3 domain-only death agonist. *Genes Dev*, *10*(22), 2859-2869. doi:10.1101/gad.10.22.2859
- Wang, L., Zhang, K., Wu, L., Liu, S., Zhang, H., Zhou, Q., . . . Fan, Z. (2012). Structural insights into the substrate specificity of human granzyme H: the functional roles of a novel RKR motif. *J Immunol*, *188*(2), 765-773. doi:10.4049/jimmunol.1101381
- Wang, W., Guo, H., Geng, J., Zheng, X., Wei, H., Sun, R., & Tian, Z. (2014). Tumor-released Galectin-3, a soluble inhibitory ligand of human NKp30, plays an

- important role in tumor escape from NK cell attack. *J Biol Chem*, 289(48), 33311-33319. doi:10.1074/jbc.M114.603464
- Wang, Y., Cheng, H., Zeng, T., Chen, S., Xing, Q., & Zhu, B. (2022). A novel 17 apoptosis-related genes signature could predict overall survival for bladder cancer and its associations with immune infiltration. *Heliyon*, 8(11), e11343. doi:10.1016/j.heliyon.2022.e11343
- Watzl, C., & Urlaub, D. (2012). Molecular mechanisms of natural killer cell regulation. *Front Biosci (Landmark Ed)*, 17(4), 1418-1432. doi:10.2741/3995
- Weinstein, A. G., Godet, I., & Gilkes, D. M. (2022). The rise of viperin: the emerging role of viperin in cancer progression. *J Clin Invest*, 132(24). doi:10.1172/JCI165907
- Wu, Y., & Zhou, B. P. (2010). TNF-alpha/NF-kappaB/Snail pathway in cancer cell migration and invasion. *Br J Cancer*, 102(4), 639-644. doi:10.1038/sj.bjc.6605530
- Yasinska, I. M., Sakhnevych, S. S., Pavlova, L., Teo Hansen Selno, A., Teuscher Abeleira, A. M., Benlaouer, O., . . . Sumbayev, V. V. (2019). The Tim-3-Galectin-9 Pathway and Its Regulatory Mechanisms in Human Breast Cancer. *Front Immunol*, 10, 1594. doi:10.3389/fimmu.2019.01594
- Zavadil, J., Haley, J., Kalluri, R., Muthuswamy, S. K., & Thompson, E. (2008). Epithelial-mesenchymal transition. *Cancer Res*, 68(23), 9574-9577. doi:10.1158/0008-5472.CAN-08-2316
- Zhang, C., Zou, Y., Zhu, Y., Liu, Y., Feng, H., Niu, F., . . . Liu, H. (2021). Three Immune-Related Prognostic mRNAs as Therapeutic Targets for Pancreatic Cancer. *Front Med (Lausanne)*, 8, 649326. doi:10.3389/fmed.2021.649326
- Zhang, D., Beresford, P. J., Greenberg, A. H., & Lieberman, J. (2001). Granzymes A and B directly cleave lamins and disrupt the nuclear lamina during granule-mediated cytotoxicity. *Proc Natl Acad Sci U S A*, 98(10), 5746-5751. doi:10.1073/pnas.101329598
- Zhang, Q., Bi, J., Zheng, X., Chen, Y., Wang, H., Wu, W., . . . Tian, Z. (2018). Blockade of the checkpoint receptor TIGIT prevents NK cell exhaustion and elicits potent anti-tumor immunity. *Nat Immunol*, 19(7), 723-732. doi:10.1038/s41590-018-0132-0
- Zhang, Z., Wu, N., Lu, Y., Davidson, D., Colonna, M., & Veillette, A. (2015). DNAM-1 controls NK cell activation via an ITT-like motif. *J Exp Med*, 212(12), 2165-2182. doi:10.1084/jem.20150792
- Zhao, W., Yang, H., Liu, L., Qu, X., Ding, J., Yu, H., . . . Chai, J. (2023). OASL knockdown inhibits the progression of stomach adenocarcinoma by regulating the mTORC1 signaling pathway. *FASEB J*, 37(3), e22824. doi:10.1096/fj.202201582R
- Zheng, L., Bidere, N., Staudt, D., Cubre, A., Orenstein, J., Chan, F. K., & Lenardo, M. (2006). Competitive control of independent programs of tumor necrosis factor receptor-induced cell death by TRADD and RIP1. *Mol Cell Biol*, 26(9), 3505-3513. doi:10.1128/MCB.26.9.3505-3513.2006
- Zhong, W., Zhang, F., Huang, C., Lin, Y., & Huang, J. (2021). Identification of an apoptosis-related prognostic gene signature and molecular subtypes of clear cell renal cell carcinoma (ccRCC). *J Cancer*, 12(11), 3265-3276. doi:10.7150/jca.51812
- Zou, R., Zhao, W., Xiao, S., & Lu, Y. (2022). A Signature of Three Apoptosis-Related Genes Predicts Overall Survival in Breast Cancer. *Front Surg*, 9, 863035. doi:10.3389/fsurg.2022.863035

Zou, X., He, R., Zhang, Z., & Yan, Y. (2022). Apoptosis-Related Signature Predicts Prognosis and Immune Microenvironment Infiltration in Lung Adenocarcinoma. *Front Genet*, 13, 818403. doi:10.3389/fgene.2022.818403

## Danksagung

An dieser Stelle möchte ich meinen besonderen Dank nachstehenden Personen entgegenbringen, ohne deren Mithilfe die Anfertigung dieser Promotionsschrift niemals zustande gekommen wäre:

Mein Dank gilt zunächst Herrn Prof. Dr. Sos, meinem Doktorvater, für die Ermöglichung und Betreuung dieser Arbeit, der freundlichen Hilfe und des entgegengebrachten Vertrauens, das mir einen eigenen und kritischen Zugang zu der Thematik dieser Arbeit eröffnete.

Ich danke Frau Prof. Dr. von Karstedt und Herrn Prof. Dr. Beyer für die hilfsbereite und wissenschaftliche Betreuung als Zweitgutachter.

Des weiteren bedanke ich mich bei Fabi, Natasha und Svenja für das Lesen und Korrigieren meiner Dissertation.

Ferner danke ich allen, mit denen ich im Laufe der letzten Jahre im Labor zusammengearbeitet habe, die mich unterstützt und meinen Arbeitsalltag bereichert haben.

Tief verbunden und dankbar bin ich meiner Familie. Moritz, für deine unglaublich hilfreiche Unterstützung und dein Verständnis in den letzten Jahren und während der Anfertigung dieser Doktorarbeit, und Knödelchen fürs da sein und das tägliche Zeigen der kleinen Wunder.

Mein ganz besonderer Dank gilt meinen Eltern, die mir meinen bisherigen Lebensweg ermöglichten und immer an meine Ziele geglaubt haben. Ich kann meine Dankbarkeit, auch aus Platzgründen, kaum in Worte fassen, und hoffe ihr wisst, dass ich die folgenden Beispiele auch über mehrere Seiten ausführen könnte. Papa, danke dir für unzählige Gespräche in denen ich von klein auf das kritische Denken erlernt habe. Mama, danke dir für deine selbstlose Unterstützung in allen Lebensbereichen und unzählige Stunden des Frido-sittens.

Bogdan, auch dir vielen Dank fürs Existieren!



## Erklärung

Ich versichere, dass ich die von mir vorgelegte Dissertation selbstständig angefertigt, die benutzten Quellen und Hilfsmittel vollständig angegeben und die Stellen der Arbeit -einschließlich Tabellen, Karten und Abbildungen -, die anderen Werken im Wortlaut oder dem Sinn nach entnommen sind, in jedem Einzelfall als Entlehnung kenntlich gemacht habe; dass diese Dissertation noch keiner anderen Fakultät oder Universität zur Prüfung vorgelegen hat; dass sie noch nicht veröffentlicht worden ist sowie, dass ich eine solche Veröffentlichung vor Abschluss des Promotionsverfahrens nicht vornehmen werde. Die Bestimmungen dieser Promotionsordnung sind mir bekannt. Die von mir vorgelegte Dissertation ist von Prof. Dr. Martin L. Sos betreut worden.

Ich versichere, dass ich alle Angaben wahrheitsgemäß nach bestem Wissen und Gewissen gemacht habe und verpflichte mich, jedmögliche, die obigen Angaben betreffenden Veränderungen, dem Promotionsausschuss unverzüglich mitzuteilen.

06.06.2024

.....  
Datum

.....  
Unterschrift

